Development of Nano-metal – graphene structured materials for Hydrogen Storage

MSc Chemical Engineering Dissertation

Prepared by

Athule Ngqalakwezi

1321059

Submitted to

School of Chemical and Metallurgical Engineering, Faculty of Engineering and the Built Environment, University of the Witwatersrand, Johannesburg, South Africa

Supervisor(s):

Dr Diakanua Nkazi, Prof Gotthard Seifert & Dr Thabang Ntho

14 April 2021

DECLARATION

I declare that this dissertation is my own unaided work. It is being submitted for the degree of Master of Science in Engineering to the University of the Witwatersrand, Johannesburg, South Africa. It has not been submitted before for any degree or examination to any other University.

A.NGQALAKWEZI

(Signature of Candidate)

19 April 2021

Day of year

ABSTRACT

Operative solutions in the storage of hydrogen remain the main challenge in achieving an economy that is solely based on hydrogen. Energy storage, consumption and production are the fundamental challenges that hinder this development. To date no material has met the Department of energy requirements for energy storage and due to this; a lot of research has been undertaken for the development of hydrogen storage materials for on-board applications. In material based storage of hydrogen, poor kinetics and poor thermodynamics of developed materials have hindered their progress towards practical applications. As such, a need for material that will store hydrogen and have favorable kinetics and thermodynamics is a priority.

In this work, graphene based nanocomposites were synthesized for hydrogen storage applications. The primary aim of the work was to synthesize a nanocomposite that will desorb hydrogen at low temperature. The precursor graphene was synthesized using both the improved Tours method and the modified hummer's method. The graphene was reduced using various reducing methods and the effect of the reduction method on the hydrogen storage capacity of the material was evaluated. The metal/graphene nanocomposites were evaluated for hydrogen storage capacity at various pressures. The nanocomposites were then tested. An economic evaluation of the graphene nanocomposite was conducted to determine the feasibility of the material.

The characterization done in this work, XRD, FTIR and RAMAN confirmed that the graphite was successfully oxidized and the graphite oxide was successfully reduced to graphene. Elemental analysis (XRF, TEM-EDS) confirmed that the calcium and nickel were successfully incorporated into the graphene matrix. The metal/graphene was charged with hydrogen at various pressures 5, 10 and 15 bars and a proportional relationship between increasing pressure and adsorbed hydrogen was established. The hydrogen charged metal/graphene nanocomposite was then tested using TGA and TPD to test the hydrogen storage capacity and desorption temperatures thereof. The Ca/graphene desorbed hydrogen around 150℃, a temperature significantly lower than the one reported in literature. The Ca/graphene adsorbed 3.99 wt% of hydrogen while the Ni/graphene adsorbed about 2.78 wt% hydrogen. The reducing agent does affect the hydrogen storage capacity of the metal/graphene. It was found that NH_3 reduced Ca/graphene took up more hydrogen due to

the N-doping effect of the NH_3 which enhances the uptake of hydrogen. The economic evaluation was also done successfully.

ACKNOWLEDGEMENTS

"I can do all things through CHRIST who strengths me" Phillipians 4:13

First, I would like to give thanks to GOD for guiding me and giving me the strength to carry out my research and getting me where I am today. I would secondly like to thank my supervisor and co-supervisors Dr Diakanua Nkazi, Dr Mukai Hembe and Professor Gotthard Seifert who have been very helpful in my Masters journey with their unwavering support.

I would also like to thank my family for always being there for me, my dad especially, he would always encourage me whenever I was down and give me confidence to go back and fight and study hard. Thank you, your support was insurmountable and much appreciated.

I would lastly like to thank Mintek for the financial assistance, Mintek employees (Sibusiso Mavuso and Dr Jeffrey Baloyi) and the Advanced Materials division within Mintek for allowing and affording me the opportunity to carry out my experiments within their labs. This work would have not been completed with the assistance I got from you. Thank you!

RESEARCH OUTPUTS

PUBLICATIONS

Journals

A. **A. Ngqalakwezi**, D. Nkazi, S. Gotthard and T. Ntho**, (2019)** Effects of Reduction of Graphene Oxide on the Hydrogen Storage Capacities of Metal Graphene Nanocomposite, **Catalysis Today, ISSN 0920-5861,** (https://**doi.org/10.1016/j.cattod.2019.06.029**)

B. S.J Baloyi**, A. Ngqalakwezi,** D. Nkazi and T.A Ntho, **(2019)** Investigation of graphene-based nanocomposite for hydrogen storage, IOP Conf. Ser: Material Science Engineering, 655, 012029 (**doi:10.1088/1757-899X/655/1/012029**)

C. **Ngqalakwezi [1],** D. Nkazi, S. Gotthard and T. Ntho**,** Synthesis of graphene using Improved Tours Method and Modified Hummers Method: A reductant study, *Manuscript in preparation, 2019*

D. **Ngqalakwezi [1]**, D. Nkazi, S. Gotthard and T. Ntho**,** Development of graphene based nanocomposites for hydrogen storage applications: A review, *Manuscript submitted, 2020*

Book Chapters

A. **Ngqalakwezi [1]**, D. Nkazi, S.J. Baloyi and T. Ntho, (2019), **Hydrogen: An environmental remediation, Chapter 9,** Global Issues and Innovative Solutions in Healthcare, Culture, and the Environment, **IGI Global, *Book published,* *(*DOI: 10.4018/978-1-7998-3576-9.) ISBN13: 9781799835769**

B. **A. Ngqalakwezi** and D. Nkazi, (2020), **Hydrogen storage: Materials, kinetics and thermodynamics**, Advanced Technologies of Hydrogen and Engineering Systems in Automotive, **IntechOpen**, ***Book published***, **(DOI: 10.5772/intechopen.94300) ISBN 978-1-83968-298-8**

CONFERENCE AND SEMINAR PRESENTATIONS

- **A. Ngqalakwezi,** D. Nkazi, Hydrogen: A future energy? (Proposal Presentation) **Oral Presentation**, Wednesday Seminar. **School of Chemical and metallurgical engineering, Wits University, 22 August 2018**

- **A.Ngqalakwezi , D. Nkazi, S. Gotthard and T. Ntho,** Effects of Reduction of Graphene Oxide on the Hydrogen Storage Capacities of Metal Graphene Nanocomposite, **Poster presentation**, ***3rd International Conference on Catalysis and Chemical Engineering***, Double Tree Hotel, **Houston Texas, United States 25-27 February 2019**

- **A. Ngqalakwezi , D. Nkazi and T. Ntho,** Synthesis of a metal-graphene nanocomposite for hydrogen storage applications, **Poster presentation**, **School of Chemical and metallurgical engineering, Research Day, Wits University, 29 August 2019**

- **A. Ngqalakwezi, D. Nkazi,** Effects of Reduction of Graphene Oxide on the Hydrogen Storage Capacities of Metal Graphene Nanocomposite, **Oral presentation**, ***International Conference on Catalysis, Advanced Chemical Engineering and Technology***, Eurostars Ray Don Jaime, **Valencia, Spain. 05-07 September 2019**

- **S.J Baloyi, A. Ngqalakwezi, D. Nkazi and T.A Ntho,** Investigation of graphene-based nanocomposite for hydrogen storage, **Oral presentation**, Conference **of the South African Advanced Material Initiative**, Riverside Sun**, Vanderbijlpark, South Africa. 22-25 October 2019**

- **A. Ngqalakwezi , D Nkazi,** The synthesis of graphene using Improved Tours Method for energy storage applications in the automotive industry, **Oral presentation, International E-Meeting on Catalysis and Energy**, USG-United Scientific Group (US), **Online, 11 May 2020**

Table of Contents

LIST OF FIGURES

LIST OF TABLES

LIST OF SYMBOLS

d = *dimensionality*,

r = *lengths of the unreacted part*,

$\boldsymbol{r_0}$= *length of the whole particles*,

$\boldsymbol{\varepsilon}$ = *reaction fraction*

$\mathbf{k_{int}}$= *rate constant (interface controlled reaction)*

k = *generalized rate constant*

$\Delta \boldsymbol{C}$ = *concentration difference*

D = *diffusion constant*

$\boldsymbol{\rho}$ = *density*

z = *volume ratio of product to reactant*

I = *nucleation module*

r = *nucleation rate*

F = *impingement module defining the relationship between real reaction fraction and extended reaction fraction*

V= *Growth module*

$\Delta \boldsymbol{E_g}$= *activation energy for growth*

$\boldsymbol{G_0}$= *intrinsic growth rate*

m = *growth mode parameter*

$\frac{\boldsymbol{d}}{\boldsymbol{m}}$ = *growth index*

LIST OF ABBREVIATIONS

DFT	Density functional theory
ASME	American Society of Mechanical engineers
CVD	Chemical vapour deposition
CV	Contraction volume
GO	Graphite Oxide
G-B Model	Ginstling-Brounshtein model
JMAK	Johnson-Mehl-Avrami-Kolomogorov
DOE	Department of Energy
NMP	N-methyl-2-pyrrolidone
TEA	Triethylamine
ACS	American Chemical Society
ACE	Associate Chemical Enterprise

CHAPTER 1

1. INTRODUCTION

1.1 BACKGROUND & MOTIVATION

The increasing concerns about the security of energy supply due to the depletion of fossil fuels, has the led the world globally to research alternative energy supplies. Moreover, the impact fossil fuels have had on the environment have pushed the world into a paradigm shift where green systems have to be implemented to alleviate and reduce the environmental strains the world is facing currently (Andersson & Grönkvist, 2019). Fossil fuels have been used in various sectors and these different sectors have contributed to the environmental issues the world is facing globally due to the use of fossil fuels (Ruse et al., 2018). The figure 1-1 shows the greenhouse gas emission by the different sectors.

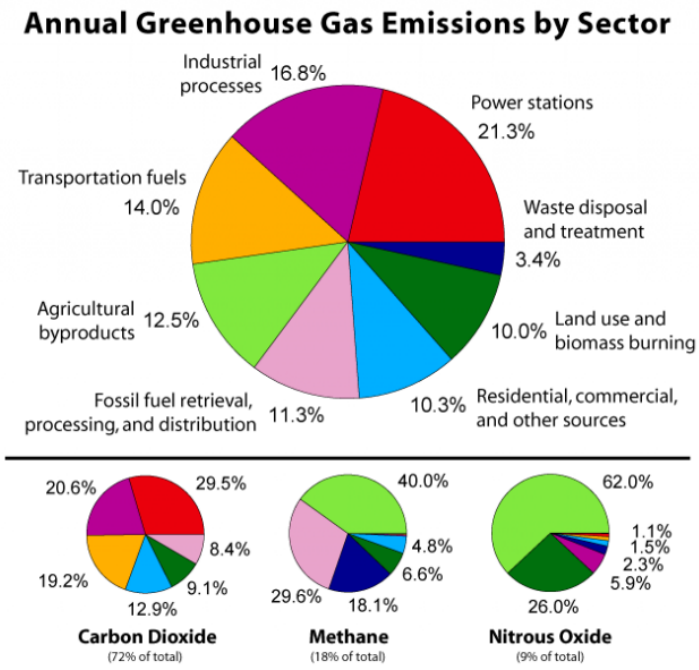

Figure 1-1: Greenhouse gas emission by different industries/ sectors (International energy agency, 2016)

The increasing concentration of these greenhouse gases on the environment has led to global warming and climate change (Houghton, 2001). Research around solutions to these issues have been prioritized and are pivotal in creating a better future for the coming generations. Legislations and regulations have been implemented to reduce the strain on the environment. However, these solutions are not long term and they do not deal with the problem head on. As such, research around alternative energy sources is very important.

Amongst alternative energy sources, hydrogen has been deemed as an alternative source of energy that can potentially replace fossil fuels for energy supply due to its zero emission and high-energy content compared to traditional fuels, namely, diesel and petrol (Abe et al., 2019; Andersson & Grönkvist, 2019). The chemical energy content on a mass basis in hydrogen is about 142 MJ kg^{-1} and 47 MJ kg^{-1} in traditional fuels such as diesel and petrol (Schlapbach & Züttel, 2001). This is almost 3 times higher than traditional fuels; this means a car using hydrogen fuel can go for a longer distance than traditional cars. The limiting factor in the application of hydrogen for commercial use has been its storage (Schlapbach & Züttel, 2001). Hydrogen occupies a large volume and the storage of it has proved to be challenging. The storage of hydrogen for commercial purposes is guided by the Department of Energy in the United States. The DoE sets the standards for material that will be applicable and practical for on-board application (Energy, 2018). The figure 1-2 shows the DoE requirements and it can be

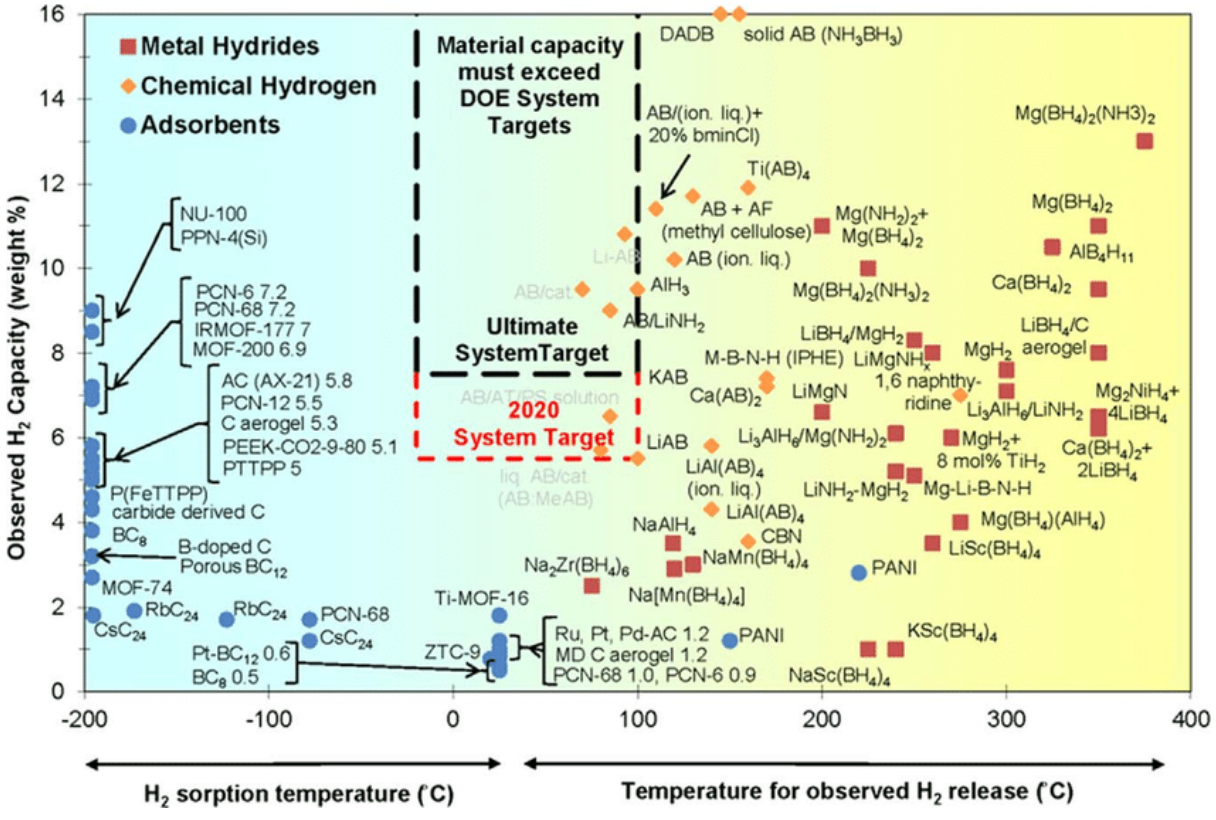

observed on the figure that to date no material has satisfied all on the requirements for onboard applications.

Figure 1-2: DoE standards for systems, target 2020 (Department of Energy-US, 2020)

The storage of hydrogen has been explored in all the three major phases, gas, liquid and solid. The storage of hydrogen in purest form, as a liquid and a gas, has been explored extensively however these methods have proved not to be practical for on-board applications. Hydrogen as a gas is stored and is compressed in composite tanks at very high pressures (Zheng et al., 2012). With this technique of storing hydrogen, a lot of money has to be invested in the material of construction to ensure that the tank integrity is not disturbed at very high pressure (Zheng et al., 2012). Material of construction such as carbon fiber, high density polymer liner, temperature sensors and others have to be used, all of this adds to the costs (Barthélémy, 2012; Hua et al., 2011; Zheng et al., 2012). The composite tanks have to be charged at pressures ranging from 350 MPa – 700 MPa, these are very high pressure and may pose safety risks and for this reasons the storage of hydrogen as a gas is not practical when considering the DoE standards for practical on-board applications (Weidenthaler & Felderhoff, 2011).

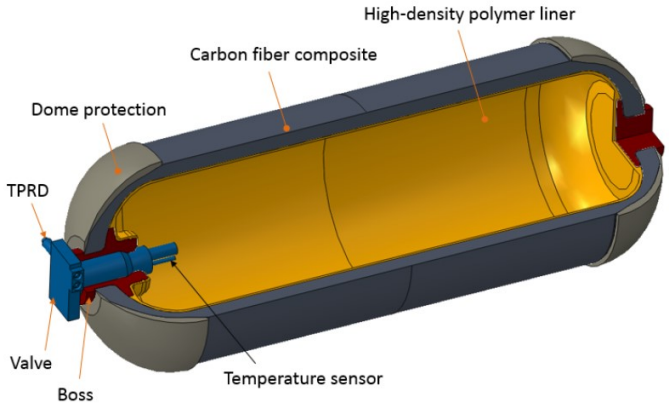

Figure 1-3: Composite tank, side-internal view (Office of energy efficiency, 2019)

Hydrogen as a gas, melts at cryogenic temperatures -253℃. Storing hydrogen as liquid requires a lot of energy to keep the hydrogen as a liquid at -253℃. This technique has a high requirement for energy and this is very expensive and costly (Schlapbach & Züttel, 2001). The storage of hydrogen as a solid is the only viable method when considering practical on-board applications. The storage of hydrogen as a solid is mainly in two parts: chemisorption material

and physisorption material (Barghi et al., 2014). Chemisorption material form a chemical bond with hydrogen and require high temperature to release the hydrogen. Physisorption material form a physical bond with hydrogen and requires low temperature to break the bond and release the hydrogen (Barghi et al., 2014). A lot of solid state hydrogen storage materials have been considered and studied, however to date no material has met the requirements of the DoE for practical on-board applications.

1.2 PROBLEM STATEMENT

The heavy use of fossil fuels and its negative effects on the environment have pushed the world to a point where green methods have to be implemented. Environmental issues like global warming and acid rain are direct consequences of utilizing fossil fuels, thus cleaner sources such as hydrogen are gathering a lot of attention as replacement sources of energy (Houghton, 2001). However, storing hydrogen in a manner that meets the DoE standards has been the hindering factor in the application of these materials because hydrogen has a large volume. When considering the DoE standards for on-board applications, solid state storage of hydrogen has gained favorable attention due to safety and less cost implications compared to storing hydrogen in its purest form as a gas and liquid (Energy, 2018).

A lot of studies and a lot of material have been synthesized for hydrogen storage. Materials such as MgH_2 (a chemisorption material) have been reported to have very high hydrogen storage capacity that meet the department of Energy's requirements, however the kinetics of these materials would not meet the requirements (Liang et al., 1999). This is mainly because these materials are thermodynamically stable and form a strong bond with hydrogen and during dehydrogenation high temperatures ranging from 250-300 ℃ would be needed to release the hydrogen (Xiong et al., 2005a) (Liang et al., 1999). A lot of metal hydrides/materials that had promising hydrogen storage capacity had the same issue, where a material would have high hydrogen storage capacity but would require a high temperature to release the hydrogen (Barthélémy, 2012). These temperatures are often outside the requirement of the DOE for on-board applications. A lot of solutions have been developed and applied in an effort to destabilize these materials such as catalysis, ball milling, thin films and alloying (Abe et al., 2019; Andersson & Grönkvist, 2019; Bououdina et al., 2006a; Xiong et al., 2005a). Some of these techniques have successfully destabilized chemisorption material, however, they still do not the meet the standards of the DOE for practical on board applications.

Physisorption material have also been developed and explored for hydrogen storage applications due to their fast kinetics (Nijkamp et al., 2001). However the main issue with these materials, is their low hydrogen storage capacity which does not meet the requirements of the DOE. In clear terms, hydrogen has been deemed as a clean source that can potentially replace traditional fuels (diesel and gasoline) however the storage of it has been an issue (Jhi et al., 2004; Nijkamp et al., 2001). The storage of hydrogen as a gas and liquid add costs, pose safety risks and has large energy requirements. With solid state storage of hydrogen, chemisorption material have kinetic issues while physisorption material have low hydrogen storage capacity (Schlapbach & Züttel, 2001). As a result, to date no material meets the DOE standards for practical on-board applications.

1.3 OBJECTIVES

Based on the problem statement description, the aim of this project is to develop a material for hydrogen storage. A graphene based nanocomposite was developed for hydrogen at low temperature. The specific steps that were taken in fulfillment of the objectives of this project are described below in point form:

To fulfill the aim of this research project, the below objectives were followed

- Synthesis of nano metals for hydrogen storage system
- Development of nano metals – graphene system as hydrogen storage material
- Characterization of the synthesised material
- Laboratory assessment of the storage systems
- Economic analysis of the developed hydrogen storage system

1.4 CONCEPTUAL MODEL FOR PROPOSED OBJECTIVES

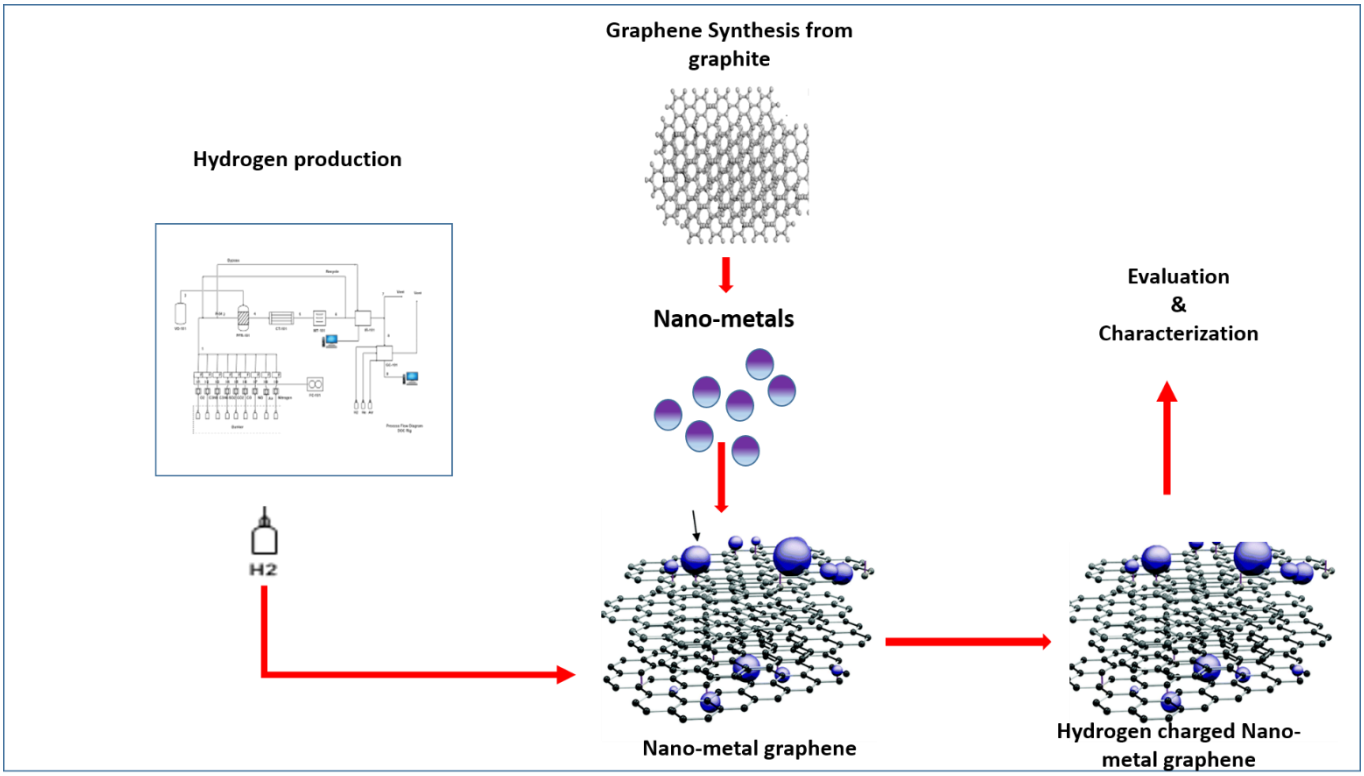

Figure 1-4: Conceptual model for proposed objectives

1.5 DEMARCATION AND LIMITATIONS OF THE RESEARCH INVESTIGATION

The work presented herein is constrained to the development of metal graphene nanocomposites using the modified hummer's method and the improved tours method. Various reductants were utilized to reduce graphite oxide to precursor graphene on the synthesis of metal graphene. The metal graphene is charged with hydrogen and subsequently tested. An economic study of this material is studied and explored. However the main focus of the study is to develop a metal on graphene nanocomposite that takes up hydrogen for on-board applications.

1.6 CONTRIBUTION OF THE STUDY TO EXISTING LITERATURE

The contribution of this master's research in the existing work done around hydrogen storage are two journal publications and a book chapter. Two other manuscripts are in preparations. In

one of the published journals, a novel metal graphene (Ca/graphene) nanocomposite was synthesized. This work was published in Catalysis Today.

1.7 PLAN OF DEVELOPMENT

This dissertation is comprised of eight chapters, described herein below:

Chapter 1:
This chapter gives a brief introduction into hydrogen storage as a research field and clearly points out the issues and gaps available that motivated the research undertaken. Furthermore, the contributions of this work to existing literature were highlighted and the scope of the research was outlined clearly.

Chapter 2:
This chapter gives an extensive idea of the hydrogen economy, specifically hydrogen storage. Hydrogen storage material such as graphene were discussed. Furthermore, the kinetics and thermodynamics of hydrogen storage materials are also discussed with equations.

Chapter 3:
The synthesis method of graphene of graphene was explored. The two synthesis methods discussed in this method are the Improved Tours Method and Modified Hummers Method. The characterization techniques used and the results thereof were discussed as well.

Chapter 4:
The synthesis of Ca/graphene and Ni/graphene nanocomposite was discussed in this chapter. The characterization and results thereof of these nanocomposites was also discussed extensively.

Chapter 5:
The metal-graphene nanocomposites synthesized were charged with hydrogen at various pressures and then characterized thereafter. The results obtained were then discussed extensively.

Chapter 6:

The effects of reduction of graphene using different reductants were evaluated in this to determine whether the reductant used on the support graphene has any effect on the hydrogen storage capacities of the graphene nanocomposites synthesized. The effects of the reductants was only evaluated on the Ca/graphene nanocomposite.

Chapter 7:

The reaction mechanism of the metal graphene nanocomposite was discussed in this chapter.

Chapter 8:

The last chapter of the dissertation explored the economics of the synthesized metal-graphene nanocomposites, as per the requirement of the Department of Energy in the US that sets the standard for practical applicable hydrogen storage materials for on-board applications.

REFERENCES

Abe, J. O., Popoola, A. P. I., Ajenifuja, E., & Popoola, O. M. (2019). Hydrogen energy, economy and storage: Review and recommendation. *International Journal of Hydrogen Energy*, *44*(29), 15072–15086. https://doi.org/10.1016/J.IJHYDENE.2019.04.068

Andersson, J., & Grönkvist, S. (2019). Large-scale storage of hydrogen. *International Journal of Hydrogen Energy*, *44*(23), 11901–11919. https://doi.org/10.1016/J.IJHYDENE.2019.03.063

Barghi, S. H., Tsotsis, T. T., & Sahimi, M. (2014). Chemisorption, physisorption and hysteresis during hydrogen storage in carbon nanotubes. *International Journal of Hydrogen Energy*, *39*(3), 1390–1397. https://doi.org/https://doi.org/10.1016/j.ijhydene.2013.10.163

Barthélémy, H. (2012). Hydrogen storage – Industrial prospectives. *International Journal of Hydrogen Energy*, *37*(22), 17364–17372. https://doi.org/https://doi.org/10.1016/j.ijhydene.2012.04.121

Energy, D. of. (2018). *Hydrogen Storage*.

Houghton, J. (2001). The science of global warming. *Interdisciplinary Science Reviews*, *26*(4), 247–257. https://doi.org/10.1179/isr.2001.26.4.247

Hua, T. Q., Ahluwalia, R. K., Peng, J.-K., Kromer, M., Lasher, S., McKenney, K., Law, K., & Sinha, J. (2011). Technical assessment of compressed hydrogen storage tank systems for automotive applications. *International Journal of Hydrogen Energy*, *36*(4), 3037–3049. https://doi.org/https://doi.org/10.1016/j.ijhydene.2010.11.090

Jhi, S.-H., Kwon, Y.-K., Bradley, K., & Gabriel, J.-C. P. (2004). Hydrogen storage by physisorption: beyond carbon. *Solid State Communications*, *129*(12), 769–773. https://doi.org/https://doi.org/10.1016/j.ssc.2003.12.032

Liang, G., Huot, J., Boily, S., Van Neste, A., & Schulz, R. (1999). Hydrogen storage properties of the mechanically milled MgH2–V nanocomposite. *Journal of Alloys and Compounds*, *291*(1), 295–299. https://doi.org/https://doi.org/10.1016/S0925-8388(99)00268-6

Nijkamp, M. G., Raaymakers, J. E. M. J., van Dillen, A. J., & de Jong, K. P. (2001). Hydrogen storage using physisorption – materials demands. *Applied Physics A*, *72*(5), 619–623. https://doi.org/10.1007/s003390100847

Ruse, E., Buzaglo, M., Pri-Bar, I., Shunak, L., Nadiv, R., Pevzner, S., Siton-Mendelson, O., Skripnyuk, V. M., Rabkin, E., & Regev, O. (2018). Hydrogen storage kinetics: The graphene nanoplatelet size effect. *Carbon*, *130*, 369–376. https://doi.org/10.1016/J.CARBON.2018.01.012

Schlapbach, L., & Züttel, A. (2001). Hydrogen-storage materials for mobile applications. *Nature*, *414*(6861), 353–358. https://doi.org/10.1038/35104634

Xiong, Z., Hu, J., Wu, G., Chen, P., Luo, W., Gross, K., & Wang, J. (2005a). Thermodynamic and kinetic investigations of the hydrogen storage in the Li–Mg–N–H system. *Journal of Alloys and Compounds*, *398*(1), 235–239. https://doi.org/https://doi.org/10.1016/j.jallcom.2005.02.010

Zheng, J., Liu, X., Xu, P., Liu, P., Zhao, Y., & Yang, J. (2012). Development of high pressure gaseous hydrogen storage technologies. *International Journal of Hydrogen Energy*, *37*(1), 1048–1057. https://doi.org/https://doi.org/10.1016/j.ijhydene.2011.02.125

CHAPTER 2

2. LITERATURE REVIEW

The prolonged reliance of mankind on energy primarily derived from fossil fuels has led to global environmental issues such as global warming (Patchkovskii et al., 2005). Combustion of fossil fuels over the past decades have contributed to a vast percentage of all greenhouse emissions globally and a significant portion to air pollution. This has incited a serious search and innovation of environmentally friendly and renewable energy sources. Renewable energy sources such as sea waves, tidal, sun, wind and biomass are explored as possible alternatives (Andersson & Grönkvist, 2019; W. Liu et al., 2018; Navlani-García et al., 2018). However hydrogen has garnered attention as a cleaner source of energy due to its increased energy density and minimized emissions to the environment. Hydrogen contains higher chemical energy per mass compared to current traditional fuel, it contains high energy content by weight than gasoline, it combusts rapidly than gasoline and is significantly less energy dense than gasoline (Schlapbach & Züttel, 2001). However the key driver or success of applied hydrogen energy lies in appropriate hydrogen storage mechanisms which remain unsolved.

Conditions practical for hydrogen storage application include high hydrogen capacities, moderate temperature (0℃-100℃) and pressure <100 atm amongst others (Energy, 2018). Solid state storage of hydrogen therefore is the viable alternative (Weidenthaler & Felderhoff, 2011). In this regard metal hydrides have been a subject of intensified research due to several reports of high hydrogen capacities however the downfall with these materials lies in their slow kinetics and uncomplimentary thermodynamics. Application of hydrogen storage materials relies on the improvement of thermodynamics and kinetics of these materials which subsequently leads to a deeper understanding of the kinetic mechanisms (Bououdina et al., 2006b; Xiong et al., 2005b). Kinetic mechanisms allow a better understanding of the intricate space and time related factors which include, morphology, hydrogen pressure, temperature, catalyst and the defects. Closer inspection of hydrogenation and dehydrogenation performance of hydrogen storage materials using kinetic models is an efficient approach to understand its kinetic mechanisms. A list of kinetic models such as Ginstling-Brounshtein, Jander model and corresponding models such as the Kissinger method, Sharp and Jones have all been explored

in an effort to establish appropriate hydrogen storage materials (Ginstling A, 1950)(Chaudhary et al., 2015; Crank 1916-, 1975).

However these kinetic models do not accurately define the hydrogenation and dehydrogenation reactions of hydrogen storage material due to existing issues; such as difficulty in deriving steps for the kinetic models and explaining the assumptions adequately, and in addition; new detailed models have not yet been introduced in hydrogen storage materials. Chaudhary et al. described the vitality of hydrogenation and dehydrogenation kinetics rates with respect to rate of charging and discharging of stored hydrogen and the importance of maintaining the power needed for such (Chaudhary et al., 2015; Crank 1916-, 1975). In addition Ley et al discovered that intrinsic factors such as equilibrium hydrogen sorption, chemical and physical behavior of materials and cycling stability and extrinsic factors such as morphology and heat transfer all affect kinetic characteristics (Ley et al., 1996) .

On the other hand, thermodynamic factors also play a crucial role in optimizing hydrogen storage systems. Properties such as temperature and pressure greatly influence the performance of hydrogen storage materials. Avdeenkov et al. developed a thermodynamic model for carbon nanostructure which took into account the inhomogeneity and non-ideality of absorbed hydrogen molecule (Avdeenkov et al., 2015). Callini et al. reported that computational modelling plays an important role in understanding the thermodynamics and kinetics of solid state material (Callini et al., 2016). Computational modelling can be used to define intricate experimental observations, to dope materials with different metals that will give optimized thermodynamics and kinetics (Callini et al., 2016).

2.1 HYDROGEN STORAGE MATERIALS

The Department of Energy in the United States of America releases hydrogen storage system targets every five years, which should be adhered to. The targets include amongst others cycle life, volumetric and gravimetric capacities, costs, refilling time and so forth. Hua et al. defined the volumetric capacity as the amount of gas in a given volume and gravimetric capacity as the amount of electricity given off by a specified weight of fuel (Energy, 2018). These two requirements are considered closely with cost and on board system efficiency. To date no material has met the DoE standards for 2015 and 2020. Figure 2-1 1 shows the 2015 targets and Figure 2-2 shows 2020.

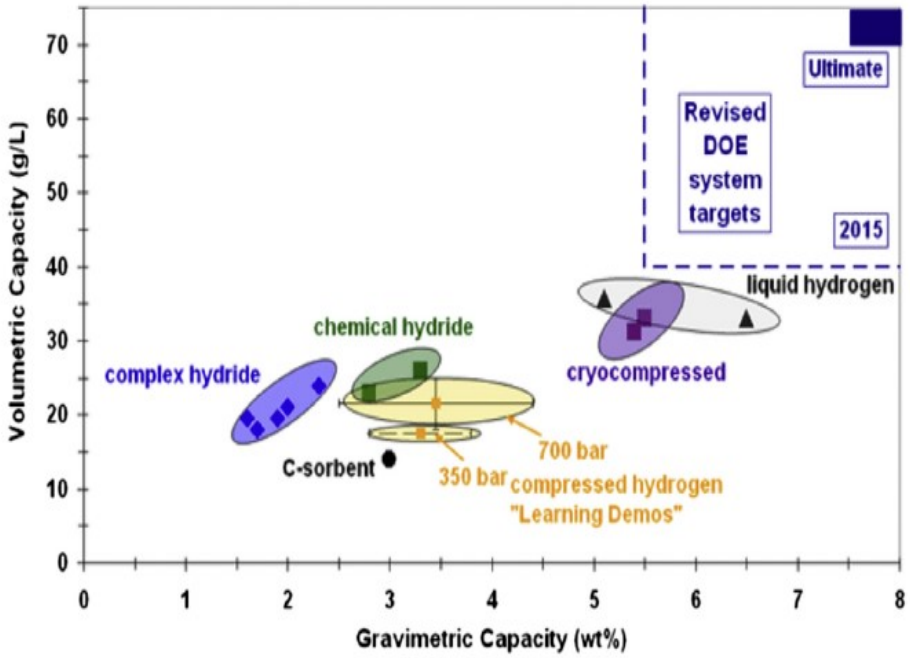

Figure 2-1: DoE 2015 targets and the ranking of hydrogen storage mechanisms and ultimate targets (Department of Energy-US, 2015)

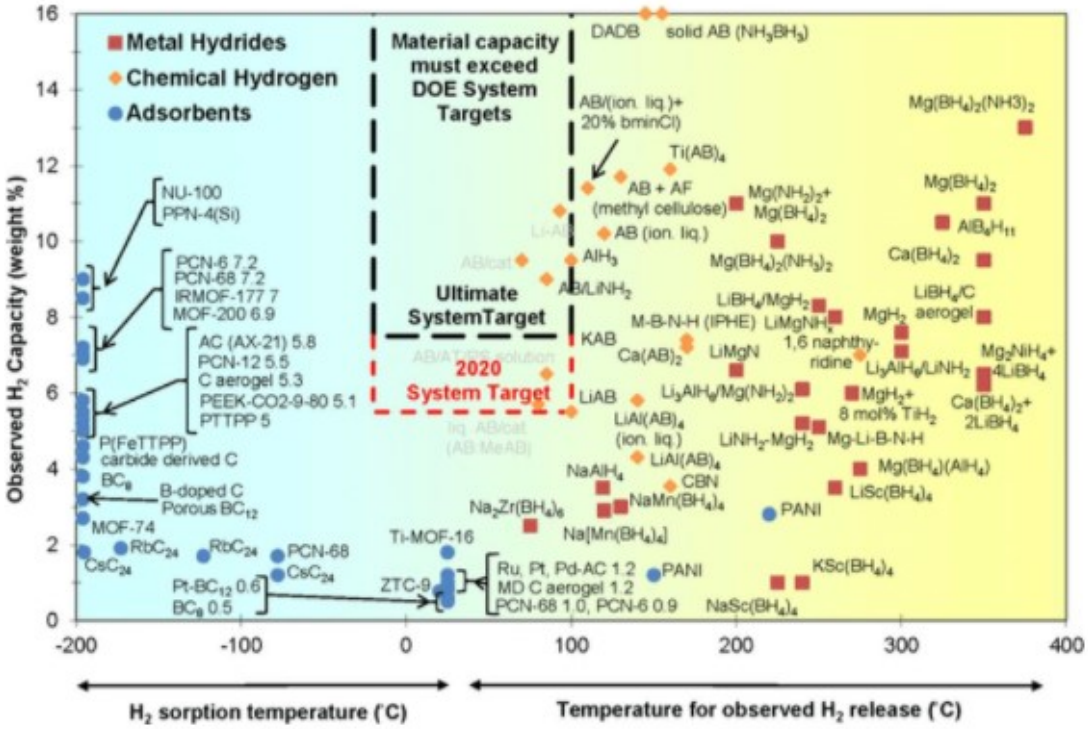

Figure 2-2: H_2 storage capacity of common materials with respect to temperature (Department of Energy-US, 2018)

The storage of hydrogen is a vital enabling advancement in the hydrogen economy and the development of hydrogen based economy, as such, this topic has attracted a lot of attention amongst researchers. The storage of hydrogen is either physical based or material based. The figure below depicts the classes of technology and materials under each storage method.

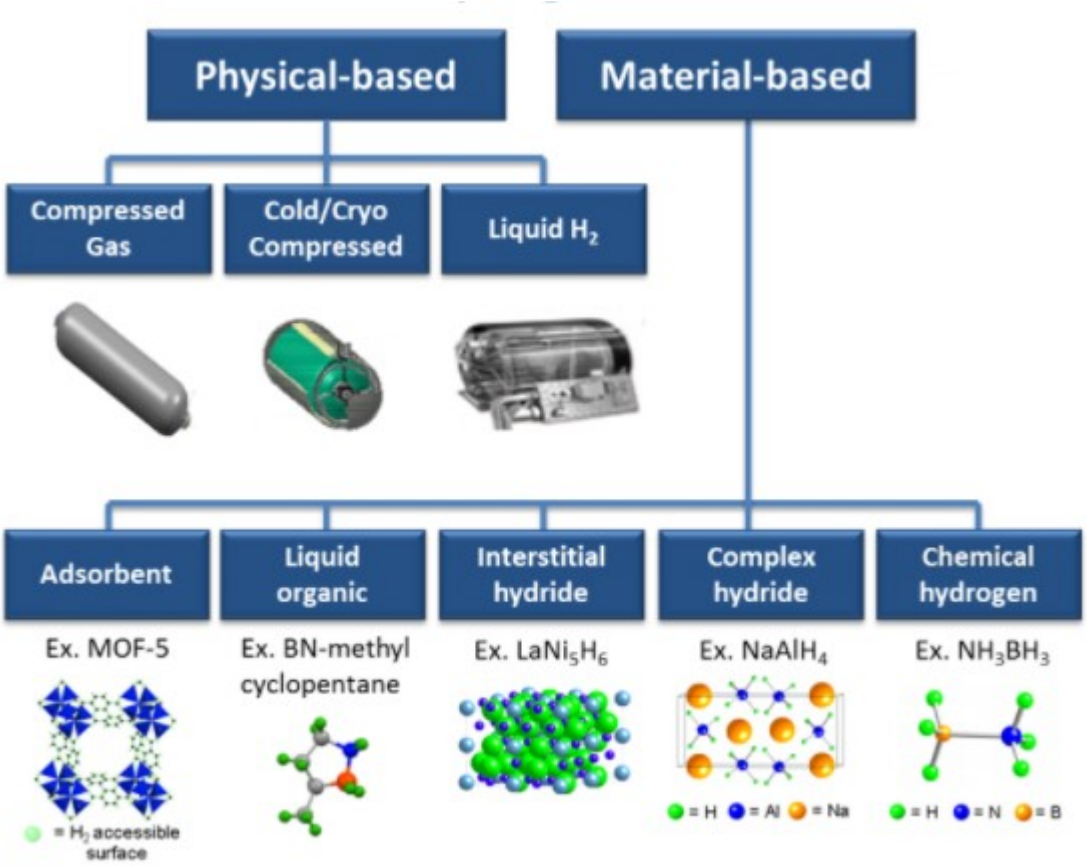

Figure 2-3: Classification of hydrogen storage materials (Energy Office, 2019)

2.1.1 Physical based storage of hydrogen

The physical based storage of hydrogen is the purest storage and the most common method of storage for hydrogen. The physical storage of hydrogen is done as either a gas or a liquid. These technologies have been extensively researched, improved and applied (Eberle et al., 2009). The gaseous storage of hydrogen typically requires composite tanks that withstand high pressures that range from 5 000 to 10 000 psi (Schlapbach & Züttel, 2001). The storage of hydrogen as a liquid is done at cryogenic temperatures, which is the boiling point of hydrogen at -253 °C

(Schlapbach & Züttel, 2001). A lot of energy is needed to maintain this temperature and keep hydrogen a liquid. Specifically NASA has commonly utilized liquid storage of hydrogen in the aerospace industry.

2.1.2 Gaseous Storage of hydrogen:

Compressed tanks and hollow spheres have been used for the gaseous storage of hydrogen. However, these materials are not practical when we consider the requirement by the Department of Energy for onboard applications (Energy, 2018). The key areas that make these technologies unsafe are kinetics, finances and safety risks. As such, material based storage has been researched intensively in this regard. In composite tanks, the hydrogen is stored at very high pressures and this means that a lot of money has to be invested on the material of construction to ensure that the integrity of the tank is not disturbed (Eberle et al., 2009). Though composite tanks are used commercially, their unsafety has prompted the need to search for more safe and reliable storage methods (Weidenthaler & Felderhoff, 2011). The figure 2-4 depicts a cross sectional area of the composite tanks and the material of construction thereof.

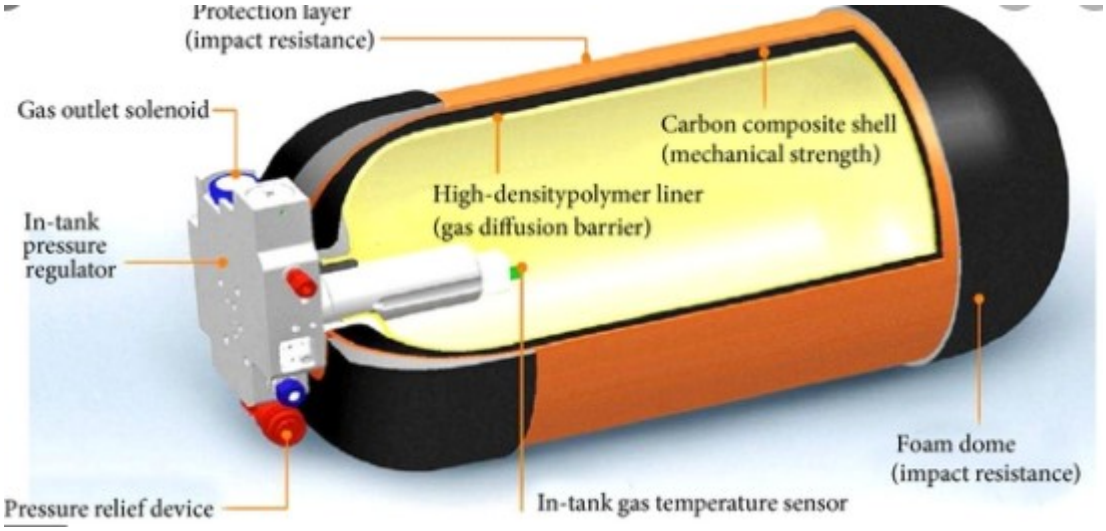

Figure 2-4: Cross sectional area of a composite tank used for hydrogen storage (von Helmolt et al., 2007)

2.1.3 Liquid Storage of hydrogen:

The storage of hydrogen in the liquid state is to cool down to cryogenic temperature at about –253 ℃ (Jiang et al., 2010)s. Liquid hydrogen is mostly utilized in application that demand high levels of purity. The maintenance of liquid hydrogen requires extra economic investment to maintain the hydrogen at cryogenic temperature and a complex technical to do this. Furthermore, the tanks that store liquid hydrogen have to be efficiently insulated in order to prevent the hydrogen from evaporating due to either conduction, convection, or radiation (Jiang et al., 2010). Liquid hydrogen however is report to have a higher energy density compared to gaseous hydrogen.

Various other techniques are used to store hydrogen as a liquid, such as sodium borohydrides solutions and rechargeable organic liquids (P. Hu et al., 2016; Nakamori et al., 2008). Borohydrides solutions have been researched because they allow for safe and controlled on-board regeneration of hydrogen. However, in the whole hydriding process $NaBO_2$ must be regenerated back to sodium borohydrides off board (Nakamori et al., 2008). This step may add extra costs and complicates the process when considering materials for practical on-board applications. The following reaction below is the ideal hydriding reactions:

$$NaBH_4\,(l) + 2H_2O\,(l) \longrightarrow 4H_2\,(g) + NaBO_2\,(s)$$

Rechargeable organic liquids are used to store hydrogen indirectly.

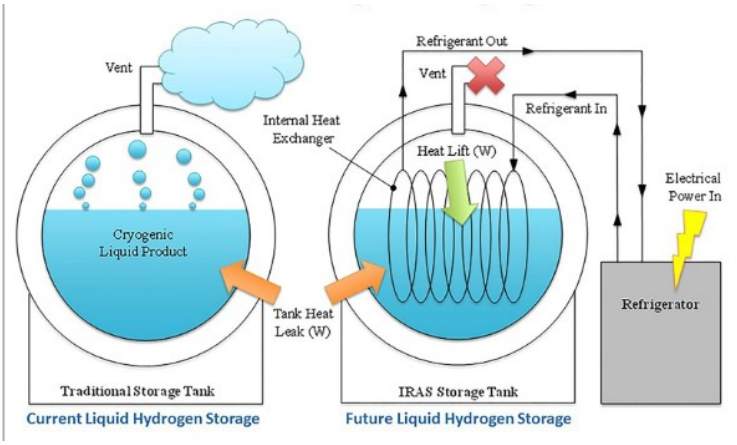

Figure 2-5: Liquid storage of hydrogen (Kennedy Space Center Cryogenic Test Laboratory, 2019)

2.1.4 Material Based storage of hydrogen

Material based storage of hydrogen in different materials as a solid has a wide range of possibilities to meet the requirements of the Department of Energy requirements. This is because storage in solid materials can reach volume and mass densities that acceptable as per the requirement of the DoE (Energy, 2018). The research surrounding hydrogen storage material is still wide open, because to date no material meets the requirements of the department of energy. Solid-state materials have to meet specific requirements to be utilized in the development of hydrogen storage technology for on-board applications (Bououdina et al., 2006b; Weidenthaler & Felderhoff, 2011). The key important factor is that these solid-state materials have to preserve its performance in terms of the total hydrogen capacity and the kinetics. The reaction of the solid-state hydrogen storage material with hydrogen has to be reversible even after the hydrogenation and dehydrogenation runs (Weidenthaler & Felderhoff, 2011)s. A lot other considerations have to be taken into account.

Either in solid-state materials, the hydrogen stored on the surface of these materials through adsorption (physisorption) or absorption (chemisorption) (Barthélémy, 2012). In physisorption, the hydrogen is bonded to the surface of the material as either a hydrogen molecule or hydrogen atoms through weak Van der Waals forces (Heine et al., 2004). In chemisorption, the hydrogen molecule is dissociated on the surface of the material into Hydrogen atoms and the hydrogen atoms are then incorporated in the lattice framework of the surface of the material (Barghi et al., 2014). Solid-state hydrogen storage materials are distinctly categorized according to these two classes. The figure 2-6 shows the chemisorption and physisorption process.

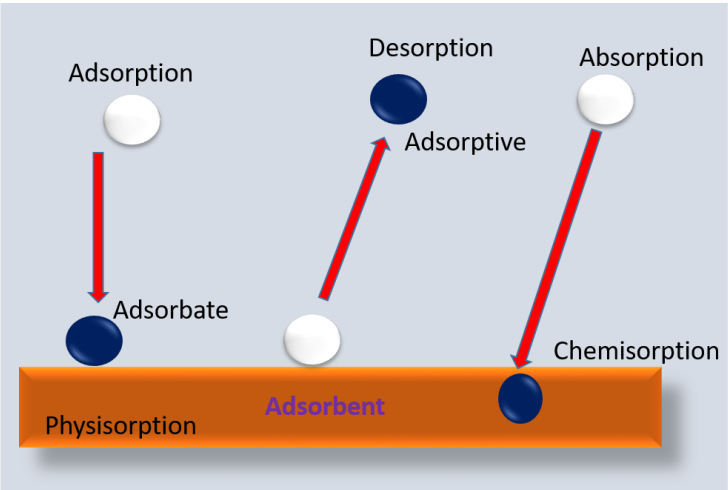

Figure 2-6: Physisorption and chemisorption (Adapted from Li et al., 2019)

In this work, physisorption material such as graphene was used as support and incorporated with different metals. Physisorption materials generally have a low hydrogen capacity but the kinetics of these materials is much faster compared to chemisorption material (Shams & Zhang, 2015). In an effort to improve the hydrogen capacity of these materials, various metals are incorporated to the graphene matrix. These materials are then referred to as hybrid materials.

2.2 GRAPHENE FOR HYDROGEN STORAGE

GRAPHENE BASED MATERIALS

Graphene, a 2D carbon allotrope that is positioned in a sp^2-bonded aromatic structure, has attracted a lot of attention for hydrogen storage application due to its low weight, cost and ability to be synthesized in large quantities (Venkatesan et al., 2015a). This two dimensional material configuration is formed by covalent bonds that are distributed on the hexagonal honeycomb lattice (M. Wang, 2012). Apart from this, graphene has intriguing properties which have made them applicable in these fields: energy storage, sensors, electrodes, field effect devices, nanocomposites and solar cells(M. Wang, 2012). The figure 2-7 the graphene 2D structure in sp^2 bonded aromatic structure.

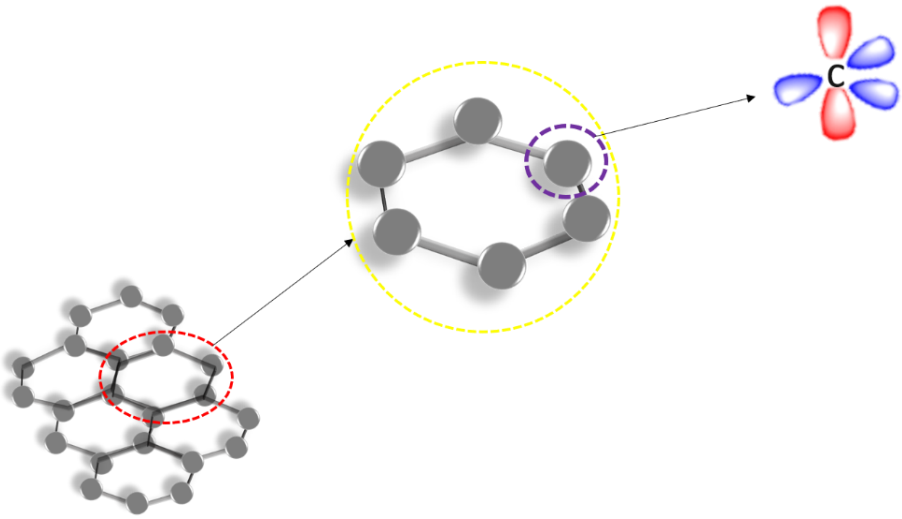

Figure 2-7: sp^2 Graphene sheet

The large surface area of graphene (2630 g^2m^{-1}) is tremendously beneficial for hydrogen storage. The interaction of graphene systems is based on instantaneous dipole-dipole induced forces because hydrogen is a non-polar molar(Pumera, 2011). A number of theoretical studies have been undertaken to explain the adsorption of hydrogen on the surface on graphene material and give more information on the pathway experimentalist need to take(Pumera, 2011)These studies have shown that the spatial distribution of adsorbed hydrogen on the surface of graphene is delocalized and that molecular hydrogen exhibits unrestricted lateral movement(Pumera, 2011).

2.2.1 Synthesis of graphene, graphene oxide and reduction thereof

The synthesis of graphene has been reported by different researchers and many methods have been reported on the exfoliation of graphite to graphene. The methods can be segregated to two main groups which are the top-down approach and bottom-up approach(Shams & Zhang, 2015). The top-down approach simply looks into breaking graphite layers to graphene while the bottom-up is the direct synthesis of graphene from carbon sources (Shams & Zhang, 2015). The most common and conventional methods of production of graphene come from the top-down approach method like the reduction of graphite oxide to graphene.

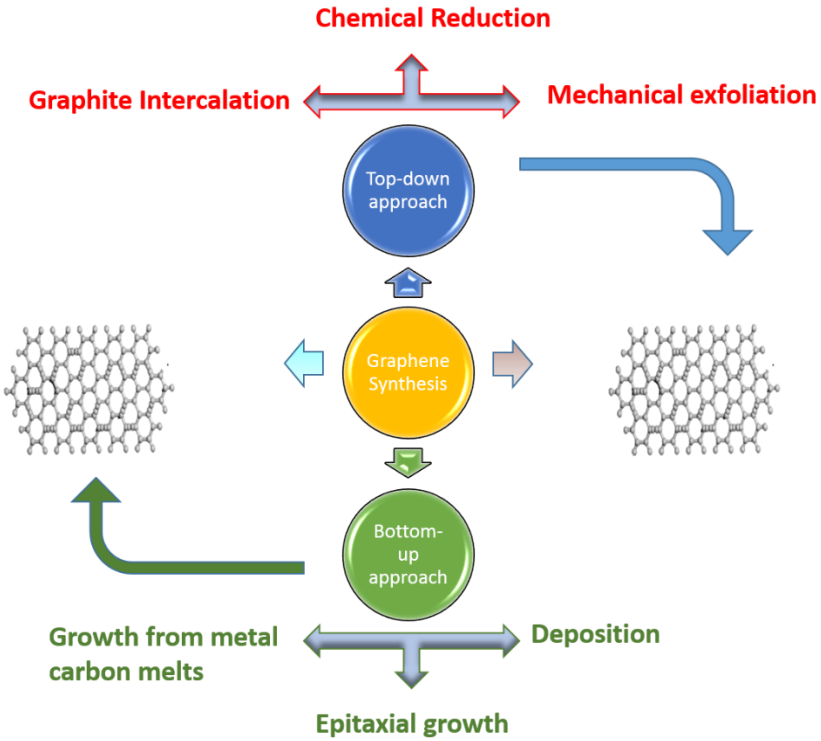

Figure 2-8: Top-down approach and bottom-up approach

2.2.1.1 Top-down Approach methods

2.1.1 Reduction of graphite oxide

The chemical reduction of precursor graphite oxide has been the most conventional and widely utilized method for the synthesis of graphene. This is due to the large production of graphene through this method. Graphene attained through this method is reportedly suitable for applications such as sensors, polymer fillers, battery electrodes, conductive paints and inks, energy storage, supercapacitors and so on(Choi et al., 2010; Shams & Zhang, 2015). Various methods have been reported on the oxidation of the precursor graphite oxide such as Modifies Hummers method, Brodie's method, Staudenmaier etc. (Poh et al., 2012). In these methods oxidants such concentrated sulphuric acid in conjunction with phosphoric acid, potassium permanganate and nitric acid are used (Poh et al., 2012).

Improved versions of these methods were also reported. Marcano et al. reported on a method that oxides the graphite better through increasing the potassium permangate and eliminating the nitric acid from the method (Marcano et al., 2010). Graphite oxide exfoliated through ultra-sonication results in the material being electrically insulative and thereby has to be reduced to restore its conductivity (Marcano et al., 2010). In that regard, graphite can be reduced either through chemical treatment or thermal treatment. The fast heating rate during the reduction process is the reported reason behind high yields of dispersed of carbon powder that are obtainable with this method. Various reductants such as hydrazine, hydroquinone, hydroxylamine, pyrrole, ammonia etc. have been used. Green reductant and less harmful reductants such as L-Ascorbic acid, coconut water, lemon juice, vinegar etc. have been reported also been reported. Recently, a novel reductant was reported by Gurunathan et al(Gurunathan et al., 2016). In this method, biomass obtained from lysogeny broth bacteria was used. The bacteria was nurtured for 21 hours at 37℃(Gurunathan et al., 2016). The subsequent graphene obtained had a high density of surface defects and it was of low purity.

2.1.2 Pyrolysis of graphene

The pyrolysis method has been deemed as a low cost method in which graphene can functionalized in low temperature. Furthermore graphene can be easily fabricated however the final graphene product comes with impurities in it and a large number of defects (Shams &

Zhang, 2015; Speyer et al., 2018). In the pyrolysis method, sodium and ethanol are used at a ratio of 1:1 and are heated for 72 hours to obtain the solid solvothermal product which is the precursor graphene (Speyer et al., 2018). The solvothermal product is then pyrolysed, washed with deionized water and then vacuum dried (Speyer et al., 2018). This method yields approximately 0.1 g per 1 ml of ethanol that has been utilized (Choucair et al., 2009).

2.1.3Mechanical Exfoliation

The mechanical exfoliation method is the most eminent method for producing high quality single layer graphene. This method is the first recognized method of producing graphene reported by Geim et al. (Geim & Novoselov, 2007). In this method graphite, which is a stacking of mono-atomic graphene layers by weak Van Der Waals forces with interlayer bond energy and distance of 2 eV/nm^2 and 3.34 Å, is exfoliated to give single layer graphene sheets (Geim & Novoselov, 2007). An external force of 300 Nn/μm^2 is needed during exfoliation to divide the graphite to graphene layers (Bhuyan et al., 2016). The uneven thickness of the graphene layers obtained by this method and high production cost render this method unattractive for mass production of graphene.

2.1.4 Sonication

In this method, ultrasonic energy is utilized to segregate the graphene layers that make up graphite. Sonication produces high quality graphene flakes and graphene produced through this method can be utilized in the field of transparent electrodes, sensors and polymer fillers (Hernandez et al., 2008; Jayasena & Subbiah, 2011; Mittal et al., 2015). However this method requires a lot of energy because sonication is the only source of energy and this issue may pose challenges when considering scaling up. A simple adjustment of the sonication is using a solvent to aid the process. The addition of the solvent in sonication process is utilized in different process to integrate graphene in composites and polymers such as vacuum filtration, drop casting, spray coating and solvent casting (Hernandez et al., 2008). Graphene is attained from graphite using the sonication process using a solvent NMP or TEA (Hernandez et al., 2008). The graphene obtained with the aid of a solvent has a yield of up 5% with an electrical conductivity of about 5000 S.m^{-1}.

Furthermore about 70% of the graphene obtained in this manner is 1 nm thick in size (W. Sun & Wang, 2014). When a solvent is used in the sonication process dispersing agents or surfactants are used to stop the graphene layers from re-stacking together again due to the weak Van Der Waals forces (Shams & Zhang, 2015). The sonication process aided by a solvent was used in the synthesis of a 3D hydrogel used as a support for BOD biosensor and microbe immobilization by Liu et al (L. Liu et al., 2015). In this process, the GO suspension was mixed with a neutral red solution and sonicated for 10 minutes and the solution was kept at 180 ℃ for 5 hours in an autoclave (L. Liu et al., 2015). The resultant hydrogel was dialyzed before characterization. Most of the graphene sheets obtained in this technique are conductive and transparent, as such this method has potential in solar panels and optoelectronics (L. Liu et al., 2015).

2.2.1.2 Bottom-up Approach

2.2.1 Chemical Vapour Deposition

Chemical vapour deposition has been widely reported because of its ease of scalability and its practicality. This method decomposes biomass material and hydrocarbon gasses such as hexane, ethylene etc. to cultivate graphene sheets on metallic catalysts at high temperatures ranging between 650 ℃ to 1000 ℃(Bhuyan et al., 2016). The graphene layers produced via this technique are high quality with low defects, they have a large surface area, are highly interconnected and are less than 75 cm (Min et al., 2014). This technique has been successfully utilized to synthesize nitrogen doped graphene, carbon nanosheets, boron-doped graphene and carbon nanofibers (Gilje et al., 2007; Reddy et al., 2010).

Chemical vapour depositions works by integrating and depositing volatile gas molecules in a reaction chamber where the material forms on the surface of the substrate while the unwanted gases are purged out (Bhuyan et al., 2016; Shams & Zhang, 2015). There are two main steps in the CVD process that are undertaken to form graphene films. The first step is the pyrolysis of the of the precursor material to form carbonaceous material on the surface of the substrate (Bhuyan et al., 2016). The pyrolysis step of the material on the substrate in this method prevents the formation of carbon clusters. High heat and a catalyst are essential in the carbon bond segregation step due to the high amount of energy required to break carbon bonds (C-H 413 kJ/mol, C=C 347 kJ/mol, C=C 839 kJ/mol and C-C 347 kJ/mol) (Bhuyan et al., 2016).

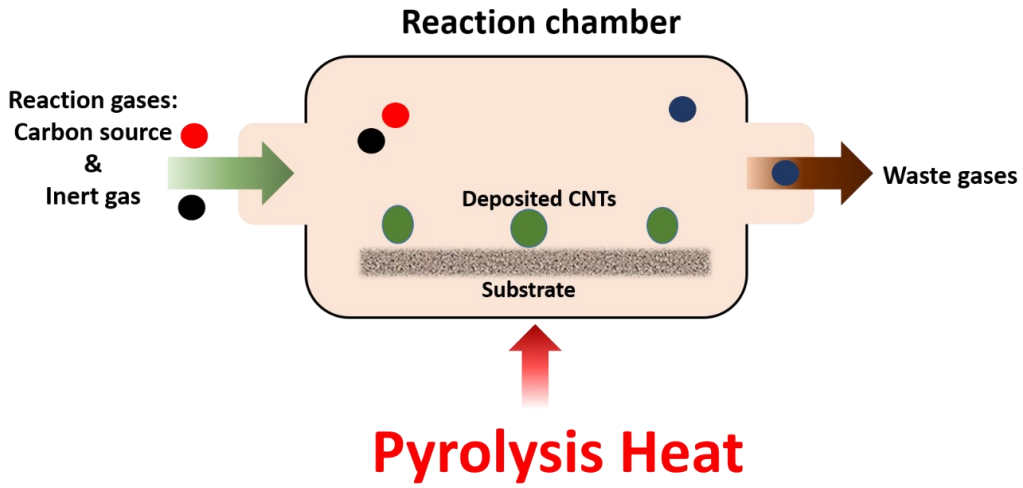

Figure 2-9: Chemical vapour deposition method (Adapted from ATL CVD Extreme Coating Solutions)

The second step in this process is the assembly of the dissociated carbon atoms onto a substrate in the presence of a catalyst (Bhuyan et al., 2016). This step is also heat intensive and forms a single layer structure on the substrate. Copper is known as a substrate that produces high quality graphene. The carbon atoms bond with the copper substrate and this provides a strong carbon-substrate interaction and this allows the single layer graphene to be easily formed (Bhuyan et al., 2016; Min et al., 2014). Graphene with fewer surface defects can be produced through treating the copper substrate. This treatment on the substrate rearranges the surface morphology of the substrate-catalyst (Min et al., 2014). The other CVD is referred to the plasma enhanced method where plasma assisted growth is introduced. Woehrl et.al. synthesized graphene using plasma assisted growth CVD (Woehrl et al., 2014). In the method, a hydrogen and methane gas mixture was used on a copper substrate. The graphene samples were then transmitted onto SiO_2 substrates (Woehrl et al., 2014). The single layer graphene attained contained some defects but it was of good quality. Bekduz et al. synthesized a defect free graphene using the plasma assisted growth method (Bekdüz et al., 2018). In this work, high quality copper foil was electropolished at 0.7 A for 1 min and 30s in an o-phosphoric acid solution. The foil was then dipped in deionized water and ethanol for a minute and blow dried with nitrogen (Bekdüz et al., 2018). The introduction of the sacrificial copper foil prevented the unintended vertical growth of graphene and the ion acceleration towards the substrate was avoided (Bekdüz et al., 2018).

2.2.2 Epitaxial Growth

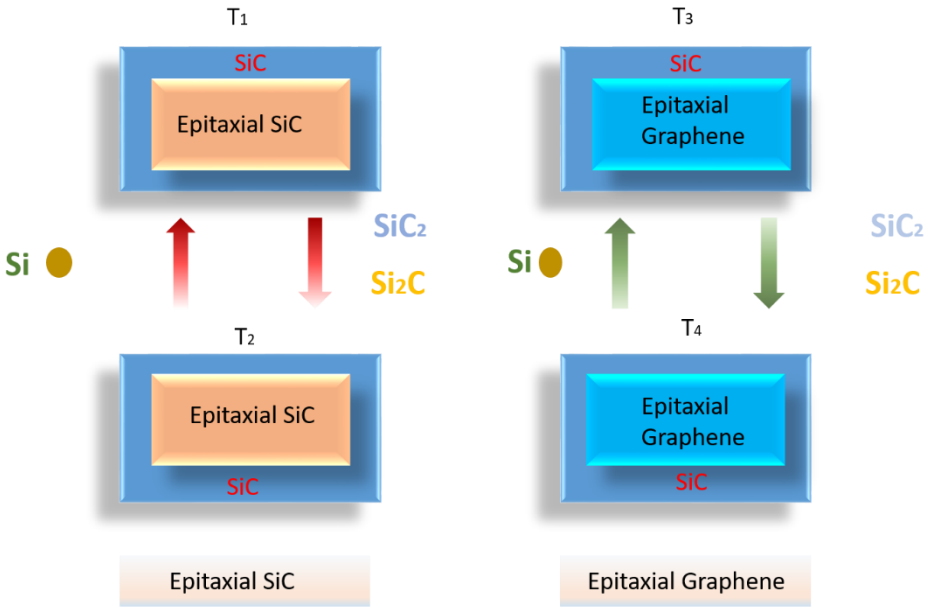

Figure 2-10: Epitaxial growth on a single crystalline substrate (Adapted from Yu et al., 2011)

Epitaxial growth is the deposition of a single crystalline substrate on a single crystalline substrate that produces an epitaxial film(Bhuyan et al., 2016). The epitaxial growth of graphene on a single crystalline silicon carbide surface is one of the most popular method of graphene synthesis.

The epitaxial growth has two main processes: hetero-epitaxial growth and homo-epitaxial growth. Hetero-epitaxial growth is when the film deposited on the substrate is different to the film and homo-epitaxial growth is when the film deposited on the substrate is of the same material (Bhuyan et al., 2016).The graphene is prepared through the thermal decomposition of silicon carbide, a hexagonal substrate, at temperatures ranging from 1200-1600 ℃ under inert conditions or under vacuum (Mishra et al., 2016). The high temperature treatment on the silicon substrate causes the silicon to sublimate, this causes the excessive carbon atoms to separate and formulate an sp^2 hybridized network which engenders the graphene grown on the substrate (Gupta et al., 2014; Mishra et al., 2016; Riedl et al., 2010). The growth rate of graphene on the face depends on the polar silicon carbide crystal face (Mishra et al., 2016). Graphene grows more rapidly on the carbon face than on the silicon face because on the carbon bigger domains of rotationally disordered, multi-layered graphene are produced (Gupta et al., 2014; Riedl et al., 2010). The ultra-high vacuum annealing on the silicon face leads to small domains and thus

the slow growth rate of graphene (Van Bommel et al., 1975). The graphene produced through the epitaxial growth on silicon carbide substrate lacks homogeneity however it is ideal to be utilized for electrical applications, in transistors and circuits, because the graphene films are very thin and are good for such applications (Gupta et al., 2014; Riedl et al., 2010). The silicon carbide substrate influences the carrier density of graphene, thickness and mobility.

2.3 GRAPHENE NANOCOMPOSITES

Nanocomposites, where nanocatalysis and nanostructure are combined, are the next research advancement of high performance of hydrogen storage materials. These materials have distinct functionalities due to the shorten diffusion distance, increased surface area and the multiplied grain boundaries(M. Wang, 2012).Graphene, graphene nanocomposites and its derivatives depict a promising potential for different applications such as automotive industry, aerospace, electronics and green energy. This is because graphene has intriguing thermal, mechanical and electrical properties(Bindumadhavan et al., 2013; M. Wang, 2012; Zhou & Szpunar, 2016).

A lot of studies have been done with graphene and nanocomposites thereof for the practical application in on-board application (Bindumadhavan et al., 2013; Ngqalakwezi et al., 2019; Pumera, 2011; Zhou & Szpunar, 2016). Graphene nanocomposites can be synthesized using various techniques. These include the self-assembly technique, solution mixing, sol-gel method, hydrothermal or the solvothermal method and other methods(C. Hu et al., 2013). Graphene nanocomposites have been preferred for hydrogen storage application mainly because of their light weight characteristic. Weight of the material is an important factor when considering the practical applications for hybrid cars according to the DoE standards. Graphene alone is a physisorbent material and does not take up a lot of hydrogen however its kinetics are interesting (Abe et al., 2019; Heine et al., 2004; C. Hu et al., 2013; Kartick et al., 2013; Ruse et al., 2018). The incorporation of metals on the graphene matrix enhances the functions of the system and improves the hydrogenation of this material to make it more appealing for practical use in hybrid cars (Nagar et al., 2017; Schniepp et al., 2006). Various metals have been used in this regard to improve the hydrogen uptake of the graphene nanocomposite. Zhou et al., synthesized a Ni/graphene nanocomposite and a Pd/graphene nanocomposite(Zhou et al., 2016). Ngqalakwezi et al. synthesized a novel Ca/graphene nanocomposite(Ngqalakwezi et al., 2019). The graphene nanocomposites can be used and applied in different industries for

hydrogen generation in the electrolysis process, in the photo degradation of pollutants, energy storage and other applications.

Furthermore, nanomaterials permit favorable charge, mass and heat transfer, these are added advantages when considering practical application of these materials for on board applications (Heine et al., 2004; Hummers & Offeman, 1958; Schniepp et al., 2006). In addition, nanomaterials assist in dimensional alteration of particular phase transitions and chemical reactions (M. Wang, 2012). Nanomaterials not only help and aid in the kinetics of hydrogen storage materials, but they also help to destabilize the thermodynamics of chemisorption materials.

2.3.1 Synthesis methods for graphene nanocomposites

2.3.1.1 Self-assembly technique

The self-assembly process is one of the primary techniques for synthesizing complex materials from molecules in macro, micro and nano scales (B. Li et al., 2010). In the bottom up techniques in nanotechnology, this method has been considered as one of the most effective (Thiruvengadathan et al., 2013). In this technique, molecules are utilized as precursor material for synthesizing graphene nanocomposites under environmentally conducive parameters. As such, graphene sheets prepared using the top down approach (mechanical and chemical exfoliation of graphite), can be utilizing as precursor material for the self-assembly technique (B. Li et al., 2010). The mechanism of self-assembly of graphene can be quite complex and understanding it necessitates the full understanding of the non-covalent and interlayer covalent interactions between graphene derivatives(Xu & Shi, 2011). These interactions include the dipole-dipole interactions, p-p interactions, van Der Waals forces and electrostatic forces. Non-covalent interactions in the self-assembly technique, aid the graphene in producing composites with novel functions and structures(Xu & Shi, 2011; Yuan et al., 2018).

These non-covalent interactions are active in various organic solvents and they permit homogenous dispersion for the anticipated self-assembly. Furthermore, graphene molecules allow for functionalization which is double sided and thus creates novel structural architecture with double-sized decoration of functional groups on the graphene sheet. These functional groups in principle, permit layer-by-layer coordinated assembly in a supramolecular manner(Yuan et al., 2018).

To take advantage of the characteristics of graphene at nanoscale in macro-sized devices, it is crucial to incorporate the graphene sheets into 3D micro-sized structures with better maneuver of the geometry and dimensionality of the material(Nine et al., 2017). Various methods have been reported for the fabrication of 3D porous structures, 2D thin films and 1 dimensional fiber-like molecules(Nine et al., 2017). For 3D porous structures these methods have been used; freeze casting self-assembly, breath figure 3D assembly, diffusion driven 3D self-assembly, 3D self-assembly through the hydrothermal process, pickering emulsions for 3D molecules and 3D assembly through chemical reduction(Chen & Yan, 2011; Deville, 2008; Putz et al., 2010; Xu et al., 2010).For 2D structures these methods have been used; vacuum assisted assembly, Rayleigh and Taylor instability and Marangoni effect self-assembly method, liquid-liquid interfacial 2D assembly method, evaporation induced 2D self-assembly method, electrophoretic method and the Langmuire-Blodgett method(Chavez-Valdez et al., 2013; F. Kim et al., 2010; Putz et al., 2010). For 1D fibers these methods have employed; 1D self-assembly self-intertwining method, direct drawing self-assembly method, electrophoretic 1D self-assembly and flow directed wet-spinning 1D self-assembly. All of these methods have been successfully employed to synthesize these different structures under various parameters(Jalili et al., 2013; X. Li et al., 2011; Yun et al., 2013).

2.3.1.2 Solution mixing method

The solution mixing method is one of the easiest method for the synthesis of polymer based graphene nanocomposites. The method comprises of three simple steps which are; the scattering of the filler, the polymer incorporation and the solvent removal through the distillation process or evaporation(Deshmukh et al., 2017). This method is also relatively cheap because it does not need the use of expensive equipment or expensive operative protocols, although it has a many steps(L.-C. Tang et al., 2019). Other advantages about this technique are; the method allows for good dispersion of thin particles because of the efficient fragmentation of organoclay agglomerates(L.-C. Tang et al., 2019; Vasudeo Rane et al., 2017). This in effect, generates greatly filled key batches that can later be mixed with pristine polymer through the melt compounding process. Furthermore this process allows for the production of highly exfoliated graphene nanocomposites that can be attained through mixing the physical coupling process with chemical reaction.

The synthesis step of this method typically involves dissipating a polymer in a solvent and suspending the filler in a different compatible solvent. Different solvents such as acetone, tetrahydrofuran (THF), toluene, chloroform, dimethylformamide and cyclohexane are utilized in this method(L.-C. Tang et al., 2019). As mentioned above, the solution blending generates ensures excellent exfoliation and dispersion of the filler within the elastomeric matrix(Chee et al., 2015).

Ultrasonication or high speed shear mixing are employed during the solution blending process to ensure the polymer solution and filler suspension are mixed thoroughly(Vasudeo Rane et al., 2017). This technique has been efficient in dispersing nanofillers irregardless of the polarity of the polymer. As much as this method has a lot of advantages, it does however have disadvantages as well. The main disadvantage of this technique is the thorough and efficient removal of solvents utilized during the process. Another major disadvantage is the scale up; the solvents utilized are very expensive and scaling up this process would pose financial difficulties and strains(L.-C. Tang et al., 2019; Vasudeo Rane et al., 2017). Lastly, the entire process involves a lot of steps and this can influence the subsequent outcome of the process.

A couple of researcher have used this method to synthesize graphene nanocomposites. Wang et.al. utilized Cu $(OH)_2$ composite sheets and reduced graphene oxide to synthesize thin micro layered structure of rGo-Cu powder(L. Wang et al., 2017). Tang et al, synthesized graphene nanosheets decorated with Ni nanoparticles utilizing the insitu chemical reduction method(X.-Z. Tang et al., 2013). The resulting nanocomposite after wet mixing electrolytic Cu to obtain Ni-graphene nanosheets/Cu nanocomposite, depicted interesting mechanical properties with a yield strength of 268 MPa and a high Young Modulus of 132 GPa(X.-Z. Tang et al., 2013). Furthermore, Zeng et al. incorporated Al powder in the GO suspension solution and ultrasonicated the mixture(Zeng et al., 2018). Al-graphene nanocomposite was obtained with a tensile strength of 255 MPa(Zeng et al., 2018). Li et.al, on the other hand used precursor organic graphite to synthesize graphene oxide using the Hummers method and decorated the graphene with Ni nanoparticles(N. Li et al., 2012). Ngqalakwezi et al, also synthesized Ca/graphene using the Improved Tours Method and chemical reduction the Ca ions on the surface of the GO(Ngqalakwezi et al., 2019).

The solution mixing method has been successfully employed to synthesis graphene nanocomposites.

2.3.1.3 Sol-gel method

The sol-gel method is also a simple method that allows the synthesis of a homogenous material that has great compositional controls(Lu et al., 2019). This method utilizes metal chlorides or metal alkoxides as the precursor material(C. Hu et al., 2013). The chlorides or alkoxides are treated through a series of condensation and hydrolysis reactions and later the cured composites are dried and calcined(C. Hu et al., 2013). A number of researchers have prepared graphene nanocomposites through the sol-gel method. A SiO_2/graphene nanocomposite was synthesized with good cyclic stability and spectacular specific capacitance of Fg^{-1} with a current density of 1 Ag^{-1} by Rezaei et al(Rezaei et al., 2016).Patil et al fabricated functional nanographene sheets using cobalt sulphide which had a good rate of cyclic ability and high reversible capacity ranging at about 466 $mAhg^{-1}$(Patil et al., 2017). Wang et al. fabricated TiC/graphene nanocomposite using the sol gel method(X. Wang et al., 2016). In this work, furfuryl alcohol was utilized as a carbon and this nanocomposite was synthesized for impact or shock absorptions(X. Wang et al., 2016). Furthermore, Sun et al synthesized various nanoparticles of platinum on sulfonated graphene and used them as anode electrocatalysts in direct ethanol fuel cell using the sol gel method(C.-L. Sun et al., 2015). The particles sized of the nanoparticles on the graphene surface ranged 1.7 nm to 13.9 nm. The sulfonic acid on the graphene improved the adsorption energy of platinum, this was observed through theoretical calculations(C.-L. Sun et al., 2015).

The synthesis work done using the sol gel method has proved to be effective in synthesis graphene nanocomposites and thin-film coating materials. This method required decreased reaction temperatures and it is also not complex to follow and conduct although the still challenges in the formation of the sol.

2.3.1.4 Hydrothermal method

The hydrothermal technique has been utilized to fabricate graphene nanocomposites using autoclaves under high pressures and temperatures. The first hydrothermal reaction was reported in 1845 by Schafhautl when he noticed the synthesis of quartz microcrystals from silicic acid(O'Hare, 2001). Since then, his method has been developed over the years by many other scientist and other novel synthesis method have also been reported. The hydrothermal technique is not restricted to the fabrication of common and advanced materials but it also

covers a wide range of interdisciplinary subdivisions in the sector of energy storage, simulating biohydrothermal and geothermal process and waste treatment(Feng & Li, 2017). In principle, the word hydrothermal, was initiated from geological sciences where it refers to a regime of water pressures and high temperatures(Byrappa & Yoshimura, 2001). Hydrothermal reaction traditionally involves water as catalyst and seldom, as a component of the solid phase during the synthesis at high pressures and temperatures. This technique has many advantages to it such as, excellent dispersion in water, the synthesis using this method is inexpensive due to instrumentation, environmentally friendly, one pot synthesis method, mild operation conditions and the material precursor are also inexpensive(A. D. Li & Liu, 2010).

Lee et al, discovered a novel hydrothermal fabrication route to synthesize graphene nanocomposites to improve the photocatalytic activity of TiO_2 under visible light. In the method, graphene was decorated or wrapped with TiO_2 particles(J. S. Lee et al., 2012).A high catalytic CeO_2/graphene was synthesized by Srivastava using the hydrothermal method(Srivastava et al., 2013). A Ag/graphene nanocomposite with exceptional electroconductivity was synthesized by Yang et al using the hydrothermal method. In this work, Yang et al, used a hydrazine reductant as a reducing agent and had control over the morphology and the size of Ag nanoparticle on the surface of graphene(J. Yang et al., 2011). Zhang et al, prepared a one pot method for the synthesis of Fe_2O_3–$Ni(OH)_2$/graphene nanocomposite. The nanocomposite had a good rate capability (at 100% retention), impressive cyclic stability (5 000 cycles) and elevated specific capacitance at approximately 857 F/g(Zhang et al., 2016). A ZnO/graphene nanocomposite was synthesized using the hydrothermal at lower temperature 90 and 80°C(Saravanakumar et al., 2013). The nanocomposites both displayed good catalytic activity during photocatalytic degradation against rhodamine-B dye(Saravanakumar et al., 2013).

2.4 KINETICS OF ENERGY STORAGE MATERIALS:

The issues of kinetics in energy storage has been tackled through many scientific interventions including ball milling, alloying, thin films and catalysis. However, to date, no material has satisfied the requirement for practical energy storage. The development of hybrid material such as graphene nanocomposites has been researched to fill in the gap. In energy storage, kinetics

of the materials considered for practical energy storage are complex and not easily understand and thus in this section, hydrogen storage kinetic models are reviewed.

2.4.1 Kinetic Models

The uptake of hydrogen and release of hydrogen in hydrogen storage systems is made of adsorption, penetration through the surface, internal diffusion and chemical reaction(Abd.Khalim Khafidz et al., 2016). Figure 2-11 shows the detailed steps of these processes:

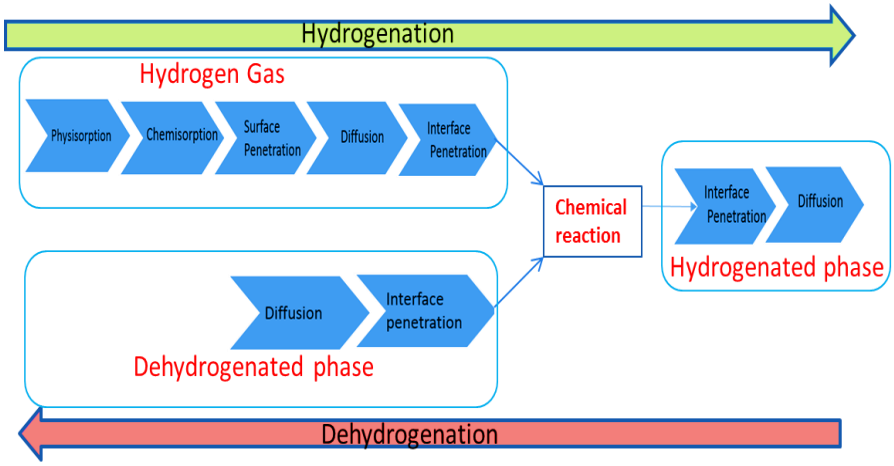

Figure 2-11: Hydrogenation and dehydrogenation steps

The two possible reaction modes for hydrogenation and dehydrogenation reactions are geometrical contraction and nucleation growth. These reaction routes are supported by theoretical and experimental research (Chou & Xu, 2007). Hydrogen storage kinetic models are thereby segregated according to these reaction routes. These models are founded on isothermal fitting and non-isothermal calculation analysis methods(Pang & Li, 2016). These methods help determine kinetic parameters and reaction modes this subsequently leads to a better understanding of the kinetic mechanism.

2.4.1.1 Geometrical Contraction Models

The basis of this model is that hydrogenation and dehydrogenation reactions transpire uniformly from the surface into the bulk of particle and the particles are uniform in size and

(1

shape(Pang & Li, 2016). The reaction fraction relationship between distances in particles of various shapes (sphere, plate and cylinder) is given by:

$$\varepsilon = 1 - \left(\frac{r}{r_0}\right)^d$$

Where d = dimensionality, r = lengths of the unreacted part, r_0= length of the whole particles, ε = reaction fraction.

The geometrical contraction models are derived from this relationship equation and assumptions of isothermal conditions(Booth, 1948; Carstensen, 1974; Crank 1916-, 1975; Khawam & Flanagan, 2006; N Koga & Criado, 1997; Nobuyoshi Koga & Criado, 1998). These are the geometrical contraction models:

2.4.1.2 Contracting volume model:

$$\frac{\mathrm{d_r}}{\mathrm{d_t}} = -\mathrm{k_{int}} \quad (2$$

$$1 - (1-\varepsilon)^{\frac{1}{d}} = \frac{k_{int}}{r_0} t = kt \quad (3$$

Where $\mathrm{k_{int}}$= rate constant (interface controlled reaction, k = generalized rate constant.

Jander Model:

$$\frac{\rho d_r}{d_t} = \frac{D\Delta C}{r_0 - r} \quad (4$$

$$\left[1 - (1-\varepsilon)^{\frac{1}{d}}\right]^2 = \frac{2D\Delta C}{r_0^2 \rho} t = kt \quad (5$$

Where ΔC = concentration difference, D = diffusion constant, ρ = density

2.4.1.3 Ginstling-Brounshtein model

$$\frac{\rho d_r}{d_t} = \frac{D\Delta C}{r \ln\left(\frac{r_0}{r}\right)} \quad (6$$

$$(1-\varepsilon)\ln(1-\varepsilon) + \varepsilon = \frac{4D\Delta C}{r_0^2 \rho} t = kt \quad (7$$

For two dimensional cylinder:

$$\frac{\rho d_r}{d_t} = \frac{D\Delta C r_0}{(r_0 - r) r} \quad (8$$

$$1 - \frac{2}{3}\varepsilon - (1-\epsilon)^{\frac{2}{3}} = \frac{2D\Delta C}{r_0^2 \rho} t = kt \quad (9$$

For three dimensional cylinder:

2.4.1.4 Valensi-Carter Model:

$$\frac{\rho d_r}{d_t} = \frac{D\Delta C}{r - \frac{r^2}{\left(Zr_0^3 + r^3(1-z)\right)^{\frac{1}{3}}}} \quad (10$$

$$\frac{z - (1 + (z-1)\varepsilon)^{\frac{2}{3}} - (z-1)(1-\varepsilon)^{\frac{2}{3}}}{z-1} = \frac{2D\Delta C}{r_0^2 \rho} t = kt \quad (11)$$

Where z = volume ratio of product to reactant

The *contracting volume model* assumes that rate of hydrogenation is regulated by the interface process. This model is deemed as the simplest method in geometrical contraction volume models because no other assumptions are made. Through this method the dimensionality and a generalized constant can be obtained through fitting a simplified isothermal curve(Carstensen, 1974; Pang & Li, 2016). Bösenberg et al.proved that LiH-MgB_2 with transition metal deposits such as Titanium and Vanadium follow the CV model very well because it is interface control(Bösenberg et al., 2010).

The *Jander Model* however is readily used for diffusion regulated reactions. The two important assumptions made in this model are: 1. the volume of hydrogen storage materials remains constant before and after absorption and desorption reactions 2. Two and three dimensional diffusion are deemed as one meaning the interface area remains constant for diffusion(Booth, 1948; Jander, 1927). However these assumptions are not always applicable for hydrogen storage materials because the volume of some materials increases during the uptake of hydrogen and decrease with the release of it. In contrast Shao et al.found that nanocrystalline Mg doped with Ti under 1Mpa of H_2 follow this model very well(Shao et al., 2012).

According to Ginstling et al and Crank the Ginstling-Brounshtein model develops the Jander Model using Fick's Law for radial diffusion for 2D and 3D spheres(Crank 1916-, 1975; Ginstling A, 1950). Although intricate; this method is regarded as a more accurate model due to its consideration of the variance in interface area due to diffusion. Chaudhary et al.reported that MgH_2-Si synthesized by ball milling, cryomilling and ultrasonicating produces desorption curves which follow this model well (Chaudhary et al., 2015). The Valensi-Carter model is an

extension of the G-B model which regards the change in volume in hydrogen storage materials during adsorption and desorption. This model is reportedly the most accurate in geometrical contraction model however it has not yet been applied to hydrogen storage materials(Carter R.E, 1967; Shimada et al., 1999; Valensi G, 1936).

2.4.1.5 Nucleation-growth impingement Models

The Nucleation growth impingement models are generally described as the Johnson-Mehl-Avrami-Kolomogorov (JMAK) models. The JMAK models define hydrogenation and dehydrogenation reactions as three synchronized processes: nucleation, growth and impingement(M. Avrami, 1941; Melvin Avrami, 1939, 1940; Johnson W.A., 1939; Kolmogorov A.N, 1937; Pang et al., 2016; Valensi G, 1936). Figure 2-12 is a diagram showing the three processes:

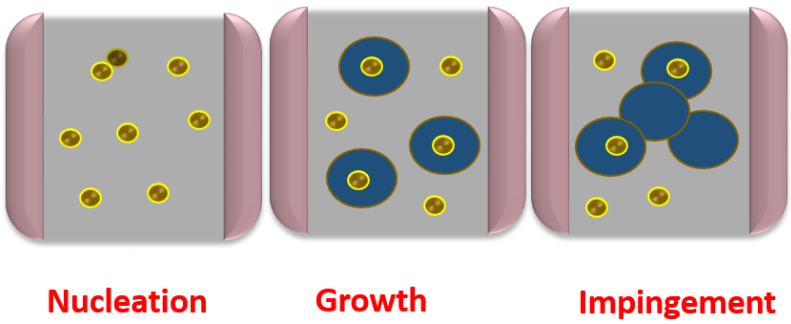

Figure 2-12: Nucleation, growth and impingement

This model is founded on the basis of; 1. Enhancing nucleation, growth and impingement 2. Solving analytical problems(Pang et al., 2016). This model is given as:

$$\varepsilon = F\left[\int_0^t I(r)V(r)d_r\right] \quad (13$$

Where I = nucleation module, r = nucleation rate, F = impingement module defining the relationship between real reaction fraction and extended reaction fraction, V= Growth module (Kempen et al., 2002).

A variation of this equation, classical JMAK (C-JMAK), which takes into consideration interface controlled growth and diffusion controlled is given by:

(14)

$$V_{(r)} = \left[G_0 \int_r^t exp\left(\frac{-\Delta E_g}{RT}\right) d\eta \right]^{\frac{d}{m}}$$

Where ΔE_g= activation energy for growth, G_0= intrinsic growth rate, m = growth mode parameter, $\frac{d}{m}$ = growth inde.

The C-JMAK model defines absorption and desorption of nucleation, growth and impingement very well. Nucleation in this regard refers to site saturation, growth mode to interface and diffusion controlled sites and impingement to randomly scattered nuclei isotropic growth(CHRISTIAN, 2002). The Avrami exponent of the desorption reaction of $NaAlH_4$ doped with Titanium was determined using this model and was found to be 3. This proved that the three dimensional interface process is the rate controlling step. Pang et al. however discovered that the actual nucleation modes propagate continuous nucleation and are not restricted to linear continuous nucleation and site saturation an assumption which this model is founded on(F. Liu et al., 2007; Pang et al., 2016). This inhibits the practical application of this model for progressive hydrogen storage applications.

Analysis methods are used to obtain kinetic mechanism by determining and comparing the best fit models and kinetic parameters that go along with it. The two most used analysis methods is isothermal fitting and non-isothermal fitting(Gross K.J., 2012). However based on literature reviewed understanding the kinetic mechanisms for hydrogen storage materials can be difficult because the analysis have downfalls which may result in misunderstanding of the kinetic mechanisms entirely (Pang & Li, 2016).

2.5 THERMODYNAMICS OF HYDROGEN STORAGE MATERIALS

Thermodynamic properties such as temperature and pressure play a vital part in the effective application of hydrogen storage materials. These two properties together with the hydrogen molecule interaction with the nanostructure and hydrogen molecule to hydrogen molecule interaction affect the gravity and volumetric capacities of hydrogen storage materials (Song et al., 2012). Hydrogen storage material thermodynamic models are founded on energy and mass balance equations derived from principles of energy and mass conservation of thermodynamics (Song et al., 2012). From an engineering perspective the effective heat removal during

adsorption of hydrogen and effective heat supply during recovery of the adsorbed hydrogen molecules, are areas of interest. Dedrick et al. reported that 0.7 MW is a required to for cooling during hydrogen uptake .(Dedrick et al., 2009) His work highlighted the importance of equally having an efficient storage system alongside an efficient cooling system for practical application of hydrogen. A proper design of a hydrogen storage materials would require thorough knowledge of heat of reaction; equilibrium pressure vs temperature (thermodynamic properties), reaction kinetics and thermal conductivity; heat capacity (thermal properties) (Dedrick et al., 2009; Pang & Li, 2016; Song et al., 2012).

2.5.1 Heat of Reaction

The heat of reaction is a thermodynamic property that is associated with the amount of heat that is released or the amount of heat that is consumed. The heat of reaction is also known as the Enthalpy of reaction and divided into two groups, exothermic reaction and endothermic reaction (Dedrick, 2008). The exothermic heat of reaction is straightly proportional to the heat waste generated and this in turn affects the heat exchanger volume. The heat exchanger volume is dependent on the materials heat capacity, heat released in a reaction and the needed temperatures for both reactants and product (Song et al., 2012). Semelsberger et al. reported that escalated exothermic reaction enthalpy yields a greater adiabatic temperature which increases the dimensions (length and mass) of heat exchangers (Semelsberger & Borup, 2005). His work recorded the three steps which are undertaken to calculate the influence of heat of reaction on the mass of radiators in hydrogen storage systems: 1. Calculation of the adiabatic temperature 2. The time it takes for the gas and spent fuel heat exchangers to bring their products to the required temperatures and lastly the total volume and mass of the heat exchangers (Semelsberger & Borup, 2005). In addition it has been found in these calculations that the hydrogen mass flow rate is inversely proportional to the gravimetric storage capacity of hydrogen storage materials. Consequently decreased gravimetric capacities lead to the achievement of desired flowrate of the storage materials in the heat exchanger and increased flowrate need longer heat exchangers to bring the temperature to the desired temperature. In essence hydrogen storage material with higher hydrogen capacities useful in decreasing heat exchanger volume or mass (Dedrick et al., 2009; Semelsberger & Borup, 2005).

Troy et al. did further analysis of endothermic heat of reactions in hydrogen systems. Endothermic heat of reaction affect the on board effectiveness of hydrogen storage systems

due to the parasitic heat loss accompanying them. The analysis he performed considered the sensible heat of the reactor, sensible heat of the storage media, endothermic heat of reaction and the number of vehicles start-ups. The DoE requirements of an on board system efficiency of 90% is met when the system is adiabatic with full heat recovery, this means the only parasitic loss considered is the endothermic heat of reaction. The maximum allowed endothermic reaction in these systems must be 24 kJ/mol H_2.

Avdeenkov et al. developed a thermodynamic model for hydrogen storage in carbon nanostructures (Avdeenkov et al., 2015). The interaction of nanostructured material with hydrogen molecule is of paramount importance in hydrogen storage systems. Better methods of calculating these interactions such as the calculation of potential energy surface in light of effective pair interaction have been explored (Avdeenkov et al., 2015)s. The effective pair interactions are attained from model energy calculations of relevant molecular systems. Alonso et al. developed a thermodynamic model which is appropriate for improving the topology of nanostructure material and their geometry (Alonso et al., 2013) . Current theoretical methods that define the non-ideality such Monte Carlo and Density functional theory are not simple to verify and can be numerically costly.

CONCLUSION

There is a range of materials that have attracted many researchers for progressive hydrogen storage research. In this chapter, hydrogen storage challenges were reviewed, hydrogen storage materials such as graphene, graphene synthesis and graphene nanocomposites were reviewed intensely. The kinetic and thermodynamic behavior related to these materials was reviewed. Upon the review of the kinetics and thermodynamics, it was concluded that the success in solving kinetic and thermodynamics issues would lead to the successful application of hydrogen storage materials. More work needs to be done in terms of the practical application of these material for energy storage, because to date, no material meets the standards for practical application in energy storage.

REFERENCES

Abd.Khalim Khafidz, N. Z., Yaakob, Z., Lim, K. L., & Timmiati, S. N. (2016). The kinetics of lightweight solid-state hydrogen storage materials: A review. *International Journal of Hydrogen Energy*, *41*(30), 13131–13151. https://doi.org/https://doi.org/10.1016/j.ijhydene.2016.05.169

Abe, J. O., Popoola, A. P. I., Ajenifuja, E., & Popoola, O. M. (2019). Hydrogen energy, economy and storage: Review and recommendation. *International Journal of Hydrogen Energy*, *44*(29), 15072–15086. https://doi.org/10.1016/J.IJHYDENE.2019.04.068

Abulizi, A., Okitsu, K., & Zhu, J.-J. (2014). Ultrasound assisted reduction of graphene oxide to graphene in l-ascorbic acid aqueous solutions: Kinetics and effects of various factors on the rate of graphene formation. *Ultrasonics Sonochemistry*, *21*(3), 1174–1181. https://doi.org/https://doi.org/10.1016/j.ultsonch.2013.10.019

Alonso, J. A., Cabria, I., & López, M. J. (2013). Simulation of hydrogen storage in porous carbons. *Journal of Materials Research*, *28*(4), 589–604. https://doi.org/DOI: 10.1557/jmr.2012.370

Andersson, J., & Grönkvist, S. (2019). Large-scale storage of hydrogen. *International Journal of Hydrogen Energy*, *44*(23), 11901–11919. https://doi.org/10.1016/J.IJHYDENE.2019.03.063

Avdeenkov, A. V, Bodrenko, I. V, Bessarabov, D. G., Bibikov, A. V, Nikolaev, A. V, Taran, M. D., Tokarev, A., & Tkalya, E. V. (2015). Thermodynamical model for hydrogen storage capacity in carbon nanostructures. *International Journal of Hydrogen Energy*, *40*(11), 4184–4193. https://doi.org/https://doi.org/10.1016/j.ijhydene.2015.01.129

Avrami, M. (1941). Kinetics of Phase Change III: Granulation, Phase Change, and Microstructure. *J. Chem. Phys., 9*, 177–184.

Avrami, Melvin. (1939). Kinetics of Phase Change. I General Theory. *The Journal of Chemical Physics*, *7*(12), 1103–1112. https://doi.org/10.1063/1.1750380

Avrami, Melvin. (1940). Kinetics of Phase Change. II Transformation-Time Relations for Random Distribution of Nuclei. *The Journal of Chemical Physics*, *8*(2), 212–224. https://doi.org/10.1063/1.1750631

Balandin, A., Ghosh, S., Bao, W., Calizo, I., Teweldebrhan, D., Miao, F., & Lau, J. (2008). Superior Thermal Conductivity of Single-Layer Graphene. *Nano Letters*, *8*, 902–907. https://doi.org/10.1021/nl0731872

Barthelemy, H., Weber, M., & Barbie, F. (2017). Hydrogen storage: Recent improvements and industrial perspectives. International Journal of Hydrogen Energy, 42(11), 7254-7262

Bekdüz, B., Beckmann, Y., Mischke, J., Twellmann, J., Mertin, W., & Bacher, G. (2018). Graphene growth through a recrystallization process in plasma enhanced chemical vapor deposition. *Nanotechnology*, *29*(45), 455603. https://doi.org/10.1088/1361-6528/aadd74

Bhuyan, M. S. A., Uddin, M. N., Islam, M. M., Bipasha, F. A., & Hossain, S. S. (2016). Synthesis of graphene. *International Nano Letters*, *6*(2), 65–83. https://doi.org/10.1007/s40089-015-0176-1

Bindumadhavan, K., Srivastava, S., & Srivastava, I. (2013). Green Synthesis of Graphene. *Journal of Nanoscience and Nanotechnology*, *13*, 4320–4324. https://doi.org/10.1166/jnn.2013.7461

Booth, F. (1948). A note on the theory of surface diffusion reactions. *Transactions of the Faraday Society*, *44*(0), 796–801. https://doi.org/10.1039/TF9484400796

Bösenberg, U., Kim, J. W., Gosslar, D., Eigen, N., Jensen, T. R., Von Colbe, J. M. B., Zhou, Y., Dahms, M., Kim, D. H., Günther, R., Cho, Y. W., Oh, K. H., Klassen, T., Bormann, R., & Dornheim, M. (2010). Role of additives in LiBH 4–MgH 2 reactive hydride composites for sorption kinetics. *Acta Materialia*, *58*(9), 3381–3389.

Bououdina, M., Grant, D., & Walker, G. (2006a). Review on hydrogen absorbing materials—structure, microstructure, and thermodynamic properties. *International Journal of Hydrogen Energy*, *31*(2), 177–182.

https://doi.org/https://doi.org/10.1016/j.ijhydene.2005.04.049

Bououdina, M., Grant, D., & Walker, G. (2006b). Review on hydrogen absorbing materials—structure, microstructure, and thermodynamic properties. *International Journal of Hydrogen Energy*, *31*(2), 177–182. https://doi.org/10.1016/J.IJHYDENE.2005.04.049

Byrappa, K., & Yoshimura, M. (2001). *2 - History of Hydrothermal Technology* (K. Byrappa & M. B. T.-H. of H. T. Yoshimura (eds.); pp. 53–81). William Andrew Publishing. https://doi.org/https://doi.org/10.1016/B978-081551445-9.50003-9

Callini, E., Aguey-Zinsou, K.-F., Ahuja, R., Ares, J. R., Bals, S., Biliškov, N., Chakraborty, S., Charalambopoulou, G., Chaudhary, A.-L., Cuevas, F., Dam, B., de Jongh, P., Dornheim, M., Filinchuk, Y., Grbović Novaković, J., Hirscher, M., Jensen, T. R., Jensen, P. B., Novaković, N., … Montone, A. (2016). Nanostructured materials for solid-state hydrogen storage: A review of the achievement of COST Action MP1103. *International Journal of Hydrogen Energy*, *41*(32), 14404–14428. https://doi.org/https://doi.org/10.1016/j.ijhydene.2016.04.025

Carstensen, J. T. (1974). Stability of Solids and Solid Dosage Forms. *Journal of Pharmaceutical Sciences*, *63*(1), 1–14. https://doi.org/https://doi.org/10.1002/jps.2600630103

Carter R.E. (1967). Kinetic model for solid-state reactions. *J Chem Phys*, *34*, 2010–2015.

Chaudhary, A.-L., Sheppard, D. A., Paskevicius, M., Pistidda, C., Dornheim, M., & Buckley, C. E. (2015). Reaction kinetic behaviour with relation to crystallite/grain size dependency in the Mg–Si–H system. *Acta Materialia*, *95*, 244–253. https://doi.org/https://doi.org/10.1016/j.actamat.2015.05.046

Chavez-Valdez, A., Shaffer, M. S. P., & Boccaccini, A. R. (2013). Applications of Graphene Electrophoretic Deposition. A Review. *The Journal of Physical Chemistry B*, *117*(6), 1502–1515. https://doi.org/10.1021/jp3064917

Chee, W. K., Lim, H. N., Huang, N. M., & Harrison, I. (2015). Nanocomposites of

graphene/polymers: a review. *RSC Advances*, *5*(83), 68014–68051. https://doi.org/10.1039/C5RA07989F

Chen, W., & Yan, L. (2011). In situ self-assembly of mild chemical reduction graphene for three-dimensional architectures. *Nanoscale*, *3*(8), 3132–3137. https://doi.org/10.1039/C1NR10355E

Choi, W., Lahiri, I., Seelaboyina, R., & Kang, Y. S. (2010). Synthesis of Graphene and Its Applications: A Review. *Critical Reviews in Solid State and Materials Sciences*, *35*(1), 52–71. https://doi.org/10.1080/10408430903505036

Chong, S. W., Lai, C. W., & Abdul Hamid, S. B. (2015). Green preparation of reduced graphene oxide using a natural reducing agent. *Ceramics International*, *41*(8), 9505–9513. https://doi.org/https://doi.org/10.1016/j.ceramint.2015.04.008

Chou, K.-C., & Xu, K. (2007). A new model for hydriding and dehydriding reactions in intermetallics. *Intermetallics*, *15*(5), 767–777. https://doi.org/https://doi.org/10.1016/j.intermet.2006.10.004

Choucair, M., Thordarson, P., & Stride, J. A. (2009). Gram-scale production of graphene based on solvothermal synthesis and sonication. *Nature Nanotechnology*, *4*(1), 30–33. https://doi.org/10.1038/nnano.2008.365

CHRISTIAN, J. W. (2002). *CHAPTER 10 - The Classical Theory of Nucleation* (J. W. B. T.-T. T. of T. in M. and A. CHRISTIAN (ed.); pp. 422–479). Pergamon. https://doi.org/https://doi.org/10.1016/B978-008044019-4/50014-3

Crank 1916-, J. (John). (1975). *The mathematics of diffusion / by J. Crank*. Clarendon Press.

De Silva, K. K. H., Huang, H.-H., & Yoshimura, M. (2018). Progress of reduction of graphene oxide by ascorbic acid. *Applied Surface Science*, *447*, 338–346. https://doi.org/https://doi.org/10.1016/j.apsusc.2018.03.243

DEDRICK, D. E. (2008). 4 - Solid-state hydrogen storage system design. In G. B. T.-S.-S. H.

S. Walker (Ed.), *Woodhead Publishing Series in Electronic and Optical Materials* (pp. 82–103). Woodhead Publishing. https://doi.org/https://doi.org/10.1533/9781845694944.1.82

Deville, S. (2008). Freeze-Casting of Porous Ceramics: A Review of Current Achievements and Issues. *Advanced Engineering Materials*, *10*(3), 155–169. https://doi.org/10.1002/adem.200700270

Diana C. Tranca & Gotthard Seifert. (2016). A First-Principles Study of Metal-Decorated Graphene Nanoribbons for Hydrogen Storage. *De Gruyter*, *230*, 791-808,.

Dutta, S., & Pati, S. K. (2010). Novel properties of graphene nanoribbons: a review. *Journal of Materials Chemistry*, *20*(38), 8207–8223. https://doi.org/10.1039/C0JM00261E

Eberle, U., Felderhoff, M., & Schüth, F. (2009). Chemical and Physical Solutions for Hydrogen Storage. *Angewandte Chemie International Edition*, *48*(36), 6608–6630. https://doi.org/10.1002/anie.200806293

Energy, D. of. (2018). *Hydrogen Storage*.

Feng, S.-H., & Li, G.-H. (2017). *Chapter 4 - Hydrothermal and Solvothermal Syntheses* (R. Xu & Y. B. T.-M. I. S. C. (Second E. Xu (eds.); pp. 73–104). Elsevier. https://doi.org/https://doi.org/10.1016/B978-0-444-63591-4.00004-5

Geim, A. K., & Novoselov, K. S. (2007). The Rise of Graphene. *Nat. Mater.*, *6*, 183.

Geng, J., Kong, B.-S., Yang, S. B., & Jung, H.-T. (2010). Preparation of graphene relying on porphyrin exfoliation of graphite. *Chemical Communications*, *46*(28), 5091–5093. https://doi.org/10.1039/C001609H

Ginstling A, B. B. (1950). Concerning the diffusion kinetics of reactions in spherical particles. *Journal of Applied Chemistry*, *23*, 1327–1338.

Gross K.J., C. K. R. (2012). *Recommended best practices for the characterization of storage properties of hydrogen storage materials*.

Gupta, B., Notarianni, M., Mishra, N., Shafiei, M., Iacopi, F., & Motta, N. (2014). Evolution of epitaxial graphene layers on 3C SiC/Si (111) as a function of annealing temperature in UHV. *Carbon*, *68*, 563–572. https://doi.org/https://doi.org/10.1016/j.carbon.2013.11.035

Gurunathan, S., Park, J., Choi, Y., jae woong, H., & Kim, J.-H. (2016). Synthesis of Graphene Oxide-Silver Nanoparticle Nanocomposites: An Efficient Novel Antibacterial Agent. *Current Nanoscience*, *12*, 762–773. https://doi.org/10.2174/1573413712666160721143424

Heine, T., Zhechkov, L., & Seifert, G. (2004). Hydrogen storage by physisorption on nanostructured graphite platelets. *Physical Chemistry Chemical Physics*, *6*(5), 980–984. https://doi.org/10.1039/B316209E

Hernandez, Y., Nicolosi, V., Lotya, M., Blighe, F. M., Sun, Z., De, S., McGovern, I. T., Holland, B., Byrne, M., Gun'Ko, Y. K., Boland, J. J., Niraj, P., Duesberg, G., Krishnamurthy, S., Goodhue, R., Hutchison, J., Scardaci, V., Ferrari, A. C., & Coleman, J. N. (2008). High-yield production of graphene by liquid-phase exfoliation of graphite. *Nature Nanotechnology*, *3*(9), 563–568. https://doi.org/10.1038/nnano.2008.215

Hu, C., Lu, T., Chen, F., & Zhang, R. (2013). A brief review of graphene–metal oxide composites synthesis and applications in photocatalysis. *Journal of the Chinese Advanced Materials Society*, *1*(1), 21–39. https://doi.org/10.1080/22243682.2013.771917

Hua, T. Q., Ahluwalia, R. K., Peng, J.-K., Kromer, M., Lasher, S., McKenney, K., Law, K., & Sinha, J. (2011). Technical assessment of compressed hydrogen storage tank systems for automotive applications. *International Journal of Hydrogen Energy*, *36*(4), 3037–3049. https://doi.org/https://doi.org/10.1016/j.ijhydene.2010.11.090

Jander, W. (1927). Reaktionen im festen Zustande bei höheren Temperaturen. Reaktionsgeschwindigkeiten endotherm verlaufender Umsetzungen. *Zeitschrift Für*

Anorganische Und Allgemeine Chemie, *163*(1), 1–30. https://doi.org/10.1002/zaac.19271630102

Jayasena, B., & Subbiah, S. (2011). A novel mechanical cleavage method for synthesizing few-layer graphenes. *Nanoscale Research Letters*, *6*(1), 95. https://doi.org/10.1186/1556-276X-6-95

Jhi, S.-H., Kwon, Y.-K., Bradley, K., & Gabriel, J.-C. P. (2004). Hydrogen storage by physisorption: beyond carbon. *Solid State Communications*, *129*(12), 769–773. https://doi.org/https://doi.org/10.1016/j.ssc.2003.12.032

Jiang, H.-L., Singh, S. K., Yan, J.-M., Zhang, X.-B., & Xu, Q. (2010). Liquid-Phase Chemical Hydrogen Storage: Catalytic Hydrogen Generation under Ambient Conditions. *ChemSusChem*, *3*(5), 541–549. https://doi.org/10.1002/cssc.201000023

Johnson W.A., M. R. F. (1939). Reaction kinetics in processes of nucleation and growth. *Trans AIME*, *135*, 396–415.

Kempen, A. T. W., Sommer, F., & Mittemeijer, E. J. (2002). Determination and interpretation of isothermal and non-isothermal transformation kinetics; the effective activation energies in terms of nucleation and growth. *Journal of Materials Science*, *37*(7), 1321–1332. https://doi.org/10.1023/A:1014556109351

Khawam, A., & Flanagan, D. R. (2006). Solid-State Kinetic Models: Basics and Mathematical Fundamentals. *The Journal of Physical Chemistry B*, *110*(35), 17315–17328. https://doi.org/10.1021/jp062746a

Kim, F., Cote, L. J., & Huang, J. (2010). Graphene Oxide: Surface Activity and Two-Dimensional Assembly. *Advanced Materials*, *22*(17), 1954–1958. https://doi.org/10.1002/adma.200903932

Kim, K. S., Zhao, Y., Jang, H., Lee, S. Y., Kim, J. M., Kim, K. S., Ahn, J.-H., Kim, P., Choi, J.-Y., & Hong, B. H. (2009). Large-scale pattern growth of graphene films for

stretchable transparent electrodes. *Nature*, *457*(7230), 706–710. https://doi.org/10.1038/nature07719

Koga, Nobuyoshi, & Criado, J. M. (1998). Kinetic Analyses of Solid-State Reactions with a Particle-Size Distribution. *Journal of the American Ceramic Society*, *81*(11), 2901–2909. https://doi.org/10.1111/j.1151-2916.1998.tb02712.x

Kolmogorov A.N. (1937). On the statistical theory of the crystallization of metals. *Bull Acad Sci USSR Math Ser*, *1*, 355–359.

Kosynkin, D., Higginbotham, A., Sinitskii, A., Lomeda, J., Dimiev, A., Price, K., & Tour, J. (2009). Longitudinal Unzipping of Carbon Nanotubes To Form Graphene Nanoribbons. *Nature*, *458*, 872.

Lee, C., Wei, X., Kysar, J. W., & Hone, J. (2008). Measurement of the Elastic Properties and Intrinsic Strength of Monolayer Graphene. *Science*, *321*(5887), 385 LP – 388. https://doi.org/10.1126/science.1157996

Lee, J. S., You, K. H., & Park, C. B. (2012). Highly photoactive, low bandgap TiO2 nanoparticles wrapped by graphene. *Advanced Materials (Deerfield Beach, Fla.)*, *24*(8), 1084–1088. https://doi.org/10.1002/adma.201104110

Ley, L., Teuschler, T., Mahr, K., Miyazaki, S., & Hundhausen, M. (1996). Kinetics of field-induced oxidation of hydrogen-terminated Si(111). *Journal of Vacuum Science & Technology B: Microelectronics and Nanometer Structures Processing, Measurement, and Phenomena*, *14*(4), 2845–2849. https://doi.org/10.1116/1.588843

Li, A. D., & Liu, W. C. (2010). 4 - Optical properties of ferroelectric nanocrystal/polymer composites. In S. C. Tjong & Y.-W. B. T.-P. P. and A. of P. N. Mai (Eds.), *Woodhead Publishing Series in Composites Science and Engineering* (pp. 108–158). Woodhead Publishing. https://doi.org/https://doi.org/10.1533/9780857090249.1.108

Li, B., Cao, X., Ong, H. G., Cheah, J. W., Zhou, X., Yin, Z., Li, H., Wang, J., Boey, F., Huang, W., & Zhang, H. (2010). All-carbon electronic devices fabricated by directly

grown single-walled carbon nanotubes on reduced graphene oxide electrodes. *Advanced Materials (Deerfield Beach, Fla.)*, *22*(28), 3058–3061. https://doi.org/10.1002/adma.201000736

Li, N., Cao, M., Wu, Q., & Hu, C. (2012). A facile one-step method to produce Ni/graphene nanocomposites and their application to the thermal decomposition of ammonium perchlorate. *CrystEngComm*, *14*(2), 428–434. https://doi.org/10.1039/C1CE05858D

Li, X., Zhao, T., Wang, K., Yang, Y., Wei, J., Kang, F., Wu, D., & Zhu, H. (2011). Directly Drawing Self-Assembled, Porous, and Monolithic Graphene Fiber from Chemical Vapor Deposition Grown Graphene Film and Its Electrochemical Properties. *Langmuir*, *27*(19), 12164–12171. https://doi.org/10.1021/la202380g

Liu, F., Sommer, F., Bos, C., & Mittemeijer, E. J. (2007). Analysis of solid state phase transformation kinetics: models and recipes. *International Materials Reviews*, *52*(4), 193–212. https://doi.org/10.1179/174328007X160308

Marcano, D. C., Kosynkin, D. V, Berlin, J. M., Sinitskii, A., Sun, Z., Slesarev, A., Alemany, L. B., Lu, W., & Tour, J. M. (2010). Improved Synthesis of Graphene Oxide. *ACS Nano*, *4*(8), 4806–4814. https://doi.org/10.1021/nn1006368

Mittal, G., Dhand, V., Rhee, K. Y., Park, S.-J., & Lee, W. R. (2015). A review on carbon nanotubes and graphene as fillers in reinforced polymer nanocomposites. *Journal of Industrial and Engineering Chemistry*, *21*, 11–25. https://doi.org/https://doi.org/10.1016/j.jiec.2014.03.022

Nagar, R., Vinayan, B. P., Samantaray, S. S., & Ramaprabhu, S. (2017). Recent advances in hydrogen storage using catalytically and chemically modified graphene nanocomposites. *J. Mater. Chem. A*, *5*(44), 22897–22912. https://doi.org/10.1039/C7TA05068B

Nakamori, Y., Li, H.-W., Matsuo, M., Miwa, K., Towata, S., & Orimo, S. (2008). Development of metal borohydrides for hydrogen storage. *Journal of Physics and Chemistry of Solids*, *69*(9), 2292–2296. https://doi.org/https://doi.org/10.1016/j.jpcs.2008.04.017

Navlani-García, M., Mori, K., Kuwahara, Y., & Yamashita, H. (2018). Recent strategies targeting efficient hydrogen production from chemical hydrogen storage materials over carbon-supported catalysts. *NPG Asia Materials*, *10*(4), 277–292. https://doi.org/10.1038/s41427-018-0025-6

Ngqalakwezi, A., Nkazi, D., Seifert, G., & Ntho, T. (2019). Effects of reduction of graphene oxide on the hydrogen storage capacities of metal graphene nanocomposite. *Catalysis Today*. https://doi.org/https://doi.org/10.1016/j.cattod.2019.06.029

Niaz, S., Manzoor, T., & Pandith, A.H. (2015). Hydrogen storage: Materials, methods and persperctives. Renewable and Sustainable Energy Reviews, 50, 457-469

Nine, M. J., Tung, T., & Losic, D. (2017). Self-Assembly of Graphene Derivatives: Methods, Structures, and Applications. In *Comprehensive Supramolecular Chemistry II* (pp. 47–74). https://doi.org/10.1016/B978-0-12-409547-2.12634-4

O'Hare, D. (2001). *Hydrothermal Synthesis* (K. H. J. Buschow, R. W. Cahn, M. C. Flemings, B. Ilschner, E. J. Kramer, S. Mahajan, & P. B. T.-E. of M. S. and T. Veyssière (eds.); pp. 3989–3992). Elsevier. https://doi.org/https://doi.org/10.1016/B0-08-043152-6/00701-4

Oliveira, A. E. F., Braga, G. B., Tarley, C. R. T., & Pereira, A. C. (2018). Thermally reduced graphene oxide: synthesis, studies and characterization. *Journal of Materials Science*, *53*(17), 12005–12015. https://doi.org/10.1007/s10853-018-2473-3

Pang, Y., & Li, Q. (2016). A review on kinetic models and corresponding analysis methods for hydrogen storage materials. *International Journal of Hydrogen Energy*, *41*(40), 18072–18087. https://doi.org/https://doi.org/10.1016/j.ijhydene.2016.08.018

Pang, Y., Sun, D., Gu, Q., Chou, K.-C., Wang, X., & Li, Q. (2016). Comprehensive Determination of Kinetic Parameters in Solid-State Phase Transitions: An Extended Jonhson–Mehl–Avrami–Kolomogorov Model with Analytical Solutions. *Crystal Growth & Design*, *16*(4), 2404–2415. https://doi.org/10.1021/acs.cgd.6b00187

Patchkovskii, S., Tse, J. S., Yurchenko, S. N., Zhechkov, L., Heine, T., & Seifert, G. (2005).

Graphene nanostructures as tunable storage media for molecular hydrogen. *Proceedings of the National Academy of Sciences of the United States of America*, *102*(30), 10439–10444. https://doi.org/10.1073/pnas.0501030102

Patil, S. J., Kim, J. H., & Lee, D. W. (2017). Graphene-nanosheet wrapped cobalt sulphide as a binder free hybrid electrode for asymmetric solid-state supercapacitor. *Journal of Power Sources*, *342*, 652–665. https://doi.org/https://doi.org/10.1016/j.jpowsour.2016.12.096

Pei, S., Wei, Q., Huang, K., Cheng, H.-M., & Ren, W. (2018). Green synthesis of graphene oxide by seconds timescale water electrolytic oxidation. *Nature Communications*, *9*(1), 145. https://doi.org/10.1038/s41467-017-02479-z

Poh, H., Šaněk, F., Ambrosi, A., Guanjia, Z., Sofer, Z., & Pumera, M. (2012). Graphenes prepared by Staudenmaier, Hofmann and Hummers methods with consequent thermal exfoliation exhibit very different electrochemical properties. *Nanoscale*, *4*, 3515–3522. https://doi.org/10.1039/c2nr30490b

Pumera, M. (2011). Graphene-based nanomaterials for energy storage. *Energy & Environmental Science*, *4*(3), 668–674. https://doi.org/10.1039/C0EE00295J

Putz, K. W., Compton, O. C., Palmeri, M. J., Nguyen, S. T., & Brinson, L. C. (2010). High-Nanofiller-Content Graphene Oxide–Polymer Nanocomposites via Vacuum-Assisted Self-Assembly. *Advanced Functional Materials*, *20*(19), 3322–3329. https://doi.org/10.1002/adfm.201000723

Reddy, A. L. M., Srivastava, A., Gowda, S. R., Gullapalli, H., Dubey, M., & Ajayan, P. M. (2010). Synthesis Of Nitrogen-Doped Graphene Films For Lithium Battery Application. *ACS Nano*, *4*(11), 6337–6342. https://doi.org/10.1021/nn101926g

Rezaei, R., Deng, C., Tavakoli-Anbaran, H., & Shariati, M. (2016). Deformation twinning-mediated pseudoelasticity in metal–graphene nanolayered membrane. *Philosophical Magazine Letters*, *96*(8), 322–329. https://doi.org/10.1080/09500839.2016.1216195

Riedl, C., Coletti, C., & Starke, U. (2010). Structural and electronic properties of epitaxial graphene on SiC(0 0 0 1): a review of growth, characterization, transfer doping and hydrogen intercalation. *Journal of Physics D: Applied Physics*, *43*(37), 374009. https://doi.org/10.1088/0022-3727/43/37/374009

Ruse, E., Buzaglo, M., Pri-Bar, I., Shunak, L., Nadiv, R., Pevzner, S., Siton-Mendelson, O., Skripnyuk, V. M., Rabkin, E., & Regev, O. (2018). Hydrogen storage kinetics: The graphene nanoplatelet size effect. *Carbon*, *130*, 369–376. https://doi.org/10.1016/J.CARBON.2018.01.012

Saravanakumar, B., Mohan, R., & Kim, S.-J. (2013). Facile synthesis of graphene/ZnO nanocomposites by low temperature hydrothermal method. *Materials Research Bulletin*, *48*(2), 878–883. https://doi.org/https://doi.org/10.1016/j.materresbull.2012.11.048

Schlapbach, L., & Züttel, A. (2001). Hydrogen-storage materials for mobile applications. *Nature*, *414*(6861), 353–358. https://doi.org/10.1038/35104634

Schniepp, H. C., Li, J. L., McAllister, M. J., Sai, H., Herrera-Alonso, M., Adamson, D. H., Prud'homme, R. K., Car, R., Saville, D. A., & Aksay, I. A. (2006). Functionalized Single Graphene Sheets Derived from Splitting Graphite Oxide. *J. Phys. Chem. B*, *110*, 8535.

Semelsberger, T. A., & Borup, R. L. (2005). Thermodynamic equilibrium calculations of dimethyl ether steam reforming and dimethyl ether hydrolysis. *Journal of Power Sources*, *152*, 87–96. https://doi.org/https://doi.org/10.1016/j.jpowsour.2005.01.056

Shams, S. S., & Zhang, R. (2015). Graphene synthesis: A Review. *Materials Science-Poland*, *33*. https://doi.org/10.1515/msp-2015-0079

Sharma, S., & Ghoshal, S.K., (2015). Hydrogen the future transportation fuel: from production to applications. Renewable and sustainable energy reviews, 43, 1151-1158

Shao, H., Xin, G., Zheng, J., Li, X., & Akiba, E. (2012). Nanotechnology in Mg-based materials for hydrogen storage. *Nano Energy*, *1*(4), 590–601. https://doi.org/https://doi.org/10.1016/j.nanoen.2012.05.005

Shimada, E., Yamashita, H., Matsumoto, S., Ikuma, Y., & Ichimura, H. (1999). The oxidation kinetics of spherically shaped palladium powder. *Journal of Materials Science*, *34*(16), 4011–4015. https://doi.org/10.1023/A:1004655713727

Song, L., Wang, S., Jiao, C., Si, X., Li, Z., Liu, S., Liu, S., Jiang, C., Li, F., Zhang, J., Sun, L., Xu, F., & Huang, F. (2012). Thermodynamics study of hydrogen storage materials. *The Journal of Chemical Thermodynamics*, *46*, 86–93. https://doi.org/https://doi.org/10.1016/j.jct.2011.06.022

Speyer, L., Fontana, S., Cahen, S., & Hérold, C. (2018). Simple production of high-quality graphene foams by pyrolysis of sodium ethoxide. *Materials Chemistry and Physics*, *219*, 57–66. https://doi.org/https://doi.org/10.1016/j.matchemphys.2018.08.020

Srivastava, M., Das, A. K., Khanra, P., Kim, N. H., & Lee, J. H. (2013). A Facile One-Step Hydrothermal Synthesis of Graphene/CeO2 Nanocomposite and its Catalytic Properties. *Advanced Materials Research*, *747*, 242–245. https://doi.org/10.4028/www.scientific.net/AMR.747.242

Sterlin Leo Hudson, M., Raghubanshi, H., Awasthi, S., Sadhasivam, T., Bhatnager, A., Simizu, S., Sankar, S. G., & Srivastava, O. N. (2014). Hydrogen uptake of reduced graphene oxide and graphene sheets decorated with Fe nanoclusters. *International Journal of Hydrogen Energy*, *39*(16), 8311–8320. https://doi.org/10.1016/J.IJHYDENE.2014.03.118

Stobinski, L., Lesiak, B., Malolepszy, A., Mazurkiewicz, M., Mierzwa, B., Zemek, J., Jiricek, P., & Bieloshapka, I. (2014). Graphene oxide and reduced graphene oxide studied by the XRD, TEM and electron spectroscopy methods. *Journal of Electron Spectroscopy and Related Phenomena*, *195*, 145–154. https://doi.org/https://doi.org/10.1016/j.elspec.2014.07.003

Sun, C.-L., Tang, J.-S., Brazeau, N., Wu, J.-J., Ntais, S., Yin, C.-W., Chou, H.-L., & Baranova, E. A. (2015). Particle size effects of sulfonated graphene supported Pt nanoparticles on ethanol electrooxidation. *Electrochimica Acta*, *162*, 282–289.

https://doi.org/https://doi.org/10.1016/j.electacta.2014.12.099

Sun, W., & Wang, Y. (2014). Graphene-based nanocomposite anodes for lithium-ion batteries. *Nanoscale*, *6*(20), 11528–11552. https://doi.org/10.1039/C4NR02999B

Tang, L.-C., Zhao, L., Qiang, F., Wu, Q., Gong, L.-X., & Peng, J.-P. (2019). *Chapter Twelve - Mechanical Properties of Rubber Nanocomposites Containing Carbon Nanofillers* (S. Yaragalla, R. K. Mishra, S. Thomas, N. Kalarikkal, & H. J. B. T.-C.-B. N. and T. R. N. Maria (eds.); pp. 367–423). Elsevier. https://doi.org/https://doi.org/10.1016/B978-0-12-817342-8.00012-3

Tang, X.-Z., Li, X., Cao, Z., Yang, J., Wang, H., Pu, X., & Yu, Z.-Z. (2013). Synthesis of graphene decorated with silver nanoparticles by simultaneous reduction of graphene oxide and silver ions with glucose. *Carbon*, *59*, 93–99. https://doi.org/10.1016/j.carbon.2013.02.058

Thakur, S., & Karak, N. (2012). Green reduction of graphene oxide by aqueous phytoextracts. *Carbon*, *50*(14), 5331–5339. https://doi.org/https://doi.org/10.1016/j.carbon.2012.07.023\

Thiruvengadathan, R., Korampally, V., Ghosh, A., Chanda, N., Gangopadhyay, K., & Gangopadhyay, S. (2013). Nanomaterial processing using self-assembly-bottom-up chemical and biological approaches. *Reports on Progress in Physics. Physical Society (Great Britain)*, *76*, 66501. https://doi.org/10.1088/0034-4885/76/6/066501

Thomsen, C., & Reich, S. (2000). Double Resonant Raman Scattering in Graphite. *Physical Review Letters*, *85*(24), 5214–5217. https://doi.org/10.1103/PhysRevLett.85.5214

Ţucureanu, V., Matei, A., & Avram, A. M. (2016). FTIR Spectroscopy for Carbon Family Study. *Critical Reviews in Analytical Chemistry*, *46*(6), 502–520. https://doi.org/10.1080/10408347.2016.1157013

Valensi G. (1936). Kinetics of the oxidation of metallic spherules and powdersNo Title. *Compt Rend*, *202*, 309–312.

Van Bommel, A. J., Crombeen, J. E., & Van Tooren, A. (1975). LEED and Auger electron observations of the SiC(0001) surface. *Surface Science*, *48*(2), 463–472. https://doi.org/https://doi.org/10.1016/0039-6028(75)90419-7

Vasudeo Rane, A., Kanny, K., Abitha, V. K., Patil, S. S., & Thomas, S. (2017). *Chapter 4 - Clay–Polymer Composites: Design of Clay Polymer Nanocomposite by Mixing* (K. Jlassi, M. M. Chehimi, & S. B. T.-C.-P. N. Thomas (eds.); pp. 113–144). Elsevier. https://doi.org/https://doi.org/10.1016/B978-0-323-46153-5.00004-5

Venkatesan, A., Patel, R. N., & Kannan, E. S. (2015a). Reduced Graphene Oxide for Room Temperature Hydrogen Storage Application. *Advanced Materials Research*, *1086*, 91–95. https://doi.org/10.4028/www.scientific.net/AMR.1086.91

Venkatesan, A., Patel, R. N., & Kannan, E. S. (2015b). Reduced Graphene Oxide for Room Temperature Hydrogen Storage Application. *Advanced Materials Research*, *1086*, 91–95. https://doi.org/10.4028/www.scientific.net/AMR.1086.91

Wall, M. (2011). *The Raman Spectroscopy of Graphene and the Determination of Layer Thickness*.

Wang, L., Yang, Z., Cui, Y., Wei, B., Xu, S., Sheng, J., Wang, M., Zhu, Y., & Fei, W. (2017). Graphene-copper composite with micro-layered grains and ultrahigh strength. *Scientific Reports*, *7*(1), 41896. https://doi.org/10.1038/srep41896

Wang, M. (2012). *Graphene Nanocomposites* (C. Yan (ed.); p. Ch. 2). IntechOpen. https://doi.org/10.5772/50840

Wang, X., Lu, M., Qiu, L., Huang, H., Li, D., Wang, H., & Cheng, Y.-B. (2016). Graphene/titanium carbide composites prepared by sol–gel infiltration and spark plasma sintering. *Ceramics International*, *42*(1, Part A), 122–131. https://doi.org/https://doi.org/10.1016/j.ceramint.2015.08.017

Woehrl, N., Ochedowski, O., Gottlieb, S., Shibasaki, K., & Schulz, S. (2014). Plasma-

enhanced chemical vapor deposition of graphene on copper substrates. *AIP Advances*, *4*. https://doi.org/10.1063/1.4873157

Xiang, Q., Yu, J., & Jaroniec, M. (2012). Synergetic effect of MoS2 and graphene as cocatalysts for enhanced photocatalytic H2 production activity of TiO2 nanoparticles. *Journal of the American Chemical Society*, *134*(15), 6575–6578. https://doi.org/10.1021/ja302846n

Xiong, Z., Hu, J., Wu, G., Chen, P., Luo, W., Gross, K., & Wang, J. (2005a). Thermodynamic and kinetic investigations of the hydrogen storage in the Li–Mg–N–H system. *Journal of Alloys and Compounds*, *398*(1), 235–239. https://doi.org/https://doi.org/10.1016/j.jallcom.2005.02.010

Xiong, Z., Hu, J., Wu, G., Chen, P., Luo, W., Gross, K., & Wang, J. (2005b). Thermodynamic and kinetic investigations of the hydrogen storage in the Li–Mg–N–H system. *Journal of Alloys and Compounds*, *398*(1–2), 235–239. https://doi.org/10.1016/J.JALLCOM.2005.02.010

Xu, Y., Sheng, K., Li, C., & Shi, G. (2010). Self-Assembled Graphene Hydrogel via a One-Step Hydrothermal Process. *ACS Nano*, *4*(7), 4324–4330. https://doi.org/10.1021/nn101187z

Xu, Y., & Shi, G. (2011). Assembly of chemically modified graphene: methods and applications. *Journal of Materials Chemistry*, *21*(10), 3311–3323. https://doi.org/10.1039/C0JM02319A

Yang, J., Zang, C., Sun, L., Zhao, N., & Cheng, X. (2011). Synthesis of graphene/Ag nanocomposite with good dispersibility and electroconductibility via solvothermal method. *Materials Chemistry and Physics*, *129*(1), 270–274. https://doi.org/https://doi.org/10.1016/j.matchemphys.2011.04.002

Yang, S., Feng, X., & Müllen, K. (2011). Sandwich-Like, Graphene-Based Titania Nanosheets with High Surface Area for Fast Lithium Storage. *Advanced Materials*, *23*(31), 3575–3579. https://doi.org/10.1002/adma.201101599

Yuan, Z., Xiao, X., Li, J., Zhao, Z., Yu, D., & Li, Q. (2018). Self-Assembled Graphene-Based Architectures and Their Applications. *Advanced Science*, *5*(2), 1700626. https://doi.org/10.1002/advs.201700626

Yun, Y. J., Hong, W. G., Kim, W.-J., Jun, Y., & Kim, B. H. (2013). A Novel Method for Applying Reduced Graphene Oxide Directly to Electronic Textiles from Yarns to Fabrics. *Advanced Materials*, *25*(40), 5701–5705. https://doi.org/10.1002/adma.201303225

Zaluska, A., Zaluski, L., & Ström-Olsen, J. O. (2001). Structure, catalysis and atomic reactions on the nano-scale: a systematic approach to metal hydrides for hydrogen storage. *Applied Physics A*, *72*(2), 157–165. https://doi.org/10.1007/s003390100783

Zhang, H., Ye, Y., Li, Z., Chen, Y., Deng, P., & Li, Y. (2016). Synthesis of Fe2O3–Ni(OH)2/graphene nanocomposite by one-step hydrothermal method for high-performance supercapacitor. *Journal of Materials Science*, *51*(6), 2877–2885. https://doi.org/10.1007/s10853-015-9596-6

Zheng, J., Liu, X., Xu, P., Liu, P., Zhao, Y., & Yang, J. (2012). Development of high pressure gaseous hydrogen storage technologies. *International Journal of Hydrogen Energy*, *37*(1), 1048–1057. https://doi.org/https://doi.org/10.1016/j.ijhydene.2011.02.125

Zhou, C., & Szpunar, J. A. (2016). Hydrogen Storage Performance in Pd/Graphene Nanocomposites. *ACS Applied Materials & Interfaces*, *8*(39), 25933–25940. https://doi.org/10.1021/acsami.6b07122

Zhou, C., Szpunar, J. A., & Cui, X. (2016). Synthesis of Ni/Graphene Nanocomposite for Hydrogen Storage. *ACS Applied Materials & Interfaces*, *8*(24), 15232–15241. https://doi.org/10.1021/acsami.6b02607

CHAPTER 3

3. SYNTHESIS AND REDUCTION OF GRAPHENE

Graphical Abstract

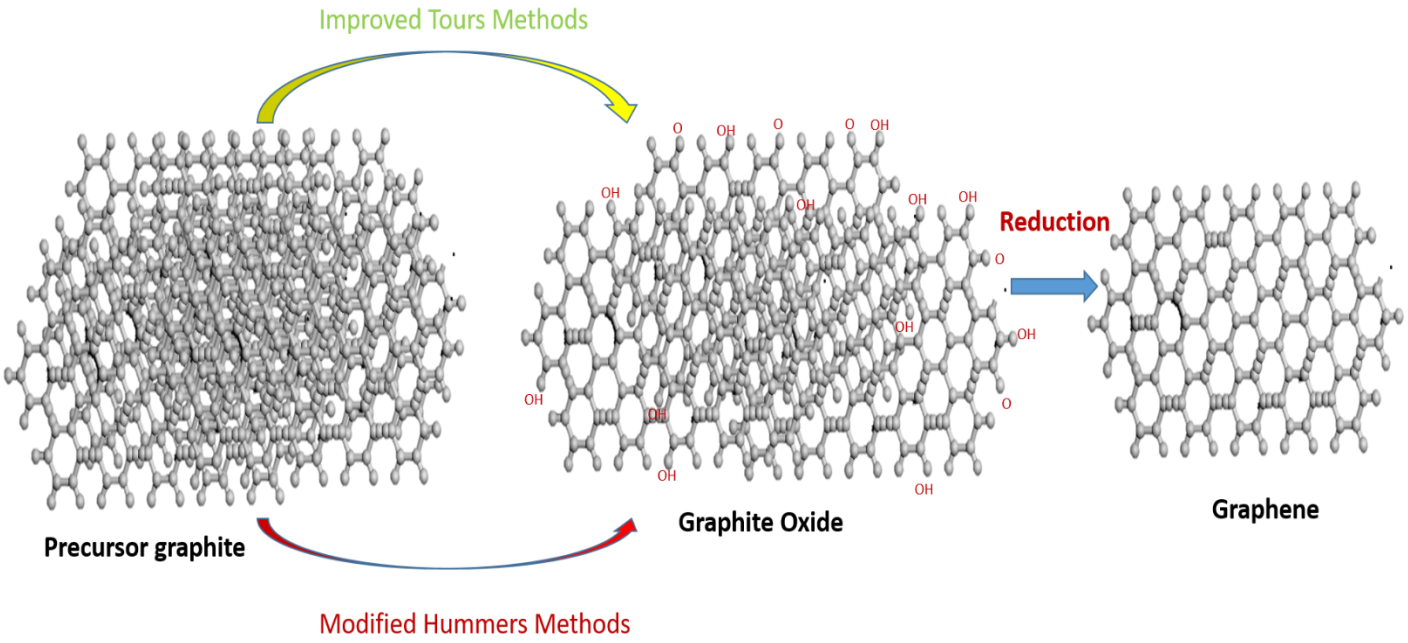

A manuscript of this chapter will be published. Manuscript in preparation

Introduction

Graphene, a carbon allotrope, embodies key advancement in modern science through its versatile properties and as such has been considered for many applications such as catalysis, hydrogen storage and sensors (Shams & Zhang, 2015). Graphene was initially discovered by Geim in 2004 using mechanical exfoliation, and many other methods since then have been employed to produce graphene such as chemical vapour deposition, graphite intercalation, micromechanical cleavage of graphite and the reduction of graphite oxide (Geim & Novoselov, 2007). A few novel methods were reported in 2013 by Kosynkin et al. and Choucair et al (Choucair et al., 2009; Kosynkin et al., 2009). Kosynkin's methods showed that the longitudinal unzipping of carbon nanotubes forms graphene nanoribbons while Choucair's method showed that graphene was produced hydrothermally and through sonication (Choucair et al., 2009; Kosynkin et al., 2009). The general graphene synthesis methods are classified to two simple approaches: the top-down approach and bottom-up approach (Choi et al., 2010). The top-down approach mainly looks into segregating the graphene layers, which form graphite, into atomic layers from the graphite i.e. graphene layer stack. The bottom-up approach concentrates on using carbon obtained from alternative sources as graphene building blocks (Shams & Zhang, 2015)

The production of graphene through the reduction of graphite oxide has become a conventional method. This method has been preferred over the other methods due to its ability to produce large of quantities of graphene compared to other methods and due to the minimized degree of exfoliation that can be obtained with expandable graphite and graphite (Gurunathan et al., 2016; Marcano et al., 2010; Venkatesan et al., 2015a). The reduction of graphene with this method can be achieved either through chemical or thermal treatment (Choi et al., 2010). The Staudenmaier method, Brodie method and Hummers method have all been used in the synthesis of the precursor graphite oxide. Oxidants such as nitric acid, potassium permanganate and

concentrated sulphuric have been used in these methods (Poh et al., 2012). Marcano et al. reported an improved method to oxidize graphite, the Improved Tours Method, where nitric acid is excluded while the amount of potassium permangate is increased. This synthesis method is reported to improve the oxidation process of graphite (Marcano et al., 2010). Various reductants have also been reported to effectively reduce graphite oxide. Gurunathan et al. developed a novel reductant procedure where biomass attained from the lysogeny broth bacteria was utilized to effectively reduce graphite oxide (Gurunathan et al., 2016). The traditional reductant (hydrazine) used in Modified Hummers method has been deemed as lethal and as such greener reductants have been studied by various researchers such as lemon juice, coconut water, L-Ascorbic acid, vinegar and many other more (Abulizi et al., 2014; Chong et al., 2015; Mas'udah et al., 2016) .

.

In this chapter, graphene was synthesized from precursor graphite utilizing the modified Hummers method and the improved Tours Method. The graphite was first oxidized to graphite oxide and then later reduced to graphene. Modified Hummers method is a conventional method used widely in the synthesis of graphene. Improved Tours Method is an improved method for the synthesis of graphite.

3.1 EXPERIMENTAL: MATERIALS AND METHOD

3.1 METHOD

3.1.1 Synthesis of Graphite Oxide Improved Tours Method

Materials

Graphite flakes (expandable-99.99%, 200 mesh) purchased from Sigma Aldrich were used as pre-cursor material. Potassium permanganate, ACS reagent, 99%) also purchased from Sigma Aldrich was used as an oxidant. Concentrated sulphuric acid and phosphoric acid purchased from ACE chemicals were also used. Hydrogen peroxide also purchased from ACE chemicals was used to quench the oxidation reaction.

Method

The Improved Tours Method was utilized to synthesize precursor graphite oxide because this method allows a large scale synthesis of hydrophilic oxidized graphene. In this method, H_3PO_4

and H_2SO_4 were mixed at a ratio of 1:9 (360 ml: 40ml) and were mixed with graphite flakes. The mixture of H_3PO_4 and H_2SO_4 and graphite flakes was stirred at 400 rpm for an hour while the temperature was kept below 10 ℃ through the use of an ice bath. About 18g of $KMnO_4$ were added very slowly to the graphite solution to avoid any explosion. After completely adding $KMnO_4$, the solution was removed from the ice bath and was heated to 50 ℃ and stirred continuously for approximately 3 hours. When the solution was completely cool, 3ml of H_2O_2 were added to quench the reaction. The resultant, was dialyzed about 7 times in 5l of deionized water to obtain a neutral pH. The washed graphite oxide was then filtered and dried at 120℃ overnight.

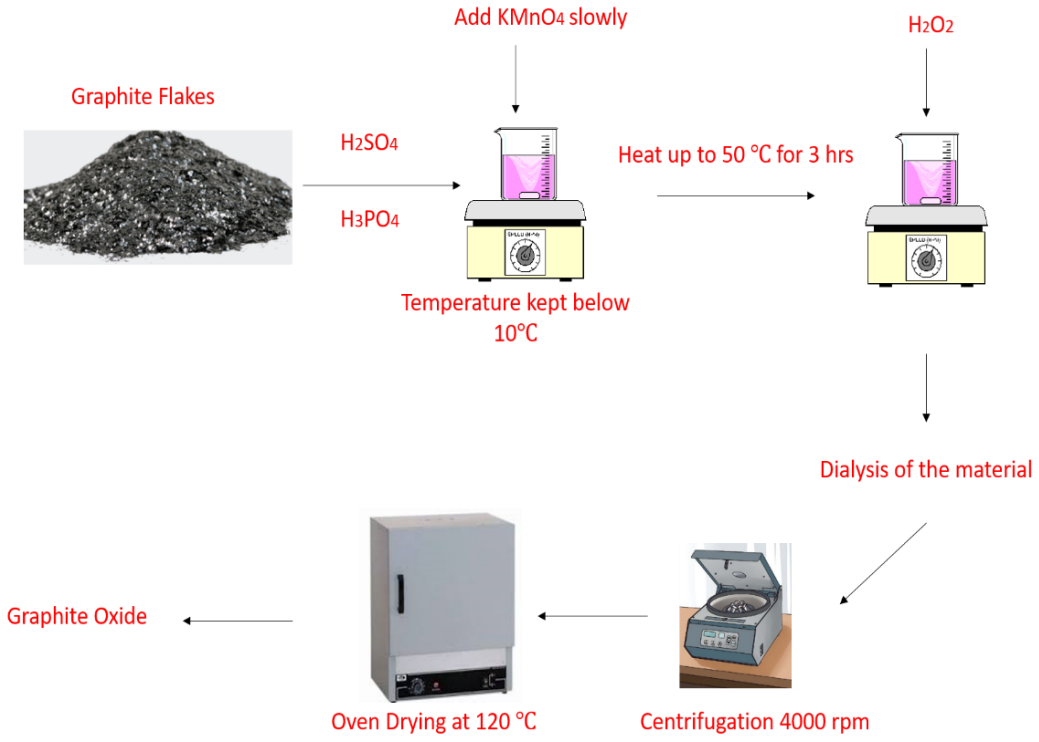

Figure 3-1*:* Graphite oxidation

3.1.2 Graphite Oxide reduction

2.2.1 Thermal reduction

Precursor graphite oxide was thermally reduced through furnace treatment. Procedurally, the graphite oxide was weighed and transferred to a crucible and then placed in the furnace for approximately 24 hours. The precursor graphite oxide was thermally reduced at 200℃. The resultant, after thermal treatment, was weighed and then taken for characterization.

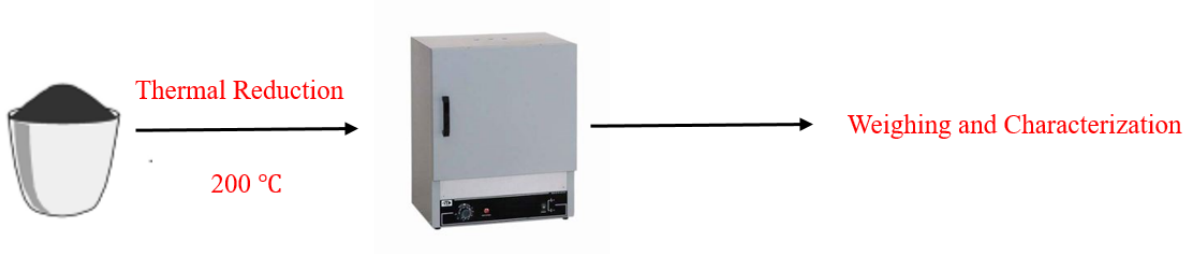

Figure 3-2: The thermal reduction process of GO

2.2.2 Chemical reduction: Ammonia

Dry precursor graphite oxide was mixed with de-ionized water (300ml) and stirred at 250 rpm until the solution was uniform. Then, about 10 ml of NH_3 were mixed with de-ionised water (100ml). While continuously stirring the graphite oxide solution, the NH_3 solution was slowly added. After completely adding the NH_3 solution, the temperature was increased to 70 ℃ and it was kept there for 2 hours. The solution of reduced graphene was aged for 2 days and then freeze dried.

2.2.3 Chemical Reduction: L-Ascorbic Acid

Lastly, precursor graphite oxide was reduced using L-Ascorbic acid. In the reduction process, precursor GO was mixed with de-ionized water (250 ml) and the solution was stirred at 250 rpm. Then, an L-Ascorbic acid solution was made through mixing about 5.28g of L-Ascorbic acid with de-ionised water (300ml). The L-Ascorbic solution and precursor GO solution were mixed together, but slowly adding the ascorbic acid solution to the graphite oxide solution. The temperature was elevated to 70 ℃ and was kept at 70 ℃ for 2 hours. The solution of reduced graphene was then aged for 2 days and then it was freeze dried.

3.1.3 Synthesis of Graphite Oxide Modified Hummers Method

Materials

Precursor graphite flakes Graphite flakes (expandable-99.99%, 200 mesh) purchased from Sigma Aldrich were used as pre-cursor material. Potassium permanganate (Analytical grade, 99%) also purchased from Sigma Aldrich was used as an oxidant. Concentrated sulphuric acid

purchased from ACE chemicals were also used. Hydrogen peroxide (30%) also purchased from ACE chemicals was used to quench the oxidation reaction. Nickel (II) acetate tetrahydrate (Ni $[(OAc)_2]_3$, sodium hydroxide (NaOH) and hydrochloric acid (HCl) were obtained from Merck Chemicals (Pty) Ltd. De-ionized water purified using the Milli-Q system Millipore with a resistivity of 18.2 MΩcm was utilized throughout the experiments.

Method

In this method, graphite oxide was prepared using Modified hummers method with expandable graphite flakes as the starting material. Expandable graphite flakes (3g) were mixed with about 70 ml of concentrated sulphuric acid and the mixture was stirred at constant while the temperature was maintained below 10 °C in an ice bath. The oxidizing agent (potassium permanganate (9g)) was slowly added to the solution. The ice water bath was removed after completely adding the oxidant and the solution was heated to 35 °C and the solution was continuously stirred for a further 30 minutes. High purity water (150 ml) were further added to the solution and the solution was heated to 95 °C. A hydrogen peroxide solution was prepared by mixing hydrogen peroxide 30% (20 ml) with deionized water (150 ml). The solution was slowly added to the graphite oxide solution to quench the reaction. The solution color changed to dark brown. After the reaction was quenched, the solution was exfoliated through sonication. The solution was sonicated for 10 min and ambient temperature and pressure. The resultant and sonicated solution was then was with hydrochloric acid 1M (15 ml) to remove any metal ions. The solution was centrifuged for half an hour at 4000 rpm. The resultant solution was dialyzed in 5l of deionized water. The process was repeated until a neutral pH was obtained. The resultant was dried at overnight in an oven and then stored.

3.1.3 Reduction of graphite oxide

In this section, graphite oxide was reduced using a green reductant and the conversional hazardous hydrazine was not used. Lemon juice purchased from Woolworths was used as a reductant in this section. The solid graphite oxide was mixed with deionized water (150 ml) and was mixed concentrated lemon juice. The solution was stirred and the temperature was increased and was kept at 50 °C for 2 hours. The solution was filtered and dried overnight.
The resultant was then taken for characterization.

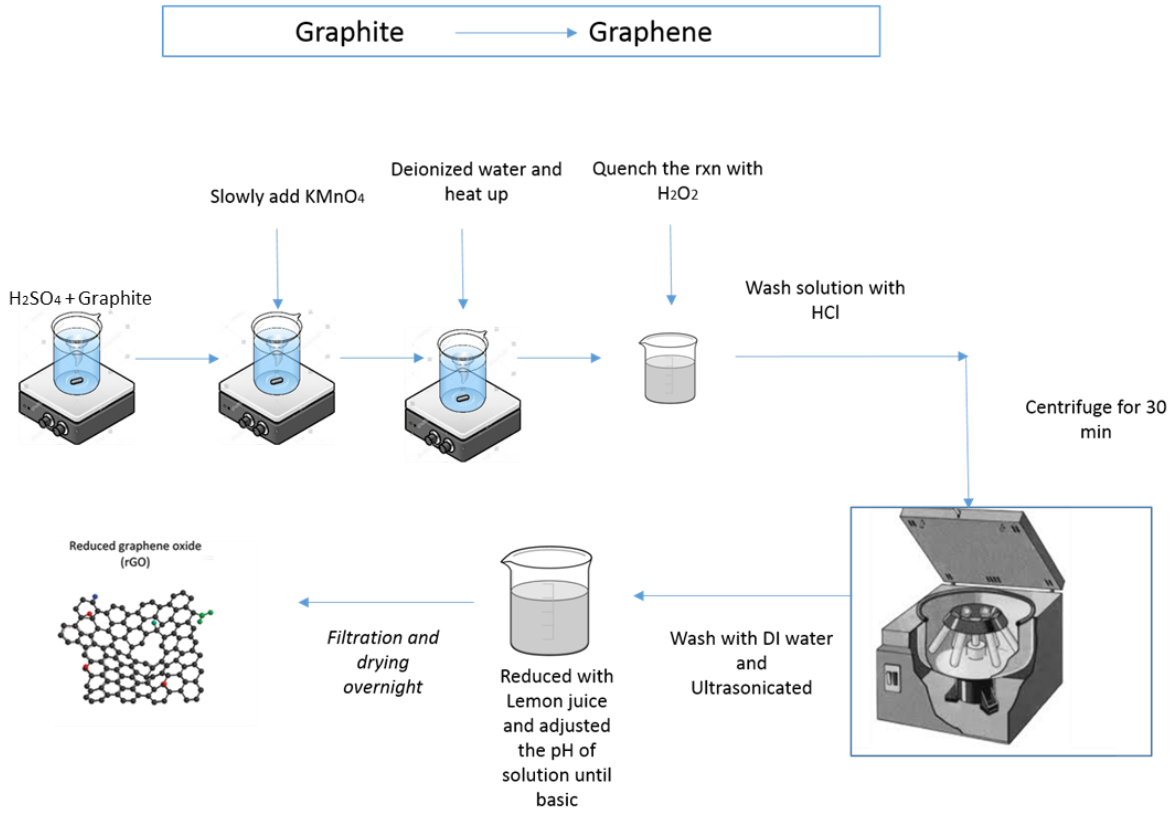

Figure 3-3: Modified hummers method

3.2 CHARACTERIZATION

XRD patterns were recorded using X-ray powder diffraction (p-XRD), an advanced powder diffractometer with CuKα-radiation (40 kV, 40 mA, 1.78897 Å). The XRD analysis machine is equipped with a LinxEye detector that detects the crystal structure of the material. The XRD patterns were captured in the 2θ range of 5 to 80◦ diffraction angle with a step size of 0.02. Raman mapping was performed using the Perkin Elmer Raman spectroscopy with a wavelength excitation of 785 nm laser that delivers the laser at 100 Mw on the sample. The Raman uses a temperature controlled detector (-50 °C) , Charged coupled device (CCD), that has a 1024 x 256 pixel sensor with a lateral resolution of approximately 1 µm. The mapping was performed with a grip spacing of 0.25 nm and at an accumulation time of 3 seconds at each spot. The obtained spectra was processed utilizing the PerkinElmer processing software. For FTIR analysis, a Perkin Elmer Spectrum two (UATR Two) was utilized. The spectra obtained was subtracted from the FTIR spectra that was recorded.

BET (Brunauer-Emmett-Teller) analysis on the sample was performed utilizing the Micromeritics ASAP TriStar 3000 unit. This units operates by adsorbing monolayer nitrogen gas at cryogenic temperatures (–196˚) and at 2 μmHg pressure for porosity measurement. A JEM2100F, JEOL Ltd. Electron microscope was utilized to capture high resolution TEM images. The machine is fitted with an EDX that uses an electron beam backscattered diffraction (EBSD) and wavelength dispersive spectroscopy (WDS). The machines utilizes the Oxford instruments software for processing.

3.3 RESULTS AND DISCUSSION

3.1.1 Raman

Raman is a vibrational characterization technique that is sensitive to geometric structure and bonding within molecules (Marcano et al., 2010; Oliveira et al., 2018). Raman, in this synthesis work, was utilized to detect the structural differences during the oxidation process of graphite flakes and the reduction processes of graphite oxide. In the Raman spectra, the important bands are the G, D and 2D bands. Figure 3-4 shows the spectra graphite flakes A, graphite oxide B, reduced graphene C.

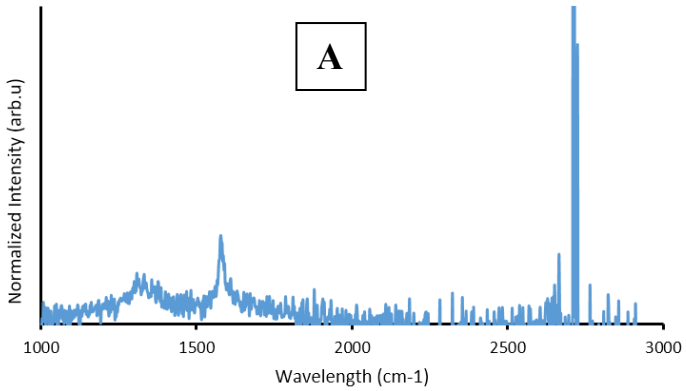

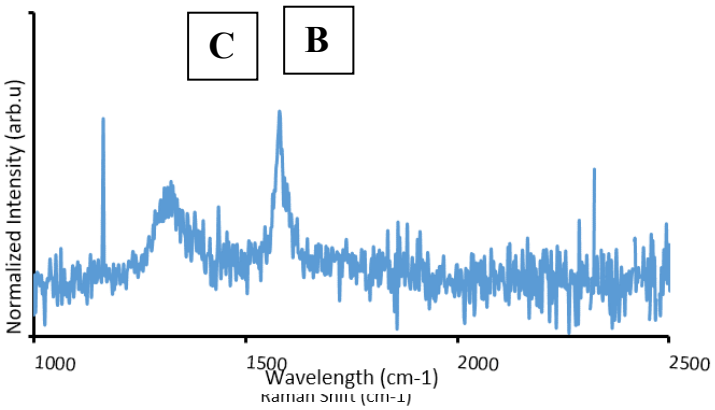

Figure 3-4: Raman characterization of graphite flakes (A), Graphtie Oxide (B), reduced graphene oxide (C)

The Raman spectra shown in figure 4(A) depicts the G band in graphite flakes at ~1582 cm^{-1}. The G band position in graphite flakes is positioned in an in-plane mode (Oliveira et al., 2018). This mode is highly sensitive to the number of layers in graphene and it involves sp^2 hybridized carbon. The G band shifted in reduced graphene to ~ 1598 cm^{-1}. This shift observed is due to the increase on the layer thickness of the material and the increase in lay thickness results in the band shifting towards a lower energy position (Wall, 2011; Zhou & Szpunar, 2016). The number of layers available in a material can be correlated to the band position using this correlation:

$$\omega_G = 1581.6 + \frac{11}{(1+n^{1.6})} \text{ [17]}$$

The temperature affects the G band and during the reduction step, as such the temperature was kept constant. The D band can be observed approximately between 1327-1342 cm^{-1} wavelength. This band is the disorder band which only appears in the presence of defects (Oliveira et al., 2018; Zhou & Szpunar, 2016). Defects occur during the oxidation and reduction processes in the synthesis of graphene. The D band for graphite flakes can be observed at ~1324 cm^{-1}, for graphite oxide at ~1332 cm^{-1} and for reduced graphene it appears around ~1340 cm^{-1}. The graphite flakes D band has a low intensity because it has defects. Again, on the graphite flakes spectrum, the 2D band can be seen at ~2714 cm^{-1} wavelength. The 2D band can be observed because of the vibrational process of the two phonon lattice. The

increase in number of layers affects the intensity of this band and symmetry resulting in the decrease of this band (Marcano et al., 2010).

3.1.2 XRD

X-ray diffraction is a non-destructive analysis for analyzing crystalline materials. XRD functions by scattering of x-ray photons using atoms in a periodic lattice (Stobinski et al., 2014). The smattered x-rays in the phase provide constructive interference. This gives an indication of structural parameters, crystals defects, phases, crystal orientation and crystallinity (Stobinski et al., 2014).

The XRD results are shown below on figure 3-5. Before the analysis of the synthesized samples, some of the samples were crushed to obtain powder. In these results, a very sharp peak at $\sim 2\theta = 30°$ can be observed in graphite flakes spectrum. This corresponds to the hexagonal arrangement in the materials and in the packing of atomic layers within the material (Diana C. Tranca & Gotthard Seifert, 2016; Venkatesan et al., 2015a). In the GO spectrum, the angle shifts lower due the oxidation of the crystalline structure that results in increased interplanar spacing. The GO peak corresponds to the d_{001} plane and can be observed at $\sim 2\theta = 11.3°$. Furthermore, the broadness of the GO peak confirms the presence of functional groups in the material due to the oxidation process (Marcano et al., 2010). The reduced graphite oxide oxidation peaks in spectrum C, are observed to decrease due to the reduction process. These results confirm that the graphite was successfully oxidized and subsequently reduced.

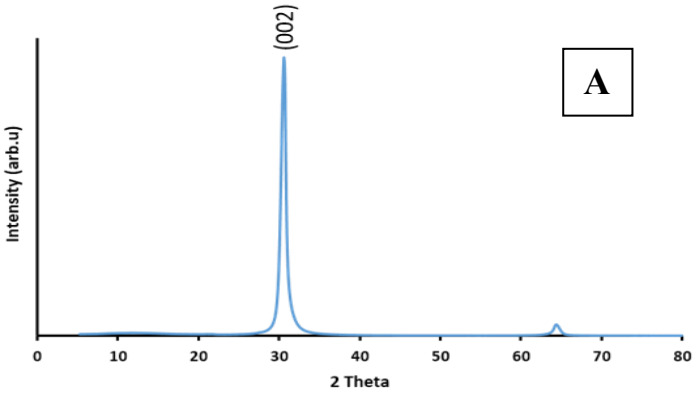

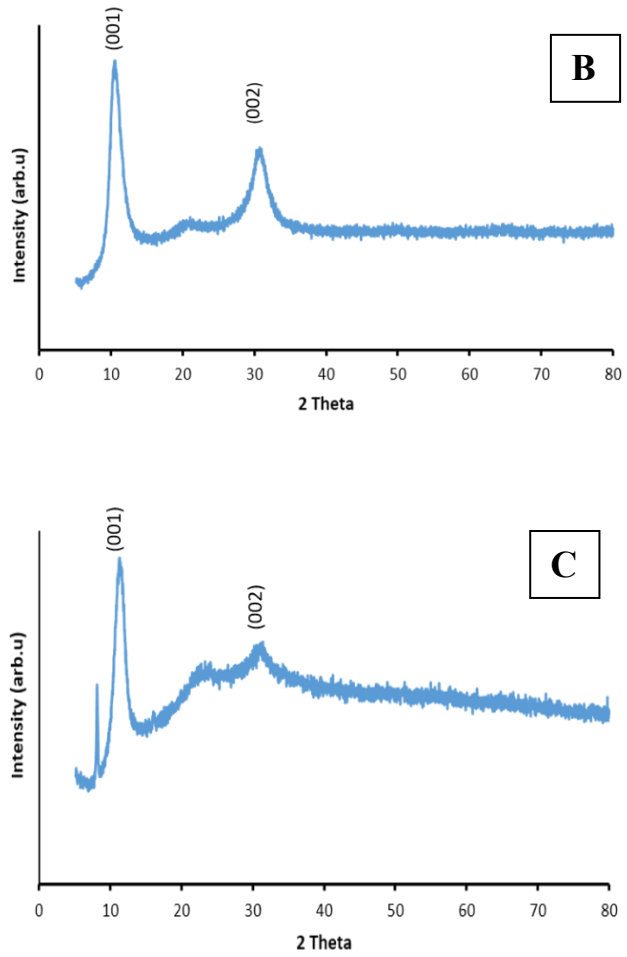

Figure 3-5: XRD characterization of graphite flakes (A), Graphite Oxide (B), and reduced graphene (C)

3.1.3 FTIR Results

Fourier transform infrared spectroscopy is an analysis method that is utilized to detect polymeric and organic materials. This method utilizes infrared light to scan test samples and detect their chemical properties (Ţucureanu et al., 2016). The bonds within and between different materials absorb light and various frequencies (Ţucureanu et al., 2016). The absorbance by the material gives indications to the materials molecular structure and composition.

The FTIR spectroscopy is also associated with molecular vibrations or atomic vibrations within a material. These vibrations are utilized to detect functional groups by analyzing the frequencies to detect molecules (Kartick et al., 2013). The FTIR spectra detected several

functional groups: O-H (3422 cm^{-1}) stretching vibrations, C=O (1719-1754 cm^{-1}) vibrations, C=C (1595-1623 cm^{-1}) vibrations and C-O (1215-1252 cm^{-1}) vibrations. The OH- stretch which can be seen on the samples is because of the presence of water in the graphene layers. The observed reduction in the intensity on the bands is due to the reduction process (Pei et al., 2018; Venkatesan et al., 2015a). Therefore, this affirms that graphite oxide was successfully reduced.

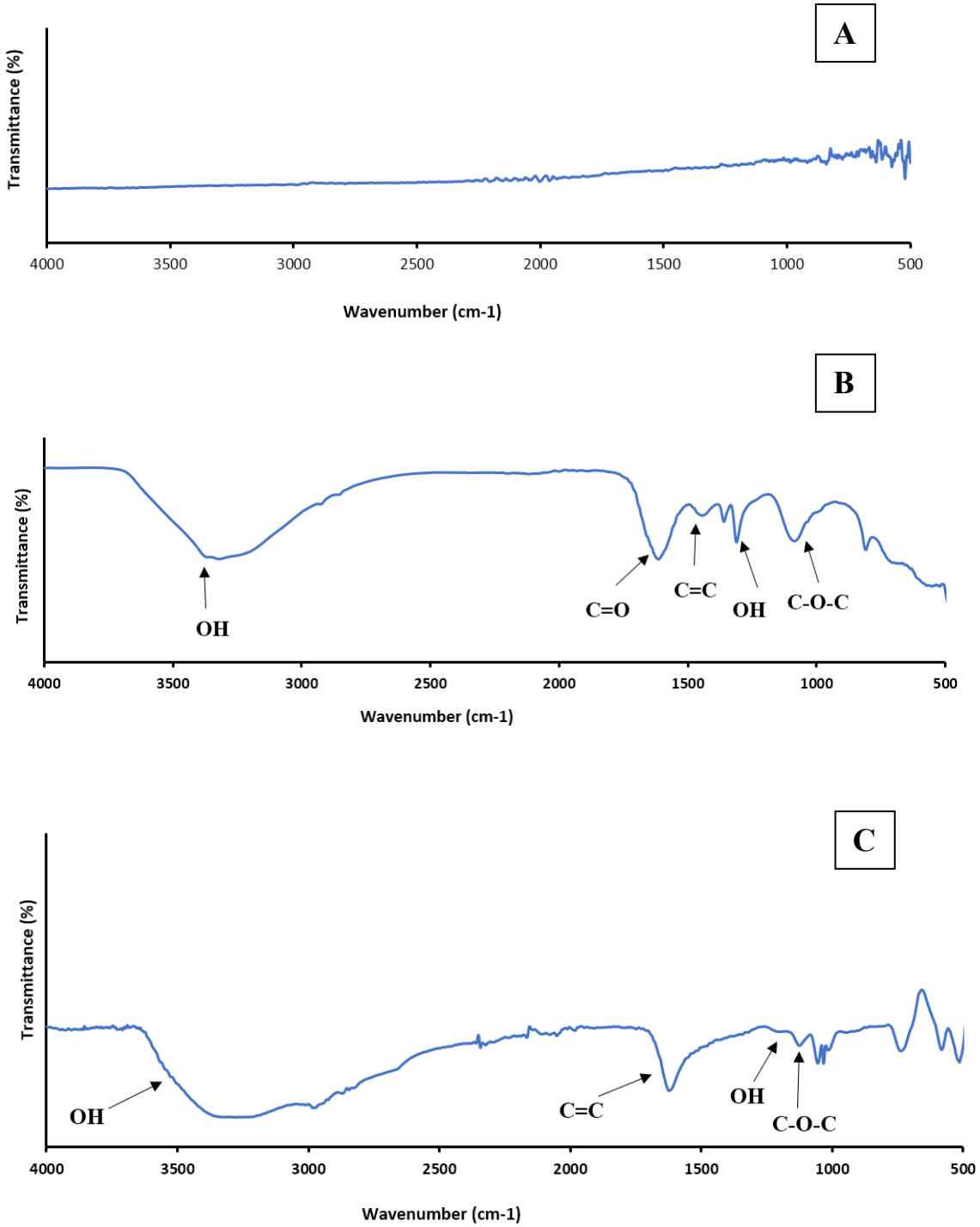

Figure 3-6: FTIR spectra A. Graphite B. GO, C. Ascorbic acid reduced graphene D. NH_3 reduced graphene

CONCLUSION

The aim of this chapter was to synthesize and characterize precursor graphene for the development of metal/graphene nanocomposite for hydrogen storage. Graphite flakes were successfully oxidized to graphite oxide. The success of this synthesis step can observed in the characterization results presented above. FTIR showed the presence of functional groups after oxidizing graphite flakes, XRD results depicted a shift in the graphite flakes peak at $\sim 2\theta = 30°$ due to the oxidation process and lastly the Raman characterization showed the defects on the graphite flakes after oxidation. The reduction of graphite oxide was also successfully completed as observed in the characterization results.

REFERENCES

Diana C. Tranca & Gotthard Seifert. (2016). A First-Principles Study of Metal-Decorated Graphene Nanoribbons for Hydrogen Storage. *De Gruyter*, *230*, 791-808,.

Kartick, B., Srivastava, S. K., & Srivastava, I. (2013). Green synthesis of graphene. *Journal of Nanoscience and Nanotechnology*, *13*(6), 4320–4324. https://doi.org/10.1166/jnn.2013.7461

Marcano, D. C., Kosynkin, D. V, Berlin, J. M., Sinitskii, A., Sun, Z., Slesarev, A., Alemany, L. B., Lu, W., & Tour, J. M. (2010). Improved Synthesis of Graphene Oxide. *ACS Nano*, *4*(8), 4806–4814. https://doi.org/10.1021/nn1006368

Oliveira, A. E. F., Braga, G. B., Tarley, C. R. T., & Pereira, A. C. (2018). Thermally reduced graphene oxide: synthesis, studies and characterization. *Journal of Materials Science*, *53*(17), 12005–12015. https://doi.org/10.1007/s10853-018-2473-3

Pei, S., Wei, Q., Huang, K., Cheng, H.-M., & Ren, W. (2018). Green synthesis of graphene oxide by seconds timescale water electrolytic oxidation. *Nature Communications*, *9*(1), 145. https://doi.org/10.1038/s41467-017-02479-z

Stobinski, L., Lesiak, B., Malolepszy, A., Mazurkiewicz, M., Mierzwa, B., Zemek, J., Jiricek, P., & Bieloshapka, I. (2014). Graphene oxide and reduced graphene oxide studied by the XRD, TEM and electron spectroscopy methods. *Journal of Electron Spectroscopy and Related Phenomena*, *195*, 145–154. https://doi.org/https://doi.org/10.1016/j.elspec.2014.07.003

Ţucureanu, V., Matei, A., & Avram, A. M. (2016). FTIR Spectroscopy for Carbon Family Study. *Critical Reviews in Analytical Chemistry*, *46*(6), 502–520. https://doi.org/10.1080/10408347.2016.1157013

Venkatesan, A., Patel, R. N., & Kannan, E. S. (2015). Reduced Graphene Oxide for Room Temperature Hydrogen Storage Application. *Advanced Materials Research*, *1086*, 91–95. https://doi.org/10.4028/www.scientific.net/AMR.1086.91

Wall, M. (2011). *The Raman Spectroscopy of Graphene and the Determination of Layer Thickness*.

Zhou, C., & Szpunar, J. A. (2016). Hydrogen Storage Performance in Pd/Graphene Nanocomposites. *ACS Applied Materials & Interfaces*, *8*(39), 25933–25940. https://doi.org/10.1021/acsami.6b07122

Zhou, C., Szpunar, J. A., & Cui, X. (2016). Synthesis of Ni/Graphene Nanocomposite for Hydrogen Storage. *ACS Applied Materials & Interfaces*, *8*(24), 15232–15241. https://doi.org/10.1021/acsami.6b02607

CHAPTER 4

4. DEVELOPMENT OF METAL-GRAPHENE NANOCOMPOSITE

Graphical Abstract

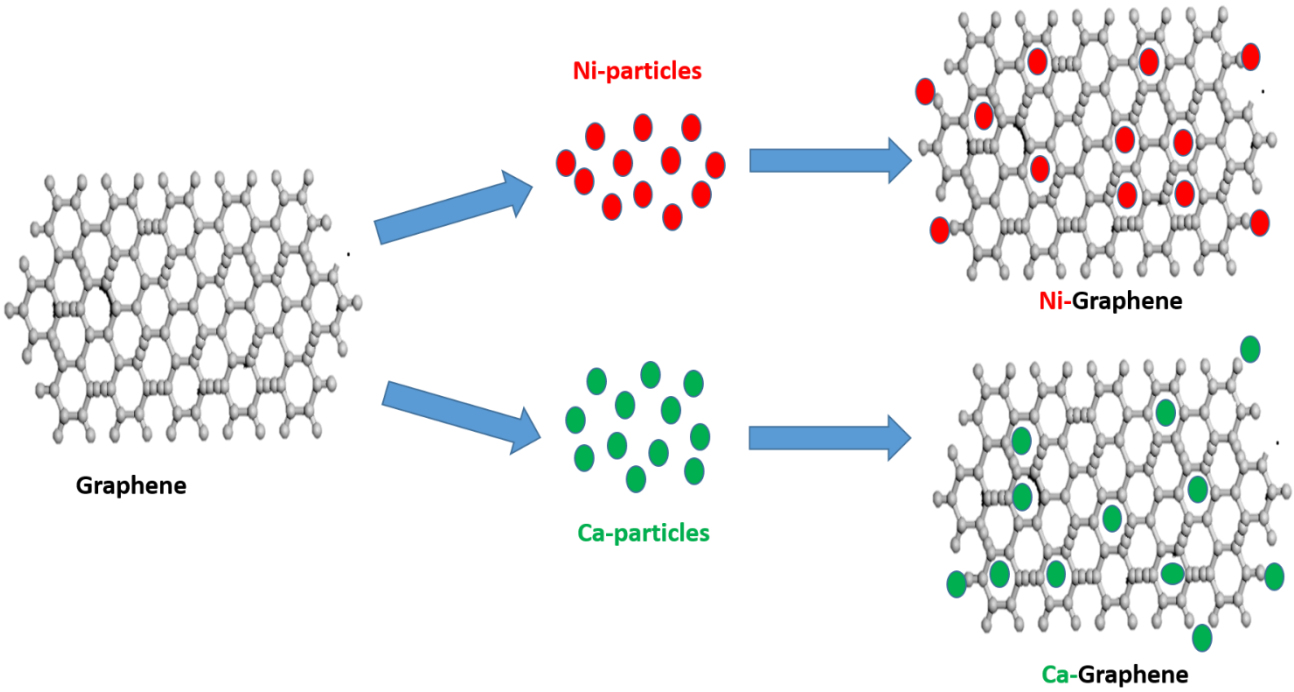

Sections of this chapter was published

Introduction

Graphene nanocomposites and its derivatives depict a promising potential for different applications such as automotive industry, aerospace, electronics and green energy (Pumera, 2011). This is because graphene has intriguing thermal, mechanical and electrical properties (Shams & Zhang, 2015). Nanocomposites, where nanocatalysis and nanostructure are combined, are the next research advancement of high performance of hydrogen storage materials. These materials have distinct functionalities due to the shorten diffusion distance, increased surface area and the multiplied grain boundaries (Gurunathan et al., 2016; Pumera, 2011; M. Wang, 2012).

A lot of studies have been done with graphene and nanocomposites thereof for the practical application in on-board application. Graphene nanocomposites can be synthesized using various techniques. These include the self-assembly technique, solution mixing, sol-gel method, hydrothermal or the solvothermal method and other methods (Ngqalakwezi et al., 2019; O'Hare, 2001; M. Wang, 2012; J. Yang et al., 2011; Zhou et al., 2016). Graphene nanocomposites have been preferred for hydrogen storage application mainly because of their light weight characteristic. Weight of the material is an important factor when considering the practical applications for hybrid cars according to the DoE standards. Graphene alone is a physisorbent material and does not take up a lot of hydrogen however its kinetics are interesting (Pei et al., 2018). The incorporation of metals on the graphene matrix enhances the functions of the system and improves the hydrogenation of this material to make it more appealing for practical use in hybrid cars (Pumera, 2011). Various metals have been used in this regard to improve the hydrogen uptake of the graphene nanocomposite. Zhou et al., synthesized a Ni/graphene nanocomposite and a Pd/graphene nanocomposite (Zhou et al., 2016)(Zhou & Szpunar, 2016). Ngqalakwezi et al. synthesized a novel Ca/graphene nanocomposite (Ngqalakwezi et al., 2019). The graphene nanocomposites can be used and applied in different industries for hydrogen generation in the electrolysis process, in the photo degradation of pollutants, energy storage and other applications.

In this chapter, the graphene synthesized using the improved tours method was loaded the calcium and nickel. The hydrothermal and solution mixing methods were utilized in this regard. The metal graphene was then characterized.

4.1 Synthesis of Ca/graphene

In the synthesis of Ca/graphene, precursor graphene gel was used. The graphene gel was obtained by mixing dried reduced graphene with deionised water. This step could be done parallel with the reduction step. A solution of Ca/Cl_2 was made by mixing 1.542g of Ca/Cl_2 (purchased from ACE) with deionised water. The solution was then slowly added to the graphene gel and the temperature was increased to 70 ℃ and was agitated for an hour. The obtained solution was ultra-sonicated and centrifuged at 4000 rpm. The resultant precipitate was washed vigorously with deionized water and centrifuged. Lastly, the obtained precipitate was oven dried at 180 ℃ and then dried in a furnace for 2 min at 300℃.

4.1.1 Characterization

For elemental and surface characterization, XRF (X-ray Fluorescence) and TEM (Transmission electron microscopy) were utilized. TEM was performed utilizing a JEOL Jem 2001F microscope that has an electron accelerating voltage. The voltage ranges from 80kV to 200Kv. The Ca/graphene samples were prepared on perforated copper grids that are coated with carbon. For XRF analysis, A NitonTM XL3t XRF analyzer was used to analyze the elemental make-up of the samples at ambient temperature.

4.1.1.1 X-ray Fluorescence (XRF)

X-ray fluorescence is an analysis technique that measures the fluorescent X-ray emitted from a sample because of excitation by X-rays, was used to analyze the elemental composition of the metal incorporated reduced graphene, reduced graphene and precursor graphite (Kalnicky & Singhvi, 2001). From the elemental analysis results, graphite flakes consisted of carbon with traces of Mn, Fe and Ca. New elements such as P and K were observed on the reduced graphene primarily because H_3PO_4 and $KMnO_4$ were used during the process of oxidizing the graphite flakes. The XRF results of the Ca/graphene showed an increase after of Ca metal on the surface of reduced graphene. The calcium content before metal incorporation was 0.516 % and increased to 8.227 %. These results prove that the Ca was successfully incorporated into the graphene matrix.

Table 4-1: Elemental comp. of the precursor graphite flakes

Graphite Flakes	
Element	**%**
Carbon	96.171
Calcium	0.516
Mn	2.623
Fe	0.47

Table 4-2: Elemental comp. of Ca decorated graphene samples

Ca-rGO	
Element	**%**
Carbon	75.426
Sulphur	3.809
Calcium	8.227
Mn	5.236
P	2.066
K	0.348

4.1.1.2 *TEM Analysis*

The surface characterization of the morphology of as-prepared metal/graphene, graphene oxide and graphene was performed using Transmission electron microscope. Transmission electron microscope is an analysis tool that utilizes an electron beam to image a high resolution nanoparticle sample. The analysis gives indication of the morphology, grain size, nanoparticle size and size distribution of materials. For the analysis, all the samples were prepared by dissolving them in a solvent and then pipetting it on the holey carbon coated copper grids (Texter, 2014).

Graphite flakes could not be exfoliated during sample preparation and the image captured shows the graphitic nature of the flakes. Graphite oxide morphology image in figure 4-1 B, depicts translucent sheets which are entangled on top of each other. Graphite Oxide was detected to be unstable when the energy beam of the microscope was elevated relative to

graphene. The reduced graphene image depicted on figure 4-1 C shows the morphology of the material to be irregular shaped, layers with rough surfaces and appears semi-transparent. The tangles and irregularity observed on the surface of reduced graphene are because of the partial reduction of graphene with the reductant used (De Silva et al., 2018).

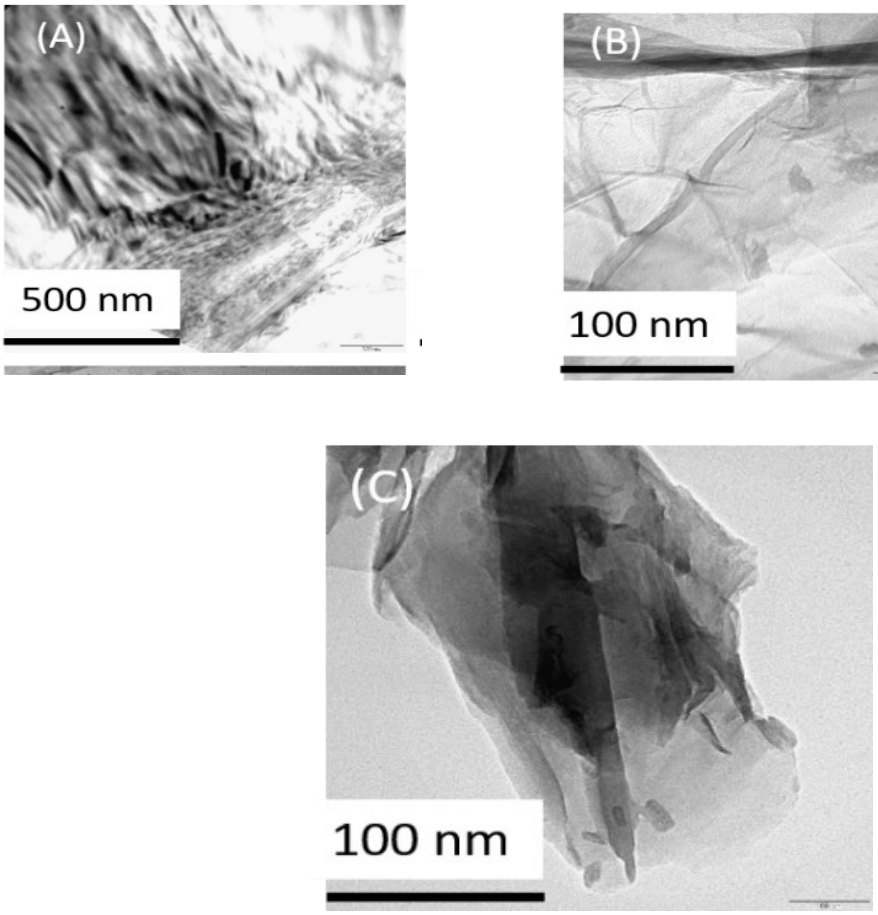

Figure 4-1: TEM morphological analysis of A. Graphite flakes B. GO, C. reduced graphene

4.2 Synthesis of Ni/Graphene

For the synthesis of Ni/Graphene nanocomposite, graphite oxide synthesized using modified Hummers methods was utilized. Graphene gel, was prepared by mixing the dry graphite oxide with de-ionized water. To prepare the nickel acetate solution, $Ni((OAc)_2)_3$ about 2.51 g was mixed with about 50 ml of deionized water. The Ni solution was added to the graphite oxide gel at a ratio of 95:5 Ni to C. The resultant solution was ultra-sonicated at room temperature for approximately 10 min. The solution turned dark brown.

Approximately 10 ml lemon juice was added to the solution. The solution was stirred for an hour. After, the pH of the solution was increased to 10 by adding 1M NaOH solution while stirring. The mixture was stirred continuously for 10 min. The solution was then placed in a tightly closed container and was heated at 70 °C for an hour. The temperature was further raised to 95 °C for another 60 min. Lastly, the uniform mixture was centrifuged and the remaining impurities were washed repeatedly with deionized water and the solution was centrifuged again. Then the resultant precipitate was vacuum dried to obtain a powder of $Ni(OH)_2$/graphene. Finally, the precursor $Ni(OH)_2$/graphene was reduced to Ni/graphene nanocomposite through hydrogen thermal treatment for 3 hours at 350 °C.

4.2.1 Characterization

In this part of the work, for elemental analysis and surface morphology, HRTEM fitted with EDX was used. HRTEM was performed utilizing a JEOL Jem 2001F microscope that has an electron accelerating voltage. The voltage ranges from 80kV to 200Kv. The Ni/graphene samples were prepared by adding the Ni/graphene powder in methanol. The solution was then prepared on carbon coated copper grids and analyzed. Elemental analysis was simultaneously using EDX on the TEM.

4.2.1.1 TEM Analysis

The TEM images of $Ni(OH)_2$/graphene before reduction (which were used as a reference) and after reduction can be observed on figure 4-2 below (images (a and c) before reduction and images (b and d) after reduction). The average particle size of the $Ni(OH)_2$ on the graphene had an average size ranging between 23 - 70 nm. It can be observed in images c and d on figure 4-2 that after the thermal reduction of $Ni(OH)_2$/graphene to Ni/graphene, the Ni particles on the graphene matrix were uniformly dispersed over the graphene surface with an average particle size of about 13 nm. The result of the elemental analysis of the Ni/graphene as depicted in Table 4-3 proves a successful preparation of Ni/graphene nanocomposite. The elemental analysis shows the presence of Ni (4.58%), O (10.29%) and C (86%) on the Ni/graphene surface, which corresponds to the component ratio utilized for the synthesis method.

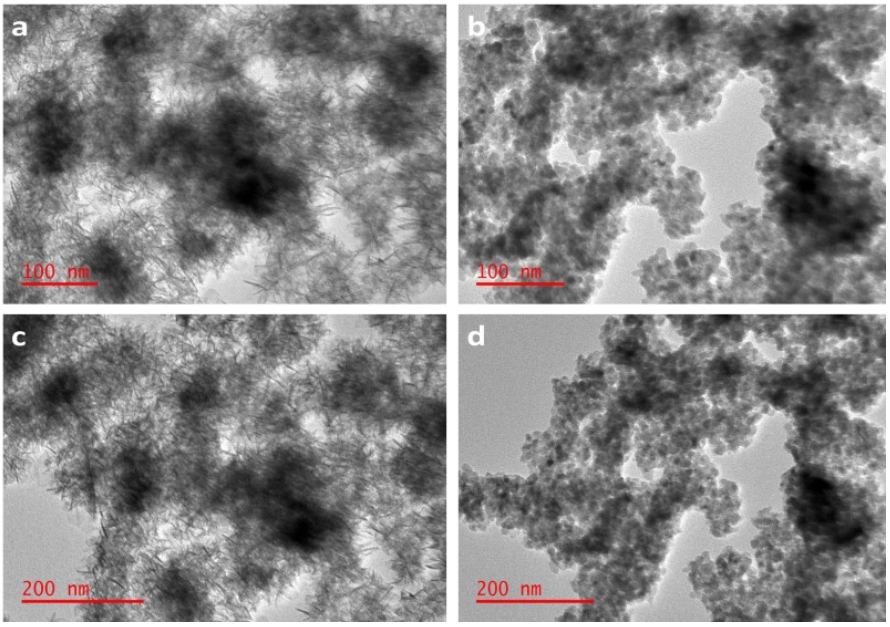

Figure 4-2. TEM images at 100 nm and 200 nm of (a & c), $Ni(OH)_2$/graphene and (b & d), Ni/graphene.

TEM Elemental Analysis:

Table 4-3. Chemical analysis of Ni/graphene sample.

Sample	C (%)	O (%)	Cu (%)	Cl (%)	Ni (%)	Total (%)
Ni/Graphene	86	10.29	0.08	0.27	4.58	100

CONCLUSION

The aim of this chapter was to develop metal/graphene nanocomposite for hydrogen storage from precursor graphene. The XRF elemental results obtained for the Ca/graphene nanocomposite showed the Ca content on the nanocomposite increased from 0.516 % to 8.227 %. The TEM images also showed the Ca particles uniformly dispersed over the graphene matrix. The EDX elemental analysis of the Ni/graphene also showed an increase on the Ni content on the surface of graphene and the TEM results also showed that the Ni particles were uniformly dispersed on the surface of the graphene. These results, in effect, prove that the aims of this chapter were successfully completed.

REFERENCES

De Silva, K. K. H., Huang, H.-H., & Yoshimura, M. (2018). Progress of reduction of graphene oxide by ascorbic acid. *Applied Surface Science*, *447*, 338–346. https://doi.org/https://doi.org/10.1016/j.apsusc.2018.03.243

Gurunathan, S., Park, J., Choi, Y., jae woong, H., & Kim, J.-H. (2016). Synthesis of Graphene Oxide-Silver Nanoparticle Nanocomposites: An Efficient Novel Antibacterial Agent. *Current Nanoscience*, *12*, 762–773. https://doi.org/10.2174/1573413712666160721143424

Ngqalakwezi, A., Nkazi, D., Seifert, G., & Ntho, T. (2019). Effects of reduction of graphene oxide on the hydrogen storage capacities of metal graphene nanocomposite. *Catalysis Today*. https://doi.org/https://doi.org/10.1016/j.cattod.2019.06.029

O'Hare, D. (2001). *Hydrothermal Synthesis* (K. H. J. Buschow, R. W. Cahn, M. C. Flemings, B. Ilschner, E. J. Kramer, S. Mahajan, & P. B. T.-E. of M. S. and T. Veyssière (eds.); pp. 3989–3992). Elsevier. https://doi.org/https://doi.org/10.1016/B0-08-043152-6/00701-4

Pei, S., Wei, Q., Huang, K., Cheng, H.-M., & Ren, W. (2018). Green synthesis of graphene oxide by seconds timescale water electrolytic oxidation. *Nature Communications*, *9*(1), 145. https://doi.org/10.1038/s41467-017-02479-z

Pumera, M. (2011). Graphene-based nanomaterials for energy storage. *Energy & Environmental Science*, *4*(3), 668–674. https://doi.org/10.1039/C0EE00295J

Shams, S. S., & Zhang, R. (2015). Graphene synthesis: A Review. *Materials Science-Poland*, *33*. https://doi.org/10.1515/msp-2015-0079

Texter, J. (2014). Graphene dispersions. *Current Opinion in Colloid & Interface Science*, *19*(2), 163–174. https://doi.org/https://doi.org/10.1016/j.cocis.2014.04.004

Wang, M. (2012). *Graphene Nanocomposites* (C. Yan (ed.); p. Ch. 2). IntechOpen.

https://doi.org/10.5772/50840

Yang, J., Zang, C., Sun, L., Zhao, N., & Cheng, X. (2011). Synthesis of graphene/Ag nanocomposite with good dispersibility and electroconductibility via solvothermal method. *Materials Chemistry and Physics*, *129*(1), 270–274. https://doi.org/https://doi.org/10.1016/j.matchemphys.2011.04.002

Zhou, C., & Szpunar, J. A. (2016). Hydrogen Storage Performance in Pd/Graphene Nanocomposites. *ACS Applied Materials & Interfaces*, *8*(39), 25933–25940. https://doi.org/10.1021/acsami.6b07122

Zhou, C., Szpunar, J. A., & Cui, X. (2016). Synthesis of Ni/Graphene Nanocomposite for Hydrogen Storage. *ACS Applied Materials & Interfaces*, *8*(24), 15232–15241. https://doi.org/10.1021/acsami.6b02607

CHAPTER 5

5. HYDROGENATION OF THE NI/GRAPHENE AND CA/GRAPHENE NANOCOMPOSITES AND CHARACTERIZATION TESTS THEREOF

Graphical Abstract

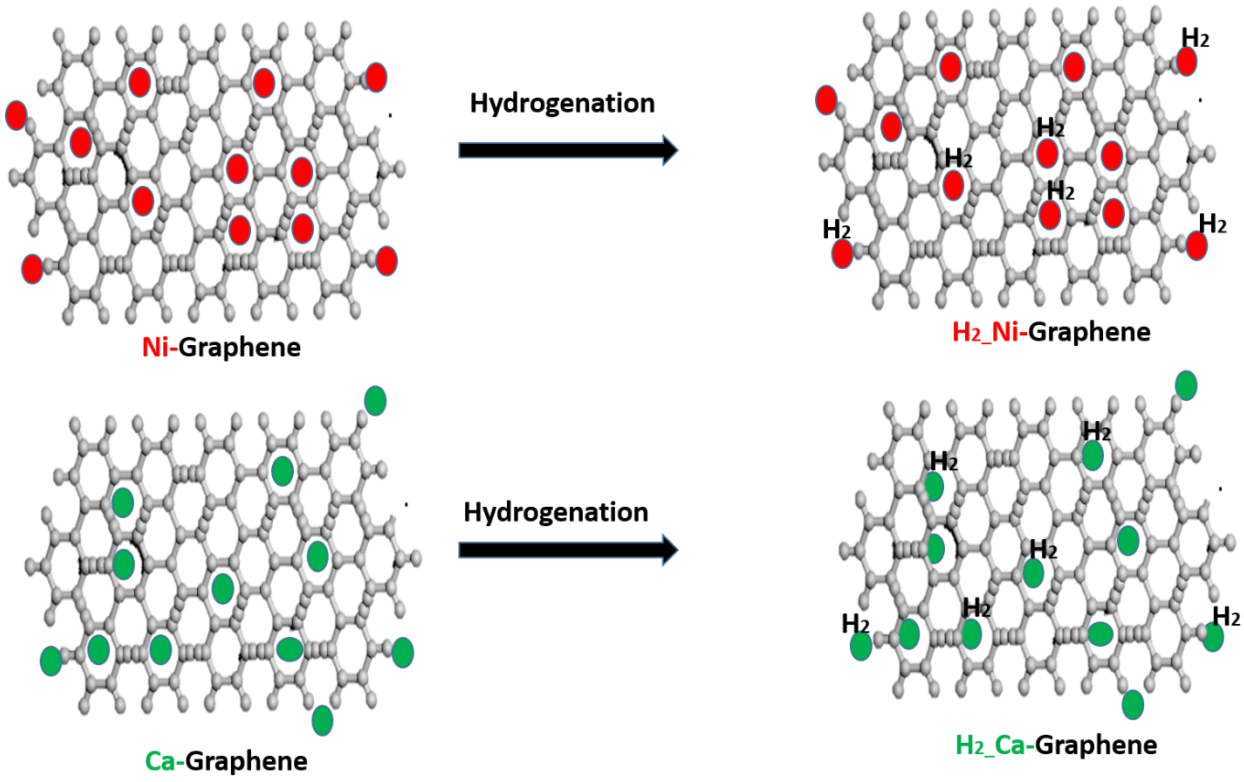

Sections of this chapter was published

Introduction

Undeniably, fossil fuels have been an integral part of the human race since their discovery and application globally. However, the impact on the environment has been severe and a need for new sources of energy became a necessity (Houghton, 2001). Hydrogen as a clean source of energy has gained a lot of attention as a replacement source for fossil fuels (Zaluska et al., 2001). Various materials have been extensively studied in this regard and a material that ticks all the on-board application requirements has not yet been developed. Amongst these materials, graphene has gained considerable amount attention for hydrogen storage applications (Venkatesan et al., 2015a). Theoretically, graphene as a single sheet of carbon atoms has been predicted to have a hydrogen capacity of about 8.3 wt.%. However it has been acknowledged that the theoretical studies around graphene for hydrogen storage are very far from practical conditions (Diana C. Tranca & Gotthard Seifert, 2016). However, the theoretical studies provide a deeper understanding for the hydrogenation process such as the strain and curvature in graphene sheets influence the adsorption capacity (Diana C. Tranca & Gotthard Seifert, 2016)s.

Furthermore, Graphene has a large surface area which is approximately 2630 m^2g^{-1}, put into practical use, this means graphene can theoretically be hydrogenated on both of its surfaces (Choi et al., 2010). A graphene with fewer layers can adsorb hydrogen molecule in the interlayer spacing and on the exposed surfaces of the top and bottom sheets (Jhi et al., 2004). However these amounts are usually less and do not meet the minimum required amounts for practical use. It then, became imperative to work around enhancing the hydrogen capacity of these material through decoration with metals that have a hydrogen storage capacity (M. Wang, 2012). As such, a lot of work has been done to functionalized graphene in an attempt to enhance its hydrogen storage capacity. In this chapter, the functionalized graphene nanocomposites were charged with hydrogen at various pressures and then were tested for hydrogen storage. To test the hydrogenation capacity of the as prepared metal/graphene nanocomposites and the desorption thereof, the thermogravimetric analysis (TGA) and TPD were used respectively.

5.1 Method: Ca/graphene nanocomposite

The Ca/graphene was charged with hydrogen in a 4540 Parr reactor at 10 bars and ambient temperature for 30 minutes. The sample results were then analysed.

The hydrogen storage capacity of the synthesized Ca/graphene was analyzed by performing a TGA analysis on hydrogen charged Ca/graphene and non-hydrogen charged Ca/graphene as a reference point. During analysis, the Ca/graphene nanocomposite was heated at a rate of 10°C/min to 500 °C under inert conditions (N_2) on the SDT Q600 Thermal Analyzer instrument.

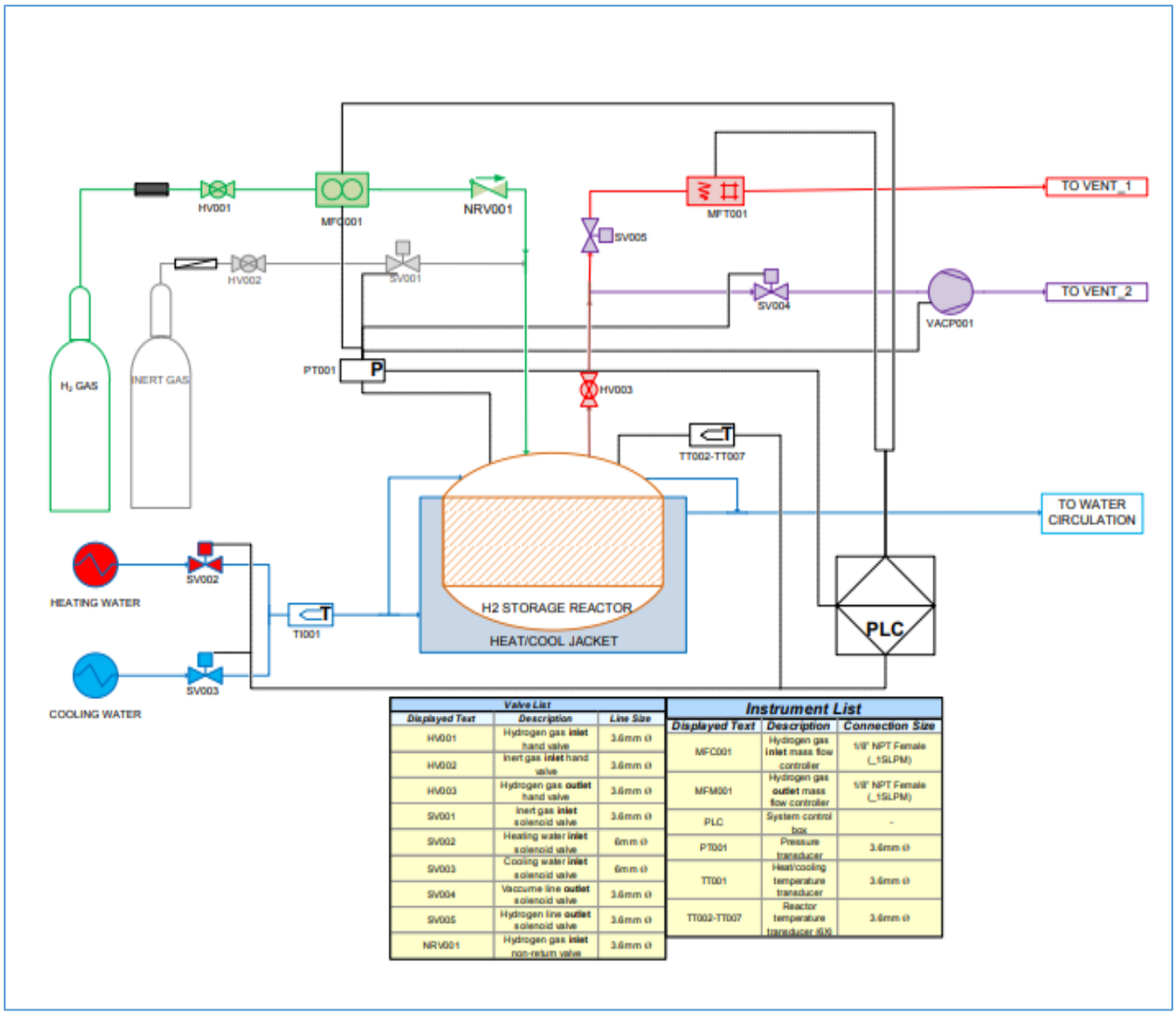

Valve List		
Displayed Text	Description	Line Size
HV001	Hydrogen gas inlet hand valve	3.6mm ø
HV002	Inert gas inlet hand valve	3.6mm ø
HV003	Hydrogen gas outlet hand valve	3.6mm ø
SV001	Inert gas inlet solenoid valve	3.6mm ø
SV002	Heating water inlet solenoid valve	6mm ø
SV003	Cooling water inlet solenoid valve	6mm ø
SV004	Vaccume line outlet solenoid valve	3.6mm ø
SV005	Hydrogen line outlet solenoid valve	3.6mm ø
NRV001	Hydrogen gas inlet non-return valve	3.6mm ø

Instrument List		
Displayed Text	Description	Connection Size
MFC001	Hydrogen gas inlet mass flow controller	1/8" NPT Female (_1SLPM)
MFM001	Hydrogen gas outlet mass flow controller	1/8" NPT Female (_1SLPM)
PLC	System control box	-
PT001	Pressure transducer	3.6mm ø
TT001	Heat/cooling temperature transducer	3.6mm ø
TT002-TT007	Reactor temperature transducer (6X)	3.6mm ø

Figure 5-1: Hydrogen charging rig

5.2 Results

Thermogravimetric analysis of Ca/graphene was performed and Figure 5-2 below shows the weight loss of nanocomposite before and after reduction. The weight loss in the Ca/graphene is ascribed to the labile oxygen groups and the adsorbed water on the Ca/graphene [23].

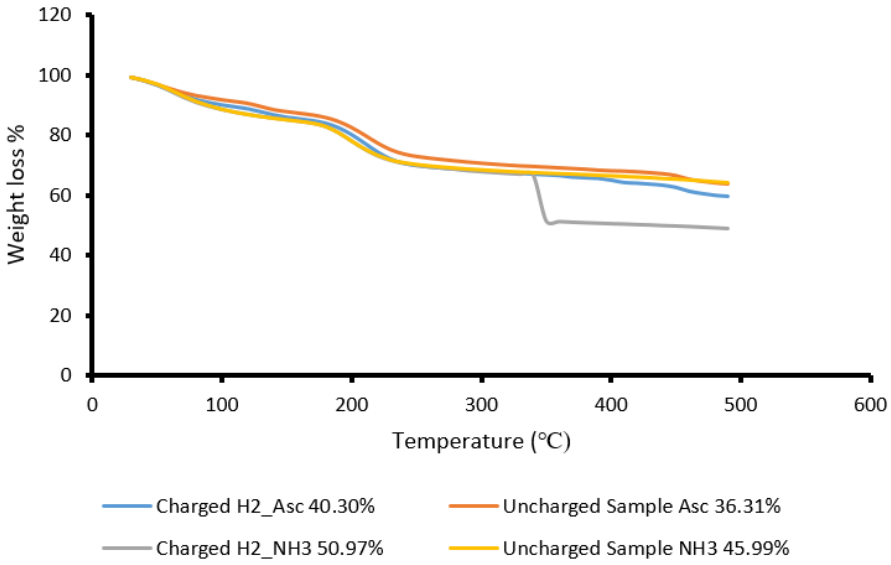

Figure: 5-2: TGA weight loss plot against temperature for the Ca/graphene samples

The hydrogen capacity of the material was examined by performing TGA on hydrogen charged Ca/graphene and non-hydrogen charged Ca/graphene. The charged Ca/graphene had a total weight loss of 50.97 wt.% and the non-charged Ca/graphene lost about 45.99%. The hydrogen uptake was calculated to be 4.98 wt.%. These results prove that the hydrogen uptake of graphene was improved through incorporating Calcium onto the graphene matrix. Graphene reportedly has hydrogen uptake of about 2 wt.% at 50 bars and 77K [23].

5.3 Method: Ni/graphene nanocomposite

The Ni/graphene was charged with hydrogen in a 4540 Parr reactor at 0, 5 and 10 bars and ambient temperature for 30 minutes. The hydrogen charged samples were firmly sealed and then analysed for hydrogen uptake.

The hydrogen storage capacity test of Ni/graphene was done on the SDT Q600 Thermal Analyzer instrument. Both the hydrogen charged Ni/graphene and non-charged Ni/graphene were heated up at a ramp rate of 10ºC/min under the constant flow of nitrogen. The hydrogen

storage uptake of the sample was quantified using the weight percentage of the sample which was taken as a function of temperature. The sample not charged with hydrogen (0 bar) was used as a reference sample.

5.4 Results

The thermogravimetric results of the Ni/graphene nanocomposite can be observed in figure 5-3 below. The Ni/Graphene used as reference point (non-hydrogen charged) depicted a lower mass loss in comparison to the charged sample. The mass loss in this sample was due to the removal of gas impurities and adsorbed moisture on the sample. The Ni/graphene charged with hydrogen charged samples depicted a rapid decrease in mass with increasing temperature as shown from Figure 5-3. Zhou et al. reported on the parameters that potentially affect the change in mass of the samples charged with hydrogen when utilizing TGA: removal of gas toxins and adsorbed water during the transfer process, elimination of water due to possible oxidation of hydrogen at the presence of Ni during the transfer process, dehydrogenation and the reduction of hydrogen in NiOx, and an irreversible interaction between hydrogen and Ni/graphene nanocomposite during thermal treatment (Thakur & Karak, 2012; Thomsen & Reich, 2000; Zhou et al., 2016).

Therefore, these assumptions were taken into account when quantifying the hydrogen uptake. As mentioned above, the uncharged nanocomposite as a reference. The Ni/graphene nanocomposite had a hydrogen uptake 0.25 wt.% at room temperature and pressure. The hydrogen storage uptake increased with an increasing charging pressure and as such at 10 bars the hydrogen storage uptake was 2.78 wt.%.

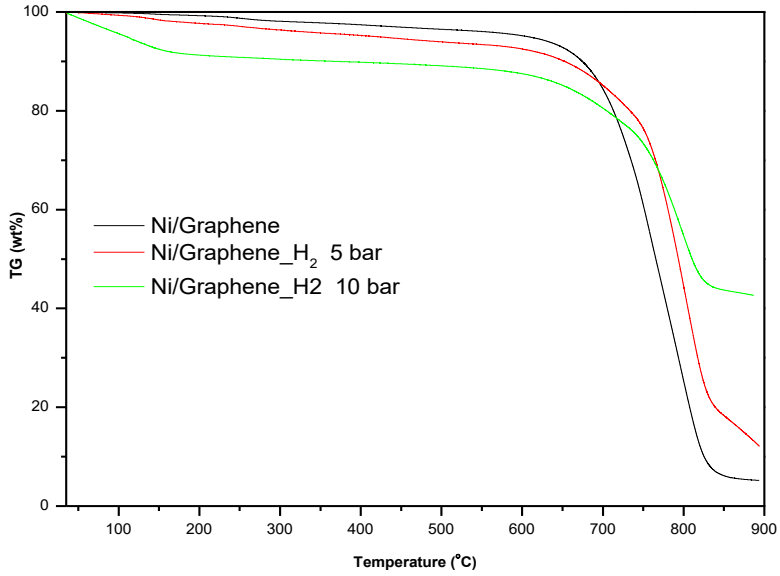

Figure: 5-3: TGA weight loss plot against temperature for the Ni/graphene samples

CONCLUSION

The aim of this chapter was to test the hydrogen storage capacity of the synthesized Ni/graphene and Ca/graphene. The synthesized nanocomposites were tested using the thermogravimetric analysis. Considerations such as the removal of gas toxins and adsorbed water were taken into account when quantifying the hydrogen storage uptake of the material. The novel Ca/graphene has a hydrogen storage capacity of about 4.98 w% and Ni/graphene has hydrogen storage capacity 2.78 wt.% both at 10 bars. The hydrogen uptake of graphene was significantly improved by the incorporation of Ni and Ca into the graphene matrix. During the hydrogenation process, it was observed that the hydrogen uptake increased with increasing pressure. The results obtained prove that the aims of this chapter were successfully accomplished.

REFERENCES

Choi, W., Lahiri, I., Seelaboyina, R., & Kang, Y. S. (2010). Synthesis of Graphene and Its Applications: A Review. *Critical Reviews in Solid State and Materials Sciences*, *35*(1), 52–71. https://doi.org/10.1080/10408430903505036

Diana C. Tranca & Gotthard Seifert. (2016). A First-Principles Study of Metal-Decorated Graphene Nanoribbons for Hydrogen Storage. *De Gruyter*, *230*, 791-808,.

Houghton, J. (2001). The science of global warming. *Interdisciplinary Science Reviews*, *26*(4), 247–257. https://doi.org/10.1179/isr.2001.26.4.247

Jhi, S.-H., Kwon, Y.-K., Bradley, K., & Gabriel, J.-C. P. (2004). Hydrogen storage by physisorption: beyond carbon. *Solid State Communications*, *129*(12), 769–773. https://doi.org/https://doi.org/10.1016/j.ssc.2003.12.032

Thakur, S., & Karak, N. (2012). Green reduction of graphene oxide by aqueous phytoextracts. *Carbon*, *50*(14), 5331–5339. https://doi.org/https://doi.org/10.1016/j.carbon.2012.07.023

Thomsen, C., & Reich, S. (2000). Double Resonant Raman Scattering in Graphite. *Physical Review Letters*, *85*(24), 5214–5217. https://doi.org/10.1103/PhysRevLett.85.5214

Venkatesan, A., Patel, R. N., & Kannan, E. S. (2015). Reduced Graphene Oxide for Room Temperature Hydrogen Storage Application. *Advanced Materials Research*, *1086*, 91–95. https://doi.org/10.4028/www.scientific.net/AMR.1086.91

Wang, M. (2012). *Graphene Nanocomposites* (C. Yan (ed.); p. Ch. 2). IntechOpen. https://doi.org/10.5772/50840

Zaluska, A., Zaluski, L., & Ström-Olsen, J. O. (2001). Structure, catalysis and atomic reactions on the nano-scale: a systematic approach to metal hydrides for hydrogen storage. *Applied Physics A*, *72*(2), 157–165. https://doi.org/10.1007/s003390100783

Zhou, C., Szpunar, J. A., & Cui, X. (2016). Synthesis of Ni/Graphene Nanocomposite for Hydrogen Storage. *ACS Applied Materials & Interfaces*, *8*(24), 15232–15241. https://doi.org/10.1021/acsami.6b02607

CHAPTER 6

6. EFFECTS OF REDUCTION OF GRAPHENE OXIDE ON THE HYDROGEN STORAGE CAPACITIES OF METAL GRAPHENE NANOCOMPOSITE

This chapter was published on Catalysis Today as is.

Graphical Abstract

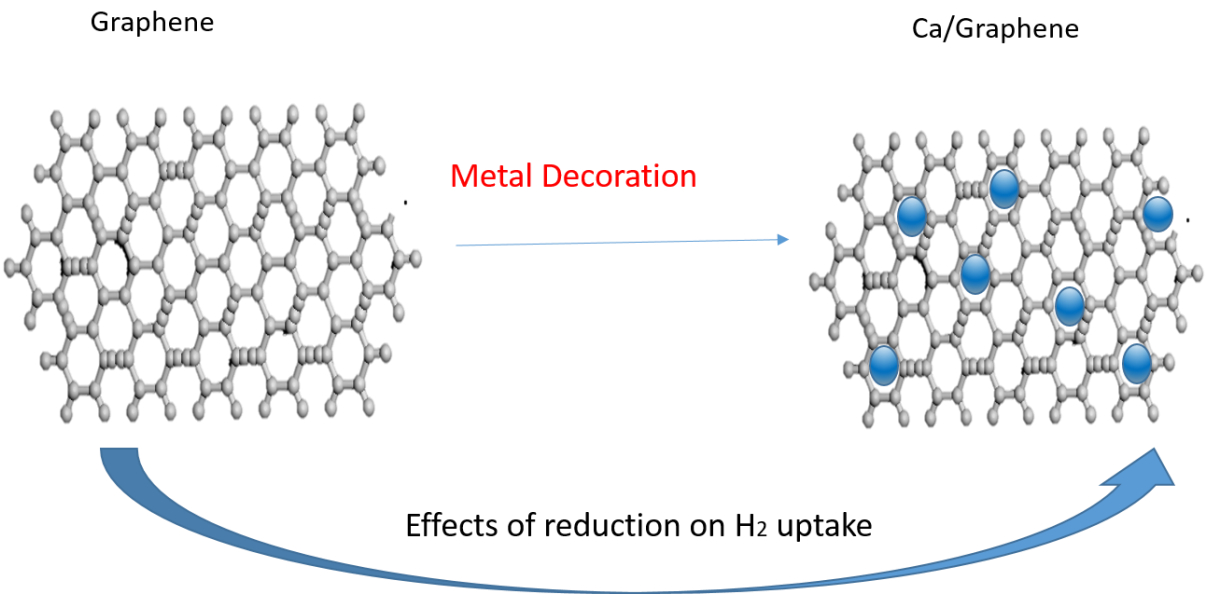

Introduction

One of the mandate of sustainable development goals globally is to make the environment a cleaner place. As such, the possibility of using hydrogen as an alternative source of energy has garnered a lot of attention due to its zero emission characteristic to the environment, high energy content and its abundant availability (Dutta & Pati, 2010) (Patchkovskii et al., 2005). However, the major challenge with hydrogen is the storage. The storage of hydrogen is governed by the US Department of Energy (DOE), which sets the standards for on-board systems (Energy, 2018). To date, no material has fully met the DOE requirements for on-board applications. Various materials have been experimentally tested for solid state storage of hydrogen because gaseous and liquid storage of hydrogen pose cost and energy challenges (Balandin et al., 2008; C. Lee et al., 2008; Venkatesan et al., 2015b). One of the material tested for solid storage of hydrogen is graphene based material because graphene has intriguing properties such as extra-ordinary mechanical strength, transport performance, increased movement of charge carriers and high surface area (Balandin et al., 2008; Jiang et al., 2010; C. Lee et al., 2008; S. Yang et al., 2011). Graphene is an allotrope of carbon which is characterized by a monolayer of sp^2 carbon atoms. Graphene can be synthesized through graphite intercalation, chemical vapour deposition, micromechanical cleavage and the reduction of graphite oxide (Geng et al., 2010; K. S. Kim et al., 2009; Xiang et al., 2012; Pei et al., 2018). The reduction of graphite oxide has been the common route of producing graphene.

The method of reduction of graphene has an effect on the structure of graphene and thereby its hydrogen storage capacity. It has been reported that thermally reduced graphene acquires a significant number of structural defects which act as binding sites for hydrogen (C. Lee et al., 2008) (Zhou & Szpunar, 2016). However Graphene alone as a physisorbent material does not take up a lot of hydrogen and thereby has to be enhanced through the addition of active metals for practical on-board applications. The incorporation of active nanometals on graphene helps in tuning the electronic structure and surface morphology of graphene (C. Hu et al., 2013). A number of metal/graphene nanocomposites have been synthesized in this regard and a lot of DFT studies have been performed (Diana C. Tranca & Gotthard Seifert, 2016). A Pd/graphene nanocomposite was synthesized with 6.7 wt.% at 50 bars (Zhou & Szpunar, 2016).

In this work ammonia and L-Ascorbic were used as reductants instead of hydrazine. Hydrazine due to its hazardous nature and cost, remains undesirable as a reductant. Furthermore in this work, different reduction techniques such as chemical reduction and thermal reduction are

explored. Calcium was also used to improve the catalytic activity of graphene in the uptake of hydrogen. The effect of the reduction techniques on the hydrogen storage capacity of graphene and the metal incorporation thereof were studied.

6.1 Method

The method of synthesis is as described in chapter 3 discussed earlier. Improved Tour's method was utilized to synthesize graphene. Different reductants such as L-ascorbic acid, thermal reduction and ammonia. The effect of the reductants on the hydrogen storage capacity was evaluated.

6.2 Results and Discussion

6.2.1 Structure/texture characterization of the materials

6.2.1.1 Raman

As mentioned in chapter 3, Raman is a vibrational characterization technique that is sensitive to geometric structure and bonding within molecules. Raman was utilized to detect the structural differences during the oxidation process of graphite flakes and the reduction processes of graphite oxide. In the Raman spectra, the important bands are the G, D and 2D bands. Figure 6-1 shows the spectra graphite flakes A, graphite oxide B, NH_3 reduced graphene C and. Ascorbic acid reduced graphene D

.

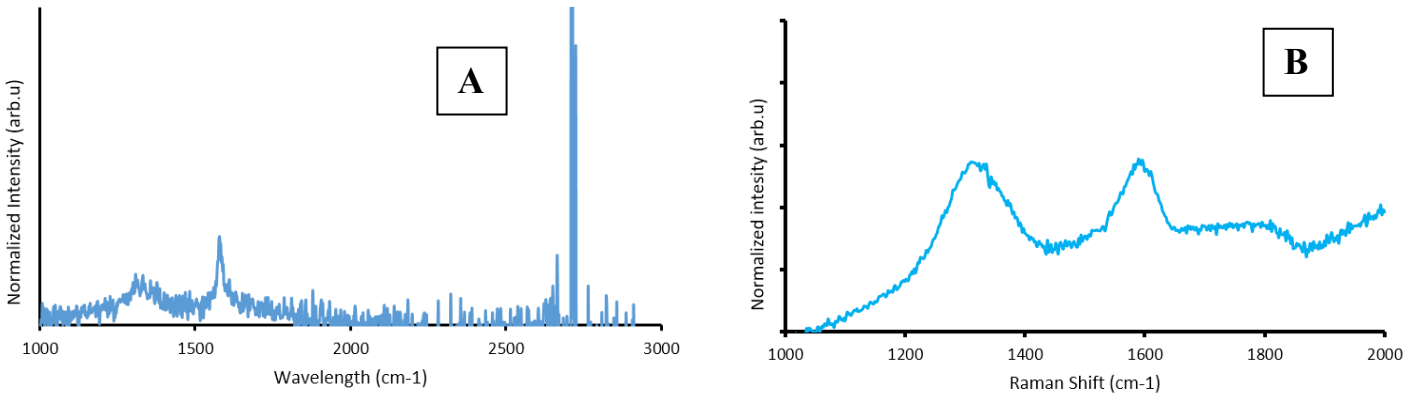

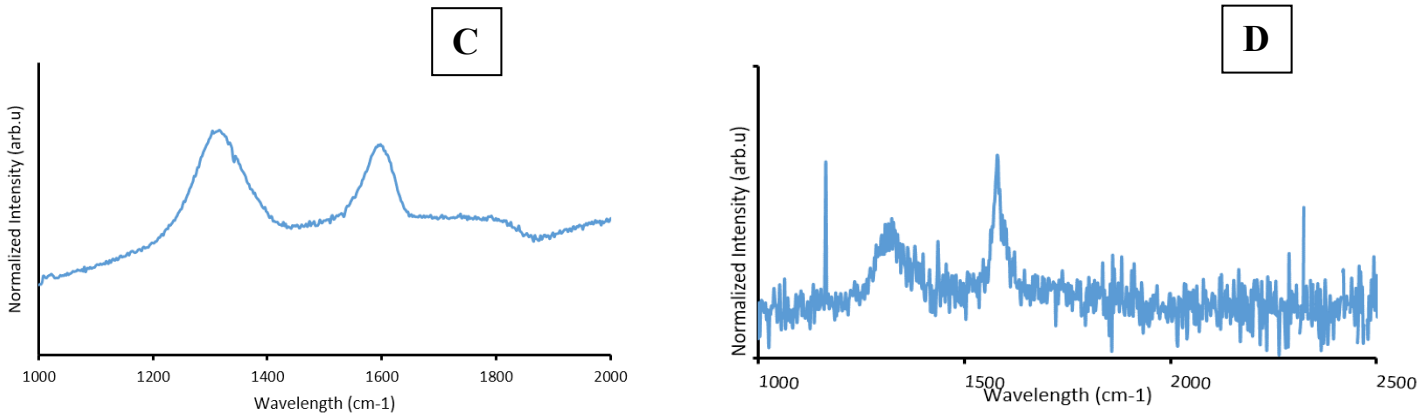

Figure 6-1: A. graphite flakes, B. GO, C. NH_3 reduced graphene D. Ascorbic acid reduced graphene

The Raman spectra shown in figure 4(A) depicts the G band in graphite flakes at ~1582 cm^{-1}. The G band position in graphite flakes is positioned in an in-plane mode. This mode is highly sensitive to the number of layers in graphene and it involves sp^2 hybridized carbon. The G band shifted in reduced graphene to ~ 1598 cm^{-1}. This shift observed is due to the increase on the layer thickness of the material and the increase in lay thickness results in the band shifting towards a lower energy position. The number of layers available in a material can be correlated to the band position using this correlation:

$$\omega_G = 1581.6 + \frac{11}{(1+n^{1.6})}\ [17]$$

The temperature affects the G band and during the reduction step, as such the temperature was kept constant. The D band can be observed approximately between 1327-1342 cm^{-1} wavelength. This band is the disorder band which only appears in the presence of defects. Defects occur during the oxidation and reduction processes in the synthesis of graphene. The D band for graphite flakes can be observed at ~1324 cm^{-1}, for graphite oxide at ~1332 cm^{-1} and for reduced graphene it appears around ~1340 cm^{-1}. The graphite flakes D band has a low intensity because it has defects. Again, on the graphite flakes spectrum, the 2D band can be seen at ~2714 cm^{-1} wavelength. The 2D band can be observed because of the vibrational process of the two phonon lattice. The increase in number of layers affects the intensity of this band and symmetry resulting in the decrease of this band.

The I_D/I_G intensity ratio was increased from 0.84 graphite oxide to 1.19 in ammonia reduced graphene and 1.21 in ascorbic reduced graphene. This was indicative of the formation sp^2 domains and the reduction of the functional groups on the plane

6.2.1.2 XRD

As discussed in chapter 3, X-ray diffraction is a non-destructive analysis for analyzing crystalline materials. XRD functions by scattering of x-ray photons using atoms in a periodic lattice. The smattered x-rays in the phase provide constructive interference. This gives an indication of structural parameters, crystals defects, phases, crystal orientation and crystallinity.

The XRD results are shown below on figure 5. Before the analysis of the synthesized samples, some of the samples were crushed to obtain powder. In these results, a very sharp peak at $\sim 2\theta = 30°$ can be observed in graphite flakes spectrum. This corresponds to the hexagonal arrangement in the materials and in the packing of atomic layers within the material. In the GO spectrum, the angle shifts lower due the oxidation of the crystalline structure that results in increased interplanar spacing. The GO peak corresponds to the d_{001} plane and can be observed at $\sim 2\theta = 11.3°$. Furthermore, the broadness of the GO peak confirms the presence of functional groups in the material due to the oxidation process. The reduced graphite oxide oxidation peaks in spectrum C, are observed to decrease due to the reduction process. These results confirm that the graphite was successfully oxidized and subsequently reduced. For the reduction step, a broad peak can be observed on the ascorbic reduced graphene which indicates loss of crystallinity and extreme decrease in the interplanar spacing (Oliveira, 2018). The results show that graphite was successfully oxidized and reduced with L-Ascorbic acid.

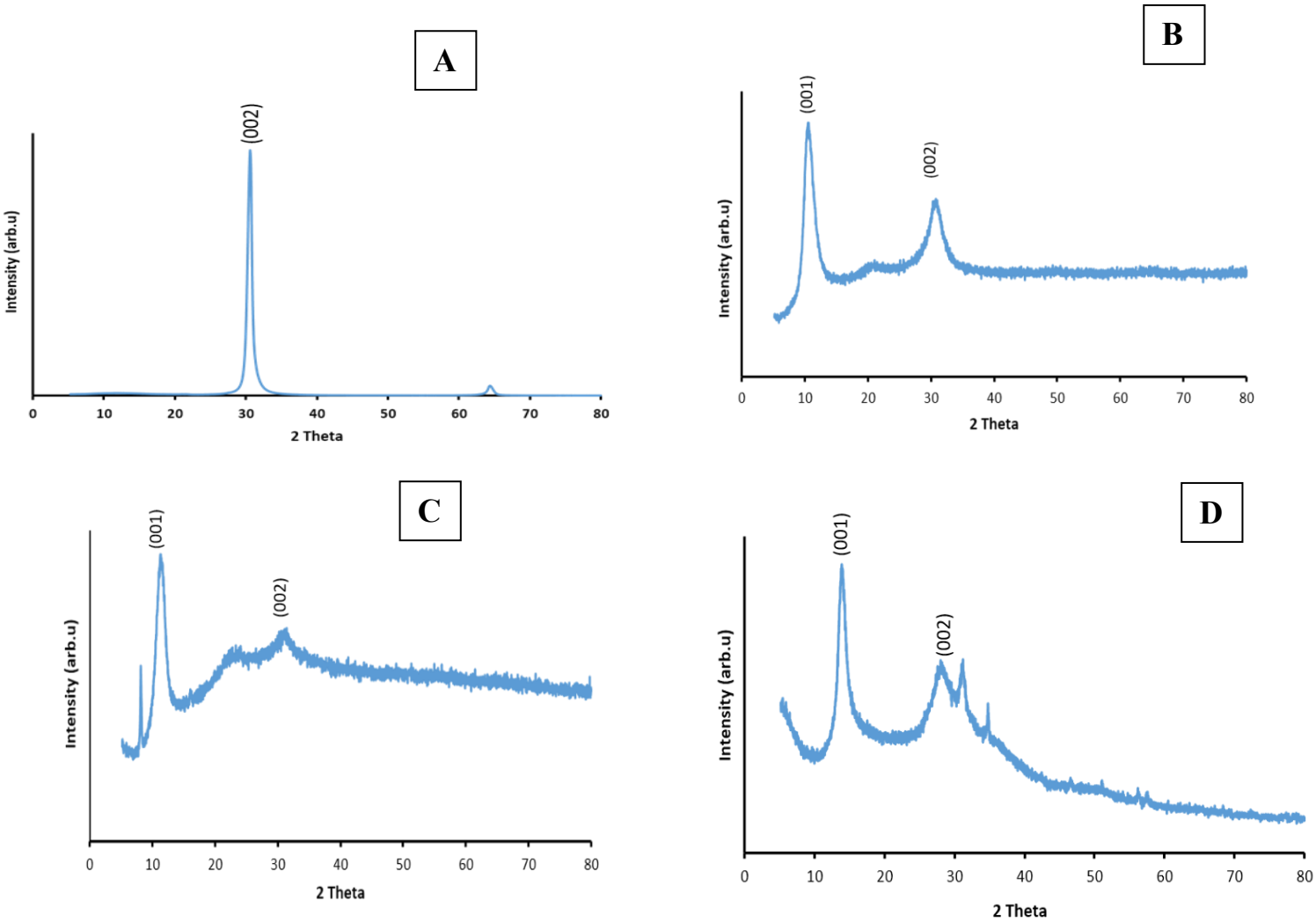

Figure 6-2: XRD patters of the samples where A. graphite flakes, B.GO, C. Ascorbic acid reduced graphene D. NH_3 reduced graphene, E. Thermally reduced graphene

6.2.1.3 FTIR Results

Fourier transform infrared spectroscopy is an analysis method that is utilized to detect polymeric and organic materials. This method utilizes infrared light to scan test samples and detect their chemical properties. The bonds within and between different materials absorb light and various frequencies. The absorbance by the material gives indications to the materials molecular structure and composition.

The FTIR spectroscopy is also associated with molecular vibrations or atomic vibrations within a material. These vibrations are utilized to detect functional groups by analyzing the frequencies to detect molecules. The FTIR spectra detected several functional groups: O-H (3422 cm^{-1}) stretching vibrations, C=O (1719-1754 cm^{-1}) vibrations, C=C (1595-1623 cm^{-1})

vibrations and C-O (1215-1252 cm^{-1}) vibrations. The OH- stretch which can be seen on the samples is because of the presence of water in the graphene layers. The observed reduction in the intensity on the bands is due to the reduction process. Therefore, this affirms that graphite oxide was successfully reduced. The decline in the intensity of the bands can be visibly observed for the samples reduced with Ascorbic acid, while the ammonia reduced graphene spectra shows minimal change in the intensity of the bands. Therefore this confirms that graphite oxide was successfully reduced with Ascorbic while it was partially reduced with ammonia.

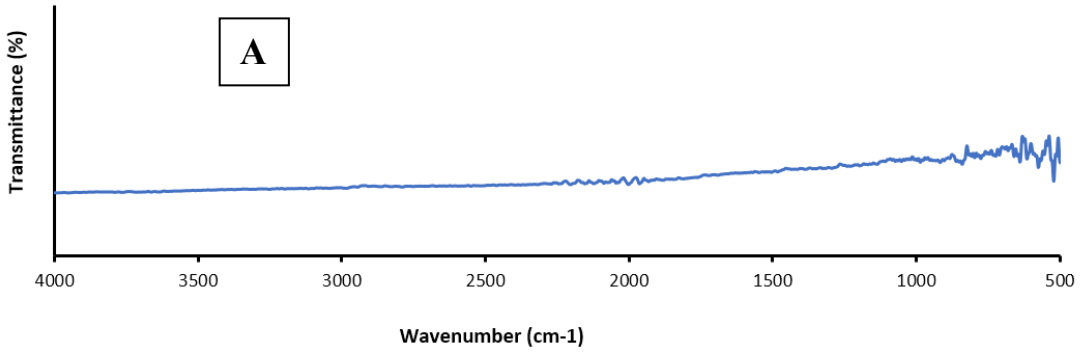

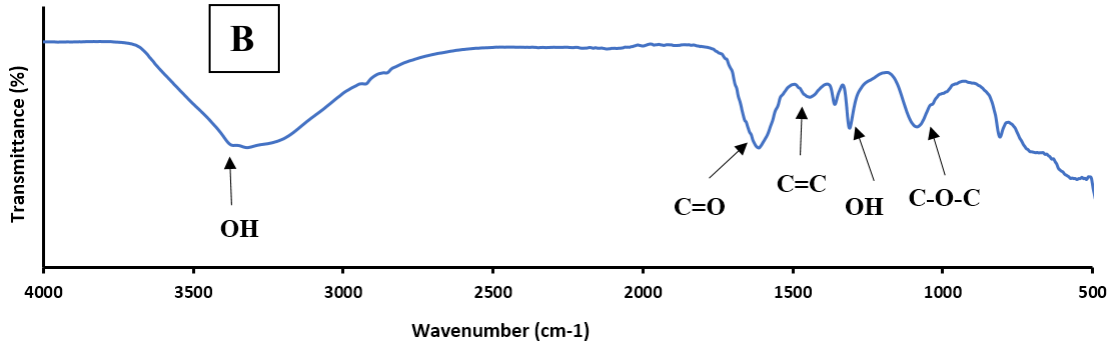

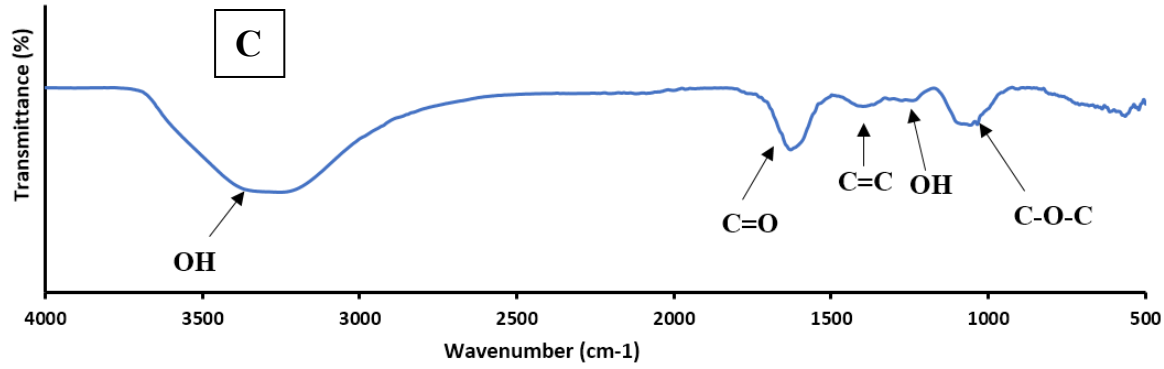

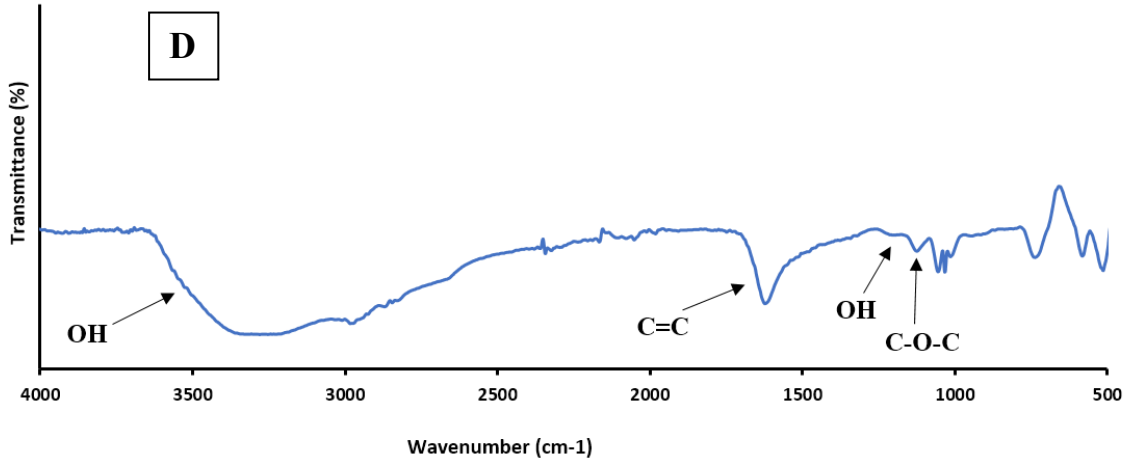

Figure 6-3: FTIR spectra A. Graphite B. GO, C. Ascorbic acid reduced graphene D. NH_3 reduced graphene

6.2.1.5 TEM Analysis

The surface characterization of the morphology of as-prepared metal/graphene, graphene oxide and graphene was performed using Transmission electron microscope. Transmission electron microscope is an analysis tool that utilizes an electron beam to image a high resolution nanoparticle sample. The analysis gives indication of the morphology, grain size, nanoparticle size and size distribution of materials. For the analysis, all the samples were prepared by dissolving them in a solvent and then pipetting it on the holey carbon coated copper grids.

Graphene reduced with ammonia, L-Ascorbic acid and thermally reduced graphene can be observed in Figure 6 C, D and E respectively. Ammonia reduced graphene (Figure 6 (C)) looks semi-transparent and the morphology depicts irregular shaped layers with irregular surfaces. The irregularity and tangles on the surface are because of the partial reduction of graphene with ammonia. L-Ascorbic reduced graphene (Figure 6 (D)) depicts more transparent layers with folding and wrinkles both on the edges and surface of the structure. Thermally reduced graphene (Figure 6 (E)) depicts flat layers which are layered. The rough surfaces on the edges and irregularity in the shape can also be seen on the captured image. Figure 6 (F) ammonia reduced and (G) L-Ascorbic reduced depicts observable particles of calcium on the surface which were previously not observed.

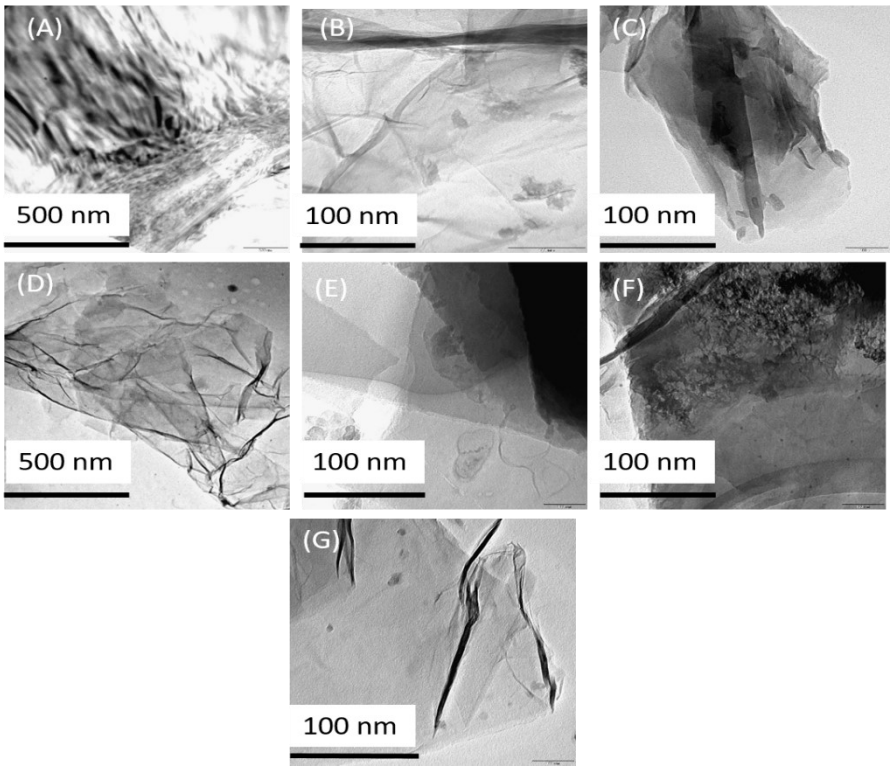

Figure 6-4: TEM morphological analysis of A. Graphite flakes B. GO, C. Ammonia acid reduced graphene D. L-Ascorbic reduced graphene E. Thermally reduced graphene F. Ca/Graphene_Ammonia G. Ca/Graphene_L-Ascorbic acid

6.3 Thermogravimetric Analysis

Thermogravimetric analysis of Ca/graphene was performed and Figure 6-5 below shows the weight loss of nanocomposite before and after reduction. The weight loss in the Ca/graphene is ascribed to the labile oxygen groups and the adsorbed water on the Ca/graphene (Kanishka et al., 2018).

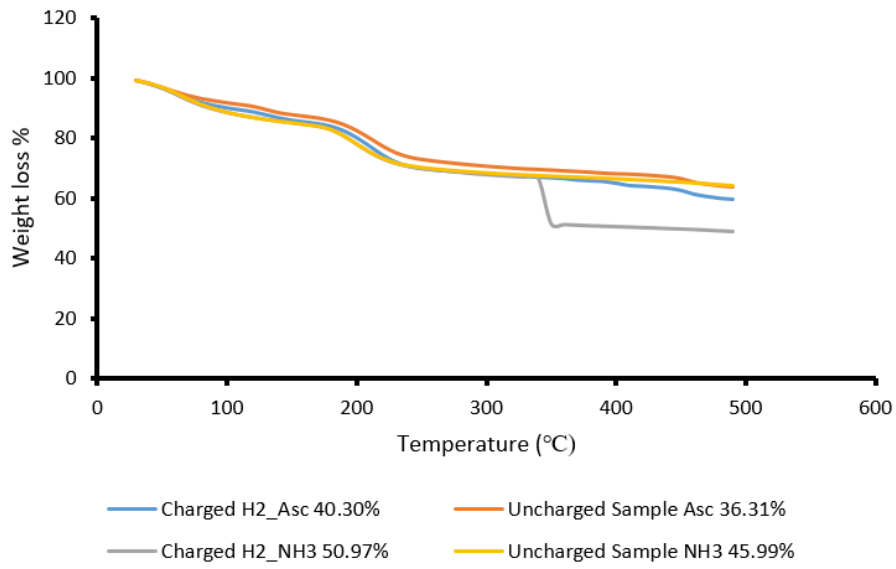

Figure 6-5: TGA weight loss plot against temperature for the Ca/graphene samples reduced with ammonia and Ascorbic acid before and after hydrogen charging

The hydrogen capacity of the material was examined by performing TGA on hydrogen charged Ca/graphene and non-hydrogen charged Ca/graphene for both samples reduced with ammonia and L-Ascorbic acid. The charged Ca/graphene reduced with ammonia had a total weight loss of 50.97 wt% and the non-charged Ca/graphene lost about 45.99%. The hydrogen uptake was calculated to be 4.98 wt.%. The charged Ca/graphene reduced with L-Ascorbic acid had a weight loss of about 36.31 wt.% and 40.30 wt% before and after charging respectively. The hydrogen uptake for the L-ascorbic reduced graphene was 3.99 wt.%. These results prove that the hydrogen uptake of graphene was improved through incorporating Calcium onto the graphene matrix. Graphene reportedly has hydrogen uptake of about 2 wt.% at 50 bars and 77K (Sterlin et al., 2014). Ammonia as a reductant has a N-doping effect on the graphene and improves the hydrogen uptake. In the results, this can be observed, the ammonia reduced Ca/graphene had a hydrogen storage capacity above that of the L-ascorbic reduced Ca/graphene.

CONCLUSION

In this chapter, the aim was to investigate the effects of reduction of graphene on the hydrogen storage capacity of the as prepared metal/graphene nanocomposite. The characterization results presented in this chapter showed from the XRD and FTIR results, L-Ascorbic acid reduced the graphene better than ammonia. However, the ammonia had a nitrogen doping effect on the graphene and this enhances the hydrogen uptake of the material. In the hydrogen storage results, it was observed that the Ca/graphene reduced with ammonia had a higher hydrogen uptake at 4.98 wt.% compared to the Ca/graphene reduced with L-Ascorbic acid which had a hydrogen storage uptake of 3.99 wt%. The reduction with ammonia enhanced the hydrogen storage capacity.

REFERENCES

Balandin, A., Ghosh, S., Bao, W., Calizo, I., Teweldebrhan, D., Miao, F., & Lau, J. (2008). Superior Thermal Conductivity of Single-Layer Graphene. *Nano Letters*, *8*, 902–907. https://doi.org/10.1021/nl0731872

Diana C. Tranca & Gotthard Seifert. (2016). A First-Principles Study of Metal-Decorated Graphene Nanoribbons for Hydrogen Storage. *De Gruyter*, *230*, 791-808,.

Dutta, S., & Pati, S. K. (2010). Novel properties of graphene nanoribbons: a review. *Journal of Materials Chemistry*, *20*(38), 8207–8223. https://doi.org/10.1039/C0JM00261E

Energy, D. of. (2018). *Hydrogen Storage*.

Geng, J., Kong, B.-S., Yang, S. B., & Jung, H.-T. (2010). Preparation of graphene relying on porphyrin exfoliation of graphite. *Chemical Communications*, *46*(28), 5091–5093. https://doi.org/10.1039/C001609H

Hu, C., Lu, T., Chen, F., & Zhang, R. (2013). A brief review of graphene–metal oxide composites synthesis and applications in photocatalysis. *Journal of the Chinese Advanced Materials Society*, *1*(1), 21–39. https://doi.org/10.1080/22243682.2013.771917

Jiang, H.-L., Singh, S. K., Yan, J.-M., Zhang, X.-B., & Xu, Q. (2010). Liquid-Phase Chemical Hydrogen Storage: Catalytic Hydrogen Generation under Ambient Conditions. *ChemSusChem*, *3*(5), 541–549. https://doi.org/10.1002/cssc.201000023

Kim, K. S., Zhao, Y., Jang, H., Lee, S. Y., Kim, J. M., Kim, K. S., Ahn, J.-H., Kim, P., Choi, J.-Y., & Hong, B. H. (2009). Large-scale pattern growth of graphene films for stretchable transparent electrodes. *Nature*, *457*(7230), 706–710. https://doi.org/10.1038/nature07719

Kosynkin, D., Higginbotham, A., Sinitskii, A., Lomeda, J., Dimiev, A., Price, K., & Tour, J. (2009). Longitudinal Unzipping of Carbon Nanotubes To Form Graphene Nanoribbons. *Nature*, *458*, 872.

Lee, C., Wei, X., Kysar, J. W., & Hone, J. (2008). Measurement of the Elastic Properties and Intrinsic Strength of Monolayer Graphene. *Science*, *321*(5887), 385 LP – 388. https://doi.org/10.1126/science.1157996

Oliveira, A. E. F., Braga, G. B., Tarley, C. R. T., & Pereira, A. C. (2018). Thermally reduced graphene oxide: synthesis, studies and characterization. *Journal of Materials Science*, *53*(17), 12005–12015. https://doi.org/10.1007/s10853-018-2473-3

Patchkovskii, S., Tse, J. S., Yurchenko, S. N., Zhechkov, L., Heine, T., & Seifert, G. (2005). Graphene nanostructures as tunable storage media for molecular hydrogen. *Proceedings of the National Academy of Sciences of the United States of America*, *102*(30), 10439–10444. https://doi.org/10.1073/pnas.0501030102

Pei, S., Wei, Q., Huang, K., Cheng, H.-M., & Ren, W. (2018). Green synthesis of graphene oxide by seconds timescale water electrolytic oxidation. *Nature Communications*, *9*(1), 145. https://doi.org/10.1038/s41467-017-02479-z

Sterlin Leo Hudson, M., Raghubanshi, H., Awasthi, S., Sadhasivam, T., Bhatnager, A., Simizu, S., Sankar, S. G., & Srivastava, O. N. (2014). Hydrogen uptake of reduced graphene oxide and graphene sheets decorated with Fe nanoclusters. *International Journal of Hydrogen Energy*, *39*(16), 8311–8320. https://doi.org/10.1016/J.IJHYDENE.2014.03.118

Venkatesan, A., Patel, R. N., & Kannan, E. S. (2015b). Reduced Graphene Oxide for Room Temperature Hydrogen Storage Application. *Advanced Materials Research*, *1086*, 91–95. https://doi.org/10.4028/www.scientific.net/AMR.1086.91

Xiang, Q., Yu, J., & Jaroniec, M. (2012). Synergetic effect of MoS2 and graphene as cocatalysts for enhanced photocatalytic H2 production activity of TiO2 nanoparticles. *Journal of the American Chemical Society*, *134*(15), 6575–6578. https://doi.org/10.1021/ja302846n

Yang, S., Feng, X., & Müllen, K. (2011). Sandwich-Like, Graphene-Based Titania Nanosheets with High Surface Area for Fast Lithium Storage. *Advanced Materials*, *23*(31), 3575–3579. https://doi.org/10.1002/adma.201101599

Zhou, C., & Szpunar, J. A. (2016). Hydrogen Storage Performance in Pd/Graphene Nanocomposites. *ACS Applied Materials & Interfaces*, *8*(39), 25933–25940. https://doi.org/10.1021/acsami.6b07122

CHAPTER 7

7. REACTION MECHANISM & DESORPTION KINETICS OF GRAPHENE BASED NANOCOMPOSITE FOR HYDROGEN STORAGE

Graphical Abstract:

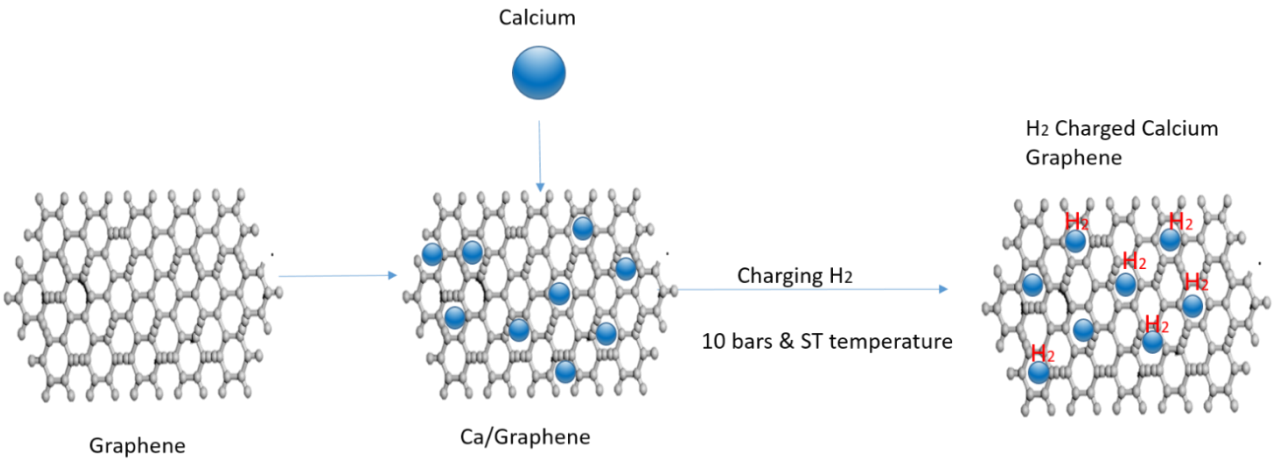

Sections of this chapter will be published. Manuscript in preparation

Introduction

The development of advanced nanocomposites, nanostructures and nanotechnologies has pioneered advanced and fast growing research that depicts potential in the fulfillment of the practical requirements for hydrogen storage (Pumera, 2011). Hydrogen as a carbon free alternative source of energy, has been researched extensively for hydrogen storage applications (Abe et al., 2019; Ruse et al., 2018; Sterlin Leo Hudson et al., 2014). A lot of materials, which are classified under chemisorption materials or physisorption materials, have been researched for practical hydrogen storage applications. Physisorption materials are materials that bind with weak Van der Waals forces resulting in these materials to have fast kinetics compared to chemisorption materials however physisorption materials have very low hydrogen storage capacity (Jhi et al., 2004; Nijkamp et al., 2001). Chemisorption materials on the other hand, form a stronger bond with materials they bond with and these materials are very stable. This results in chemisorption materials having slow kinetics and requiring very high temperatures to release the hydrogen. Chemisorption materials however have high hydrogen storage capacity (Energy, 2018; Liang et al., 1999). Nanotechnology has been effectively and efficiently employed to address the issue of kinetics in hydrogen storage materials (Schlapbach & Züttel, 2001).

Furthermore, nanomaterials permit favorable charge, mass and heat transfer, these are added advantages when considering practical application of these materials for on board applications (Bououdina et al., 2006a; Ruse et al., 2018). In addition, nanomaterials assist in dimensional alteration of particular phase transitions and chemical reactions. Nanomaterials not only help and aid in the kinetics of hydrogen storage materials, but they also help to destabilize the thermodynamics of chemisorption materials (M. Wang, 2012).

In this chapter, the kinetics of both the Ca/graphene and Ni/graphene were investigated to further understand the interaction of the graphene with molecular hydrogen. To understand the kinetics of the material various characterization techniques were done on the material. The thermodynamics of the materials, were also investigated to get a better understanding of whether the nanocomposites synthesized are within the requirements of the Department of Energy for practical on board applications in hydrogen storage.

7.1 Method

In this chapter, the reaction mechanism and desorption kinetics of the Ca/graphene and Ni/graphene were evaluated. The metal graphene nanocomposites herein were characterized using Thermo-gravimetric analysis. To avoid repetition, the detailed method of the TGA analysis procedure was detailed and described above in the previous chapters. For the TPD analysis, an AutoChemTM II 2920 with automated catalyst characterization system was used to detect the desorption kinetics of the material. The TPD instrument is coupled to a quadrupole mass spectrometer.

7.2 Reaction mechanism of Ca/graphene

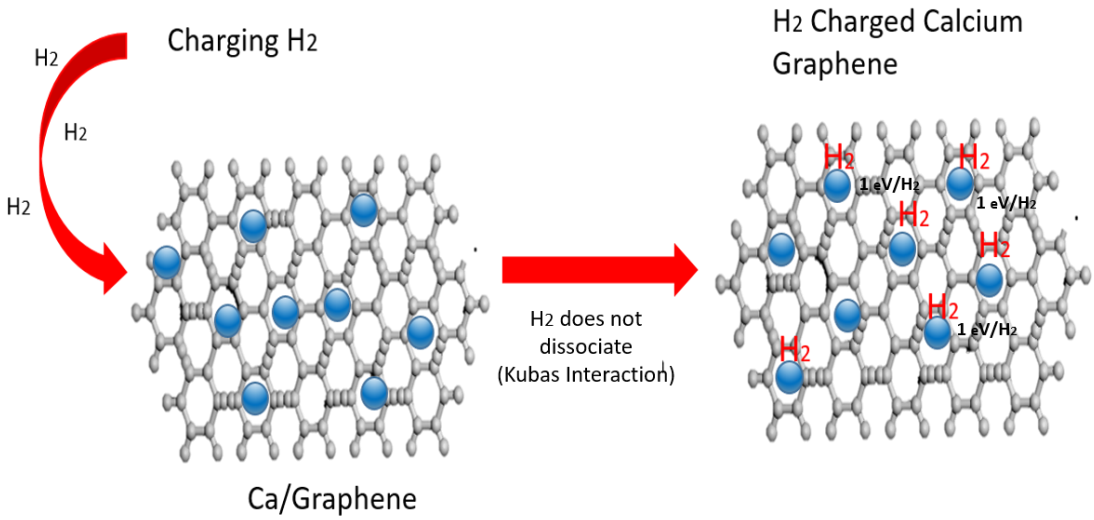

Figure 7-1: Reaction mechanism of the Ca/graphene nanocomposite

The figure 7-1 shows a graphical representation of the reaction mechanism of the Ca/graphene nanocomposite. The results attained for the structural characterization of the Ca/graphene developed and hydrogen storage properties thereof, may be explained as proposed in by Tranca et.al (Diana C. Tranca & Gotthard Seifert, 2016). The calcium clusters or atoms are restrained at the carbon nanostructure and can bind hydrogen molecules without dissociating through unidirectional polarization or the so called Kubas interaction (De Silva et al., 2018).

This results in binding energies with up to almost 1 eV/H_2-molecule considerably larger than with "pristine" graphene (0.07 eV/H_2) (Heine et al., 2004). The occurrence of Ca particles on the graphene matrix increases the binding energy and thereby facilitates the adsorption of hydrogen molecule due to the polarization of the hydrogen molecule.

7.3 Reaction mechanism of the Ni/graphene nanocomposite

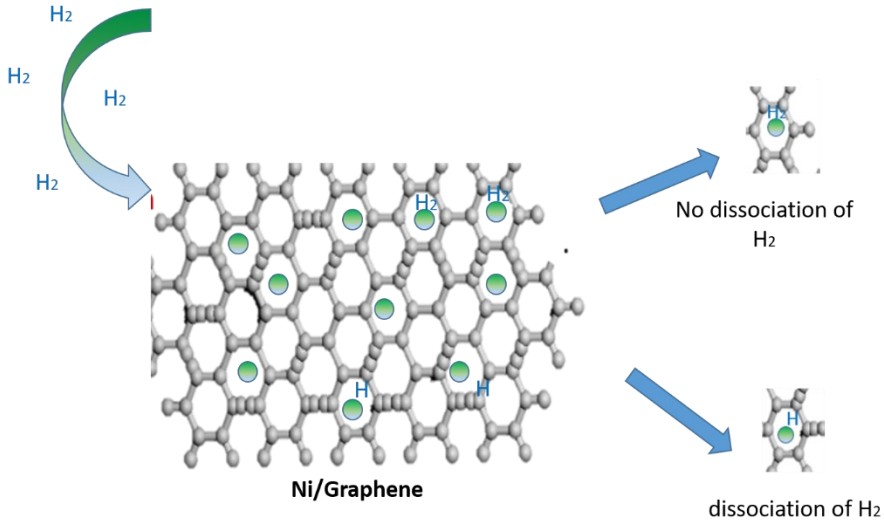

Figure 7-2: Reaction mechanism of the Ni/graphene nanocomposite

For the Ni/graphene nanocomposite, the reaction mechanism is proposed based on the structural analysis of the hydrogen charged Ni/graphene nanocomposite and the hydrogen storage properties of the nanocomposite. The results show the possibility of the non-dissociation of molecular hydrogen on the surface of the graphene. Molecular hydrogen adheres to the surface of the Ni-particles. Multiple hydrogen molecules can adhere on the Ni particles, however these anchored molecules may dissociate at the surface into atomic hydrogen atoms due to the presence of Ni (Zhou et al., 2016). The dissociation of the hydrogen molecule leads to the formation of the nickel hydride (NiHx). During the hydrogenation process of graphene, atomic hydrogen migrate into the graphene support through the Ni-graphene interface and this facilitates hydrogen spill over. The dissociated atoms are trapped at the unsaturated sites of the graphene matrix.

7.4 Temperature Programmed Desorption Method

In this step, Temperature programmed desorption (TPD) analysis was performed on the synthesized metal/graphene nanocomposites. TPD is an analysis method that gives an indication of desorbed molecules from a surface when the surface temperature is elevated. The samples were analyzed on a TPD instrument that is followed by mass spectrometry. The samples were analyzed in a continuous flow reactor connected to a quadrupole mass spectrometer. The samples were heated with a linear temperature ramp, giving:

$$T_{(t)} = T_0 + \beta t$$

Where T is the temperature, t = time and β = heating rate.

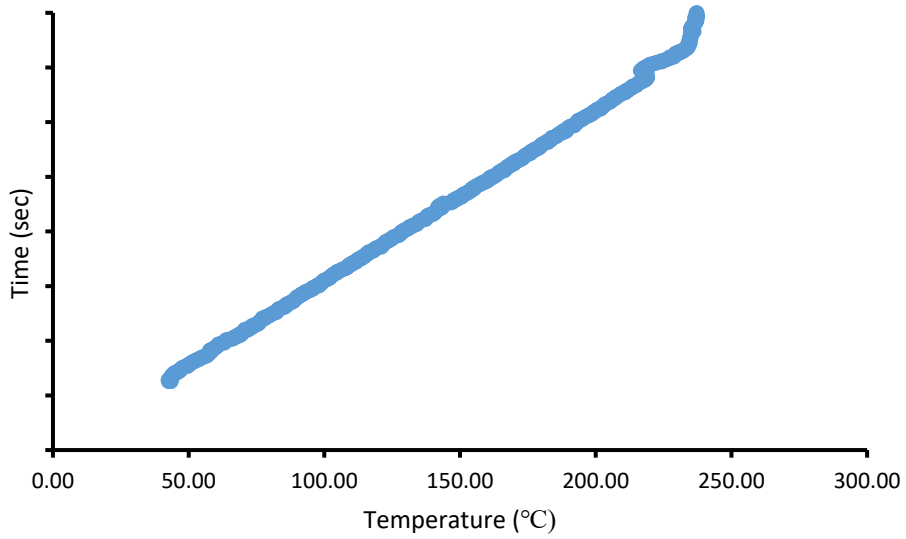

Figure 7-3: Temperature ramp rate of the metal/graphene nanocomposites.

The metal/graphene nanocomposites' desorption rate can be calculated using the Polanyi-Wigner equation which is given as:

$$v = -\frac{d\theta}{dt} = v.\theta^n.e^{\frac{E_B}{K_B T}}$$

Where T is the temperature, E_B is the binding energy, n is the desorption order, K_B is the Boltzmann constant and θ is the relative coverage of the surface. Figure (6) shows the linearity of the temperature ramp against time proving that the temperature was controlled in a stable manner. The temperature was ramped and left at 250 to make sure that all strongly bound species were removed and to activate the sample for the adsorption step. The linearity ramp of the temperature is important in the calculation of the desorption rate.

7.5 Results: Desorption profiles

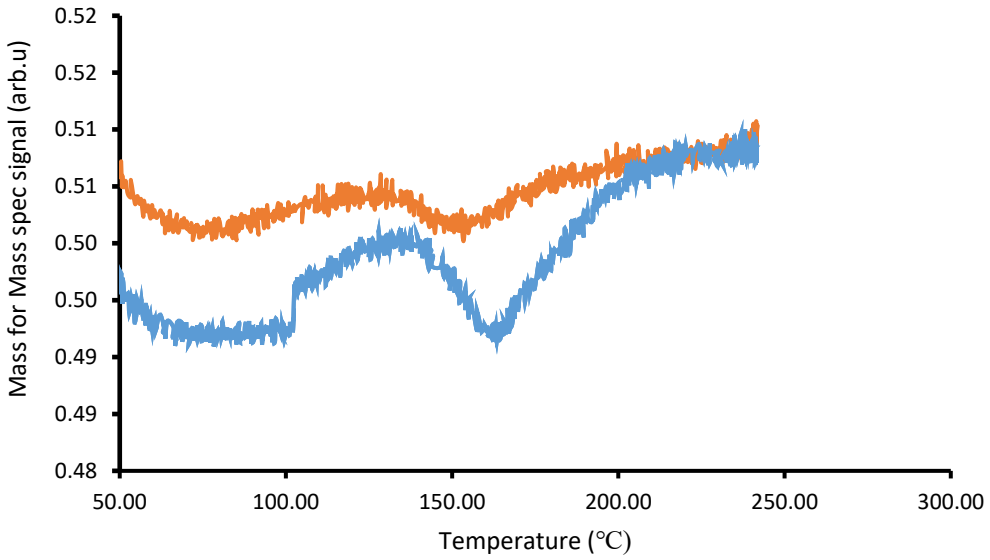

Figure 7-4: TPD-MS desorption profiles

Figure 7-4 gives an indication of the desorption profiles of the synthesized metal nanocomposite. On the figure, the area under peak, obtained from the TPD desorption profiles of this analysis is proportional to the amount of gas originally adsorbed on the surface. On the method, the temperature was ramped to 250 ℃ linearly. This is to ensure that all strongly bound species were detached and to activate the sample for the adsorption step.

The temperature ramp was done again the second to 250 ℃ at ramp rate of 10 ℃/min while flowing helium. As the temperature was elevated the hydrogen was desorbed from the surface at a temperature of about 100 ℃, the hydrogen was taken up again and then desorbed again at a temperature of about 150 ℃. The theoretical calculated desorption temperature for Ca hydride is around 250 ℃ and with these result it can be observed that the desorption temperature was significantly reduced.

CONCLUSION

The aim of this chapter was analyse the reaction mechanism of the synthesized Ni/graphene and Ca/graphene nanocomposites. The reaction mechanism proposed were based on the structural characterization of the nanocomposites and the hydrogen storage uptake of the composites. The reaction of the mechanism of the Ca/graphene was explained through the Kubas interaction theory and Ni/graphene was also explained through two possibilities, the dissociation of the hydrogen molecule at the surface and the non-dissociation of the hydrogen molecule at the surface. Furthermore, the desorption kinetics of the nanocomposites were evaluated. The desorption temperature was around 150 ℃ for Ca/graphene and according to literature the desorption temperature of the Ca hydride is around 250 ℃. The incorporation of graphene had a significant effect. These results have shown that the aims of the project were achieved through the significant decrease of the desorption temperature of Ca.

REFERENCES

Balandin, A., Ghosh, S., Bao, W., Calizo, I., Teweldebrhan, D., Miao, F., & Lau, J. (2008). Superior Thermal Conductivity of Single-Layer Graphene. *Nano Letters*, *8*, 902–907. https://doi.org/10.1021/nl0731872

Geng, J., Kong, B.-S., Yang, S. B., & Jung, H.-T. (2010). Preparation of graphene relying on porphyrin exfoliation of graphite. *Chemical Communications*, *46*(28), 5091–5093. https://doi.org/10.1039/C001609H

Heine, T., Zhechkov, L., & Seifert, G. (2004). Hydrogen storage by physisorption on nanostructured graphite platelets. *Physical Chemistry Chemical Physics*, *6*(5), 980–984. https://doi.org/10.1039/B316209E

Hu, P., Ben-David, Y., & Milstein, D. (2016). Rechargeable Hydrogen Storage System Based on the Dehydrogenative Coupling of Ethylenediamine with Ethanol. *Angewandte Chemie (International Ed. in English)*, *55*(3), 1061–1064. https://doi.org/10.1002/anie.201505704

Hua, T. Q., Ahluwalia, R. K., Peng, J.-K., Kromer, M., Lasher, S., McKenney, K., Law, K., & Sinha, J. (2011). Technical assessment of compressed hydrogen storage tank systems for automotive applications. *International Journal of Hydrogen Energy*, *36*(4), 3037–3049. https://doi.org/https://doi.org/10.1016/j.ijhydene.2010.11.090

Jiang, H.-L., Singh, S. K., Yan, J.-M., Zhang, X.-B., & Xu, Q. (2010). Liquid-Phase Chemical Hydrogen Storage: Catalytic Hydrogen Generation under Ambient Conditions. *ChemSusChem*, *3*(5), 541–549. https://doi.org/10.1002/cssc.201000023

Kim, F., Cote, L. J., & Huang, J. (2010). Graphene Oxide: Surface Activity and Two-Dimensional Assembly. *Advanced Materials*, *22*(17), 1954–1958. https://doi.org/10.1002/adma.200903932

Lee, J. S., You, K. H., & Park, C. B. (2012). Highly photoactive, low bandgap TiO2 nanoparticles wrapped by graphene. *Advanced Materials (Deerfield Beach, Fla.)*, *24*(8), 1084–1088. https://doi.org/10.1002/adma.201104110

Pei, S., Wei, Q., Huang, K., Cheng, H.-M., & Ren, W. (2018). Green synthesis of graphene oxide by seconds timescale water electrolytic oxidation. *Nature Communications*, *9*(1), 145. https://doi.org/10.1038/s41467-017-02479-z

Pumera, M. (2011). Graphene-based nanomaterials for energy storage. *Energy & Environmental Science*, *4*(3), 668–674. https://doi.org/10.1039/C0EE00295J

Ruse, E., Buzaglo, M., Pri-Bar, I., Shunak, L., Nadiv, R., Pevzner, S., Siton-Mendelson, O., Skripnyuk, V. M., Rabkin, E., & Regev, O. (2018). Hydrogen storage kinetics: The graphene nanoplatelet size effect. *Carbon*, *130*, 369–376. https://doi.org/10.1016/J.CARBON.2018.01.012

Venkatesan, A., Patel, R. N., & Kannan, E. S. (2015a). Reduced Graphene Oxide for Room Temperature Hydrogen Storage Application. *Advanced Materials Research*, *1086*, 91–95. https://doi.org/10.4028/www.scientific.net/AMR.1086.91

Xiang, Q., Yu, J., & Jaroniec, M. (2012). Synergetic effect of MoS2 and graphene as cocatalysts for enhanced photocatalytic H2 production activity of TiO2 nanoparticles. *Journal of the American Chemical Society*, *134*(15), 6575–6578. https://doi.org/10.1021/ja302846n

Yang, J., Zang, C., Sun, L., Zhao, N., & Cheng, X. (2011). Synthesis of graphene/Ag nanocomposite with good dispersibility and electroconductibility via solvothermal method. *Materials Chemistry and Physics*, *129*(1), 270–274. https://doi.org/https://doi.org/10.1016/j.matchemphys.2011.04.002

Zhou, C., & Szpunar, J. A. (2016). Hydrogen Storage Performance in Pd/Graphene Nanocomposites. *ACS Applied Materials & Interfaces*, *8*(39), 25933–25940. https://doi.org/10.1021/acsami.6b07122

CHAPTER 8

8. TECHNO-ECONOMIC ASSESSEMENT OF CA/GRAPHENE NANOCOMPOSITE

Introduction

The Department of Energy requirements for onboard applications amongst others include the system cost for practical applicable hydrogen storage materials. The research surrounding hydrogen storage has advanced in the hydrogen storage capacity spectrum, mainly in terms of volume and density storage capacity research however not much attention has been focused on the other requirements by the DOE for hydrogen storage materials. In this regard, Energy storage systems must be sustainable and all rounded in terms of the required requirements for hybrid systems. As a remainder, the department of Energy requirements for materials applicable for practical on-board storage include volumetric capacity, hydrogen storage capacity in terms of the density, specific storage system costs, durability and operability, fuel cost, minimum and maximum desorption temperature from the hydrogen tank, cycle life variation, charging and discharging rates, minimum full-flow rate, delivery pressure from hydrogen storage system, start time to full flow at minimum ambient, environment, health and safety, start time to full flow, purity, transient response 10% to 90% and 90% to 10% and lastly the hydrogen loss (Energy, 2018).

In this chapter, the cost of the ca/graphene synthesized in this work was evaluated. This encompasses costs for compression, chemical recovery, liquefaction. The cost of regenerating will also be considered for this material. The cost calculations in this chapter are independent of the hydrogen production pathway. As indicated by the DoE under their systems and fuel cost calculations, an approximate cost of hydrogen of about 1.6$/kg was used.

8.1 DOE Economic consideration

The economic evaluation performed herein below does not take into consideration the production of hydrogen, and will thereby make an assumption of the cost of hydrogen based on figures given by the Department of Energy in the US, which is estimated at 1.6$/kg (IEA, 2020). Another important fact to consider is that costs are subject to variations due to external influencers such as inflation, regulations and utilities; as such, the determination of future costs is then uncertain (Mueller-Langer et al., 2007). The economic analysis is performed as per the requirements of the DOE for hydrogen storage. To paint a clear picture with regards to the considerations and limitations taken into account, the definitions of the relevant cost are defined as per the requirements of DOE for practical hydrogen storage.

Specific storage system cost:

This DoE requirement looks at the total simulated costs for the on board hydrogen storage system. This includes the storage media, hardware media and an estimate for the costs of components that may have to be repaired and replaced in order to maintain an operative cycle of 150 000 miles (241 400 km) in a vehicle (Freedom CAR; Fuel Partnership, 2005). It is notable that the onboard hydrogen storage system will not reach low cost of fuel in present vehicles however the societal benefits of hybrid vehicles combined with the improved vehicle efficiency compensate for this. The DoE system cost in 2015 was targeted at $2/kWh (R35/kWh) (Freedom CAR; Fuel Partnership, 2005).

Fuel cost:

This DoE standard refers to the cost of chemical hydrogen storage systems that are fabricated off-board. These costs include chemical recovery, liquefaction, costs for compression and delivery. This cost, is not associated with the manufacturing pathway of hydrogen (i.e. electrolysis, methane steam reforming, electrolysis of water etc.). The fuel cost requirement by the DoE for 2020 and 2025 are 4$/gge (gallon gasoline equivalent) which is also equivalent to $/kg of hydrogen (Freedom CAR; Fuel Partnership, 2005).

Targets vs current technology status

The R&D community and technology developers have provided an approximation for current status data regarding the hydrogen storage cost. The estimates are made due to the complexity

of estimating system level costs when research is still at the stage of material development. The diagram shows the current technology status and the DoE targets over the years. From the graph it is evident that majority of the technologies do not meet the requirements for practical hydrogen storage (Freedom CAR; Fuel Partnership, 2005).

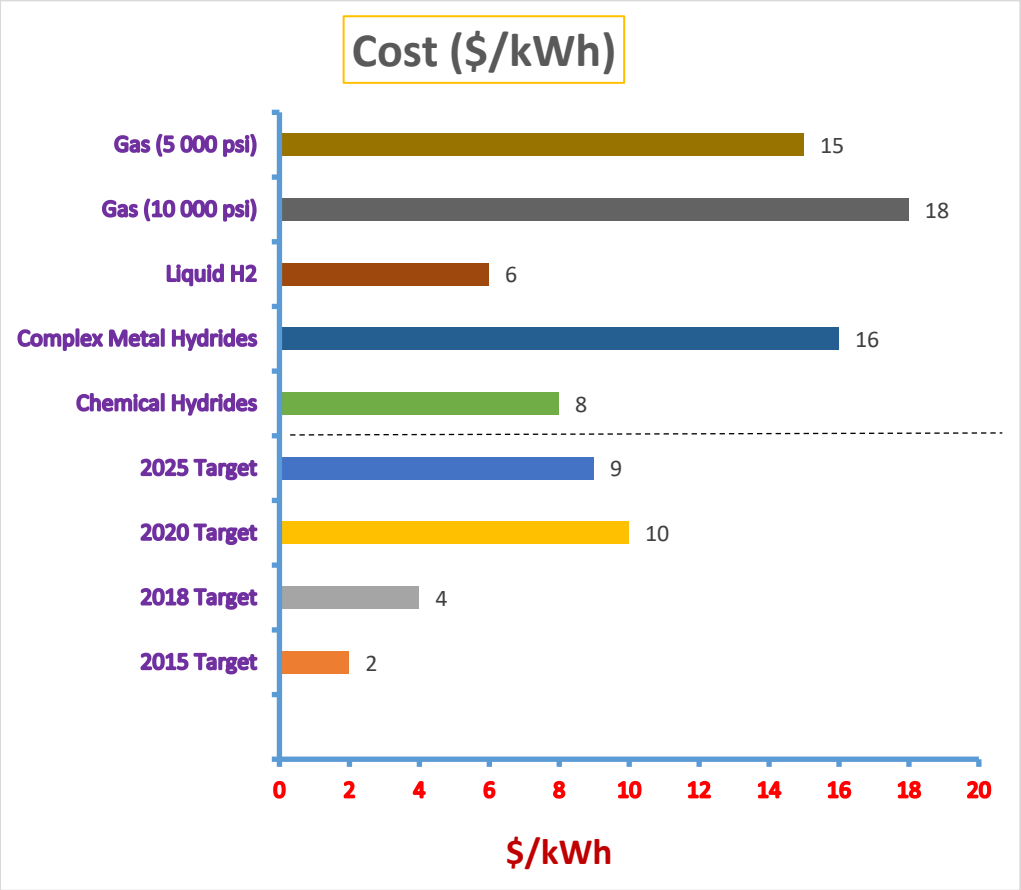

Figure 8-1: Cost of current technology vs DoE targets

It is good to note that each technology presented above has an important and unique influence on the delivery cost of hydrogen. A technology that utilized low temperatures and low pressure automatically lowers the cost of the capital investment required for heat transfer and compression during the hydrogenation and dehydrogenation cycles (Mueller-Langer et al., 2007). For this reason, in this work a cheaper material was utilized for hydrogen storage. Furthermore graphene lower the temperature needed to release the hydrogen after hydrogenation reactions.

8.2 Ca/Graphene cost analysis

Synthesis and synthesis parameters

Various synthesis methods for precursor graphene were evaluated. The experiments carried out were done at laboratory scale. The Improved Tours Method, Hummers method and Modified hummers method were evaluated in this regard. The diagram below shows the different synthesis steps from the evaluated methods for graphene synthesis:

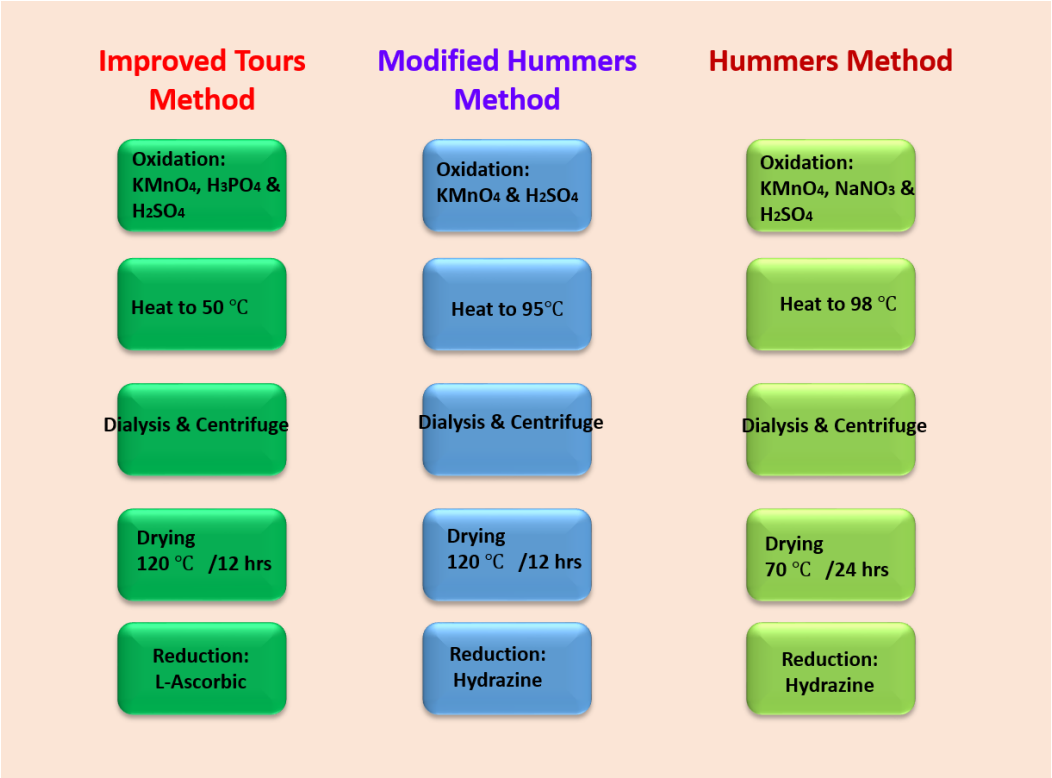

Figure 8-2: Synthesis methods for reduced graphene

The capital expenses were evaluated for the three synthesis processes above for the synthesis of precursor graphene. The graphene nanocomposite was synthesized using the simple and cheap solution mixing method.

Cost of synthesis

For the cost analysis, a process based cost estimation was utilized to evaluate the production of graphene through the 3 process synthesis methods proposed above. This methodology determines the capital cost by adding all the incurred cost in each synthesis step (oxidation, centrifugation, reduction, drying etc.) of the process and imitates the actual steps of manufacturing.

In this cost analysis method, for each step in the synthesis process the cost are simulated based on the material utilized, labor and machine operational time to finish each step in the synthesis method and the cost of the equipment utilized in the synthesis process. The cost estimation is a class 4 estimation. The price quotes for the chemical reagents utilized in each synthesis method were obtained from chemical suppliers (Sigma Aldrich) (Aldrich, 2020). The cost quotes for equipment was also obtained from equipment suppliers. To determine the subsequent manufacturing costs, standard manufacturing and labor rates were utilized (DeSantis et al., 2017). The projected capital cost (which is the cost estimate C_{est}) is calculated as the sum of the manufacturing costs (C_{man}) and the material cost (C_{mat})

$C_{est} = C_{man} + C_{mat}$

Based on the miles (km's) for hybrid car, the cost estimation was done over a 3 year period. The table below has an overview of the assumptions made:

Table 8-1: Overview of Assumptions

Description	Typical values
Inflation rate	4.7%
Internal interest rate	10%
Economic lifetime	3 years
Chemicals	Prices are subject to change yearly due to inflation rate at 4.7%
Equipment	50% of total cost will be used for maintenance and contingencies
Electricity	0.965 Rand/kWh
Water	Water costs are also subject to change due to demand

Synthesis Cost:

Table 8-2: Synthesis costs: Variable and fixed costs

Description	**Typical values**
Variable Costs	
Reagents for synthesis	
Improved Tours Method	R72 333.00
Hummers Method	R65 566.00
Modified Hummers method	R71 325.00
Utilities (Water and Electricity)	See Appendix A
Labour cost	R 1 035 198
Miscellaneous materials	Negligible
Fixed Costs	
Maintenance cost	10-12 % of total cost of equipment
Laboratory characterization	30% of the synthesis cost
Laboratory equipment	R108 015.69

The fuel cost was calculated in this section for 3 different synthesis. The cost of graphene based fuel for Improved Tours method, Hummers method and modified hummers method was 14.36$/kg of hydrogen, 13.96 $/kg of hydrogen and 14.30$/kg of hydrogen respectively. These costs are cheaper than complex metal hydrides and the gaseous storage of hydrogen. The final price was calculated by calculating the total cost of synthesis (reagents, equipment, maintenance, characterization and utilities) and using the current market size of hydrogen cars which is currently at 6558 units, according to the DOE statistics. Although the Hummers method has a cheaper synthesis method, however the synthesis method is not environmentally friendly due to the use of hydrazine as a reductant in the process. In order, to avoid governmental emission fines which may results in the overall cost increasing, Improved Tours method was opted for. The total capital cost for the Improved method was R 1 620 905.96, Hummers method: R 1 574 213.66 and modified hummers method R 1 613 950.76 over a 3

years period, the bar graph shows these figures below. Again, these cost estimates are at laboratory scale.

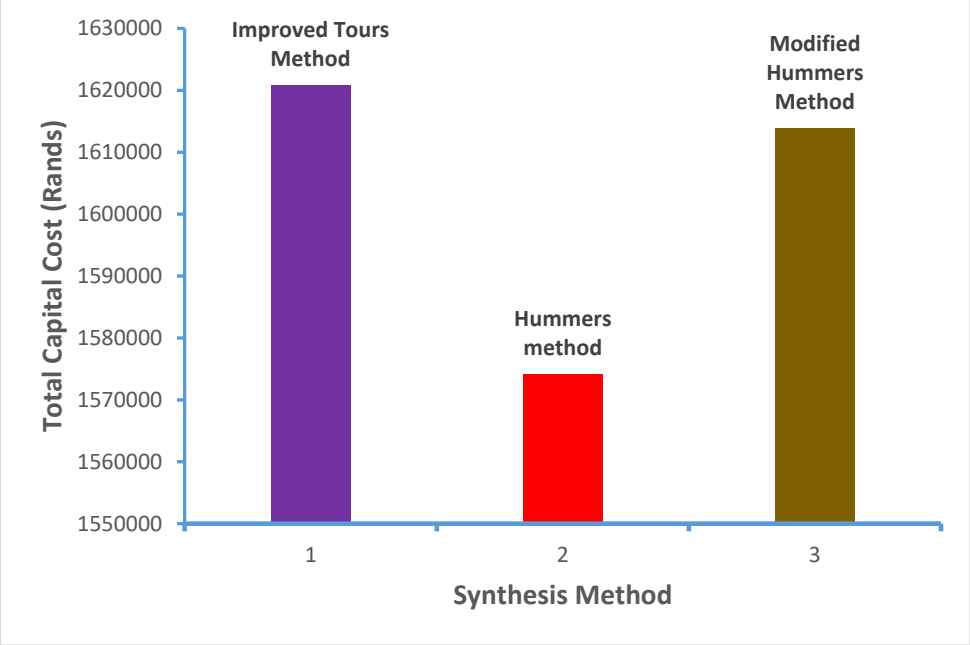

Figure 8-3: Capital Cost of Various synthesis groups

The detailed costs tables can be found in the Appendix. After the synthesis, the test were carried out on the hydrogen storage below on the figure below. However, the economics around the hydrogen rig were not done. The cost of material was considered. As mentioned above, the overall system cost calculations are complex and laboratory based. This means any results obtained would have a great margin of error because the DOE system costs are based on practical systems.

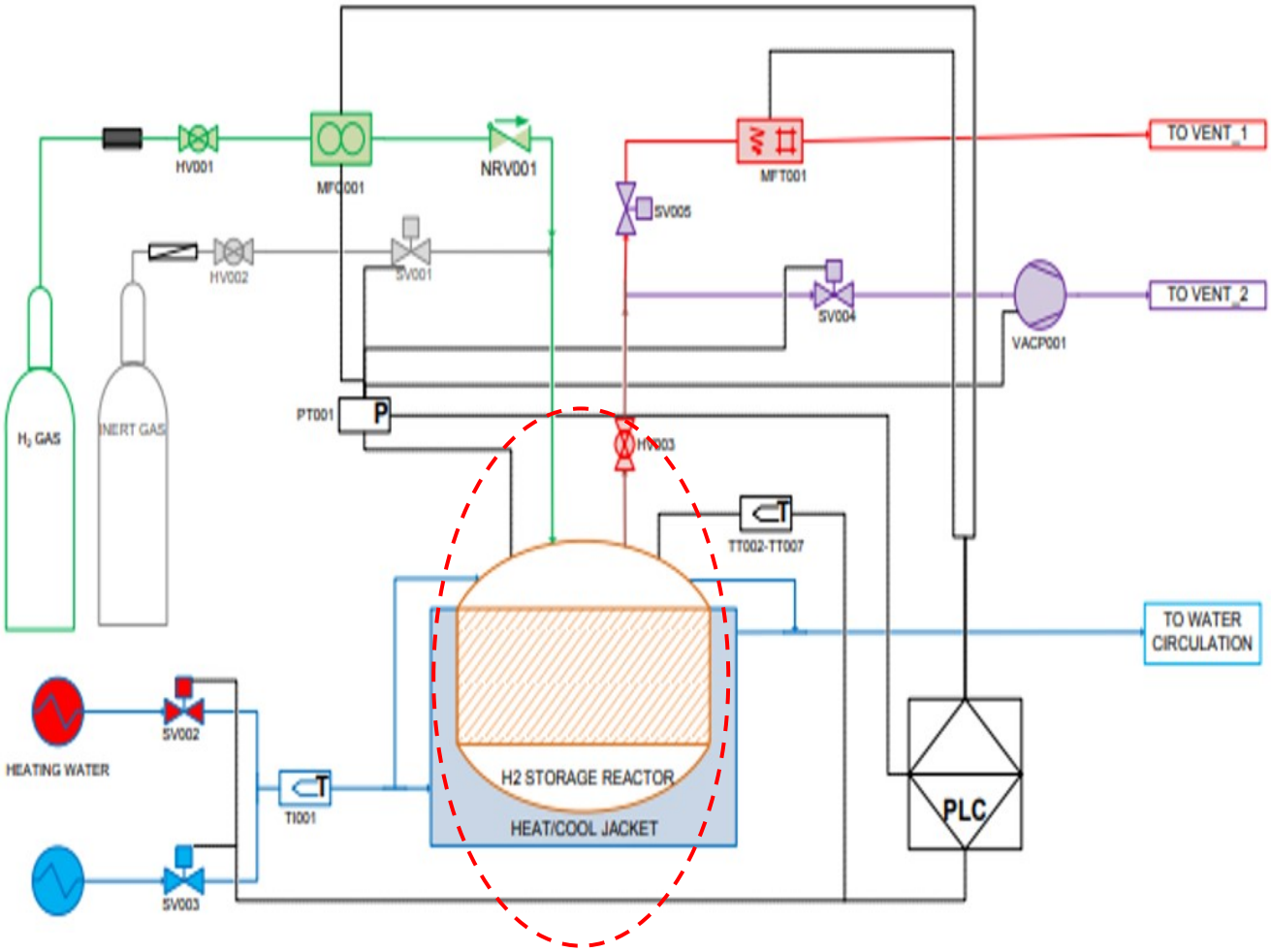

Figure 8-4: Hydrogen storage test rig

CONCLUSION

In this chapter, an economic analysis was performed for the Ca/graphene prepared for hydrogen storage. In the analysis, three synthesis methods were taken into consideration for the analysis; Improved Tours method, Hummers method and Modified Hummers Method respectively. The capital cost for each method at laboratory scale was calculated to be: R1 620 905.961, R1 574 213.661 and R1 613 950.761 respectively. The projected fuel cost was calculated to be: 14.36 \$/kg H_2, 13.96 \$/kg H_2 and 14.30 \$/kg H_2 for Improved Tours Method, Hummers method and modified Hummers method respectively (calculated at the exchange rate of 17.409 rand to dollar). The cost obtained was found to be cheaper than projected cost for complex hydrides (16\$/kg H_2) and gaseous hydrogen (at 18\$/kg H_2) however the cost was slightly more than the DOE target. More optimization and simulation would have to be performed to obtain optimum price for graphene nanocomposites.

REFERENCES

DeSantis, D., Mason, J. A., James, B. D., Houchins, C., Long, J. R., & Veenstra, M. (2017). Techno-economic Analysis of Metal–Organic Frameworks for Hydrogen and Natural Gas Storage. *Energy & Fuels*, *31*(2), 2024–2032. https://doi.org/10.1021/acs.energyfuels.6b02510

Energy, D. of. (2018). *Hydrogen Storage*.

Freedom CAR; Fuel Partnership. (2005). Hydrogen Storage technologies Roadmap. In *Department of Energy*.

Mueller-Langer, F., Tzimas, E., Kaltschmitt, M., & Peteves, S. (2007). Techno-economic assessment of hydrogen production processes for the hydrogen economy for the short and medium term. *International Journal of Hydrogen Energy*, *32*(16), 3797–3810. https://doi.org/https://doi.org/10.1016/j.ijhydene.2007.05.027

APPENDIX A:

Improved Tours Method:

Reagents quote:

Chemicals	**Sigma Aldrich**		Quantity used per run
	Unit Price		
Sulphuric acid 98% 10L	R1 818.00	R7 272.00	40 ml
Phosphoric acid 85% 10L	R3 762.00	R15 048.00	360 ml
Hydrogen peroxide 30% 2L	R2 399.00	R9 596.00	3ml
$KMnO_4$ 99%, 5kg	R1 616.00	R8 080.00	18g
Graphite flakes 24kg	R3 698.00	R7 396.00	9g
L-Ascorbic Acid 6 kg	R4 573.00	R13 719.00	5.28g
$CaCl_2$ 5kg	R5 611.00	R11 222.00	1.542 g

Equipment	**Quote**
Oven	R20 717.00
Centrifuge	R19 644.48
Ultrasonicator	R7 625.88
Thermometers	R3 829.60
pH meter	R8 471.13
Hot plate with stirrer	R2 070.34
Ice maker machine	R10 999.00
General lab equipment (Beakers, measuring cylinder etc.)	R30 000.00
Weighing balance	R4 658.26

Hummers Method:

Chemicals	Sigma Aldrich		Quantity used
	Unit Price		
Sulphuric acid 98% 10L	R1 818.00	R7 272.00	400 ml
$NaNO_3$ 10 kg	R2 550.00	R10 200.00	9g
Hydrogen peroxide 30% 2L	R2 399.00	R9 596.00	120 ml
$KMnO_4$ 99%, 5kg	R1 616.00	R8 080.00	18g
Graphite flakes 24kg	R3 698.00	R7 396.00	9g
Hydrazine 5kg	R2 360.00	R11 800.00	572 mg
$CaCl_2$ 5kg	R5 611.00	R11 222.00	1.542 g

Modified Hummers Method:

Chemicals	Sigma Aldrich		Quantity used
Sulphuric acid 98% 10L	R1 818.00	R7 272.00	70 ml
Hydrogen peroxide 30% 2L	R2 399.00	R9 596.00	20 ml
$KMnO_4$ 99%, 5kg	R1 616.00	R8 080.00	9g
Graphite flakes 24kg	R3 698.00	R7 396.00	3g
Hydrazine 5kg	R2 360.00	R11 800.00	572 mg
HCl 37% 10L	R2 125.00	R8 500.00	15 ml
NaOH 12kg ACS reagent, ≥97.0%, pellets	R7 459.00	R7 459.00	9g
$CaCl_2$ 5kg	R5 611.00	R11 222.00	1.542 g

CHAPTER 9

9. OVERALL CONCLUSION & RECOMMENDATION

9.1 SUMMARY

The heavy use of fossil fuels and its negative effects on the environment have pushed the world to a point where green methods have to be implemented. Environmental issues like global warming and acid rain are direct consequences of utilizing fossil fuels, thus cleaner sources such as hydrogen are gathering a lot of attention as replacement sources of energy. However, storing hydrogen in a manner that meets the DoE standards has been the hindering factor in the application of these materials.

The main aim of this research project according to the initial proposal submitted, is to develop graphene nanocomposites for the hydrogen storage at low temperature, taking an opportunity at the gap in this research that is has not yet been satisfied (to date, no material meets the standards of the DoE for hydrogen storage). In this regard, various materials have been studied for hydrogen storage. However, the kinetics and thermodynamics of these materials however have hindered their application as an alternative energy. The main objectives of the project are stipulated below, as stated in the initial proposal:

RESEARCH AIM AND OBJECTIVE(S):

The aim of this research project were to develop hydrogen storage system based on nano-metal – graphene materials.

To fulfill the aim of this research project, the below objectives were followed

- Synthesis of nano metals for hydrogen storage system
- Development of nano metals – graphene system as hydrogen storage material
- Characterization of the synthesised material
- Laboratory assessment of the storage systems
- Economic analysis of the developed hydrogen storage system

9.2 OUTCOMES OF RESEARCH

Precursor graphene was synthesized using Improved Tours method and modified Hummers method. The graphene thereafter was successfully decorated with Ca and Ni atoms for hydrogen storage. The graphene nanocomposites were successfully hydrogenated and tested for hydrogen storage. An economic analysis was performed for Ca/graphene. Below is summary of the overall results:

- Graphite flakes were successfully oxidized to graphite oxide. The success of this synthesis step can observed in the characterization results presented above. FTIR showed the presence of functional groups after oxidizing graphite flakes, XRD results depicted a shift in the graphite flakes peak at $\sim 2\theta = 30°$ due to the oxidation process and lastly the Raman characterization showed the defects on the graphite flakes after oxidation. The reduction of graphite oxide was also successfully completed as observed in the characterization results.

- The XRF elemental results obtained for the Ca/graphene nanocomposite showed the Ca content on the nanocomposite increased from 0.516 % to 8.227 %. The TEM images also showed the Ca particles uniformly dispersed over the graphene matrix. The EDX elemental analysis of the Ni/graphene also showed an increase on the Ni content on the surface of graphene and the TEM results also showed that the Ni particles were uniformly dispersed on the surface of the graphene. These results, in effect, prove that the aims of this chapter were successfully completed.

- The synthesized nanocomposites were tested using the thermogravimetric analysis. Considerations such as the removal of gas toxins and adsorbed water were taken into account when quantifying the hydrogen storage uptake of the material. The novel Ca/graphene has a hydrogen storage capacity of about 4.98 w% and Ni/graphene has hydrogen storage capacity 2.78 wt% both at 10 bars. The hydrogen uptake of graphene was significantly improved by the incorporation of Ni and Ca into the graphene matrix. During the hydrogenation process, it was observed that the hydrogen uptake increased with increasing pressure. The results obtained prove that the aims of this chapter were successfully accomplished.

- The reaction mechanism proposed were based on the structural characterization of the nanocomposites and the hydrogen storage uptake of the composites. The reaction of the mechanism of the Ca/graphene was explained through the Kubas interaction theory and Ni/graphene was also explained through two possibilities, the dissociation of the hydrogen molecule at the surface and the non-dissociation of the hydrogen molecule at the surface. Furthermore, the desorption kinetics of the nanocomposites were evaluated. The desorption temperature was around 150 ℃ for Ca/graphene and according to literature the desorption temperature of the Ca hydride is around 250 ℃. The incorporation of graphene had a significant effect. These results have shown that the aims of the project were achieved through the significant decrease of the desorption temperature of Ca.

- In the analysis, three synthesis methods were taken into consideration for the analysis; Improved Tours method, Hummers method and Modified Hummers Method respectively. The capital cost for each method at laboratory scale was calculated to be: R1 620 905.961, R1 574 213.661 and R1 613 950.761 respectively. The projected fuel cost was calculated to be: 14.36 $/kg H2, 13.96 $/kg H2 and 14.30 $/kg H2 for Improved Tours Method, Hummers method and modified Hummers method respectively (calculated at the exchange rate of 17.409 rand to dollar). The cost obtained was found to be cheaper than projected cost for complex hydrides (16$/kg H2) and gaseous hydrogen (at 18$/kg H2) however the cost was slightly more than the DOE target. More optimization and simulation would have to be performed to obtain optimum price for graphene nanocomposites.

9.3 HIGHLIGHTS:

- A novel Ca/graphene nanocomposite was synthesized in this work.

- According to theoretical studies on Ca for hydrogen storage, the desorption temperature of this material is around 250℃. The synthesized Ca/graphene nanocomposite released hydrogen at 150℃.

9.4 RECOMMENDATIONS:

Although a lot of research has been done with hydrogen storage material, the gap is still wide open because no material to date has met all the requirements for practical hydrogen storage materials. PhD research will be pursued to continue the work with the graphene nanocomposites for hydrogen storage.